RELATIVISTIC TREATMENTS OF THE NUCLEON-NUCLEON SYSTEM

By

DAVID JOSEPH BEACHEY B.A.Sc.

A Thesis

Submitted to the School of Graduate Studies

in Partial Fulfillment of the Requirements

for the Degree

Doctor of Philosophy

McMaster University

March 1994

RELATIVISTIC TREATMENTS OF THE NUCLEON-NUCLEON SYSTEM

DOCTOR OF PHILOSOPHY (1994) McMASTER UNIVERSITY

(Physics) Hamilton, Ontario

TITLE: Relativistic Treatments of the Nucleon-Nucleon System

AUTHOR: David Joseph Beachey, B.A.Sc. (University of Waterloo)

SUPERVISOR: Professor Y. Nogami

NUMBER OF PAGES: xiv, 169

Abstract

The relativistically minimalist Breit equation is used to study the two-nucleon system. Generally, the equation is noncovariant and its realm of applicability is limited. It is not a field-theoretical equation but, at low energy, it was thought to be a promising candidate to explore the scheme of repulsive vector and attractive scalar interactions as the dominant ingredient of the two-nucleon interaction.

In the $^1S_0$ singlet case, the equation does indeed seem viable. Dynamically sound interactions and a reasonable fit of the scattering data arise. In a specific application, the discrepancy between the $^1S_0$ isovector scattering lengths of the $p-p$ and $n-n$ interactions is explored. This novel charge-symmetry-breaking (CSB) mecharism *enlarges* the discrepancy between the two lengths, implying a still larger correction is required by other documented (CSB) mechanisms.

An all-encompassing model of the $^3S_1$-$^3D_1$ state is, on the other hand, not achieved. Models which best fit the experimental deuteron and elastic scattering data, are unphysical. The vector coupling is driven strongly negative and a dominant interference mechanism arises involving the entirely phenomenological short range OPEP. It was hoped that this parametrized short range OPEP would remain benign while the scalar/vector interference scheme took a lead role. Instead, the constraint of avoiding Klein paradox

difficulties defeats this picture and achieves the short-range repulsion in the $N-N$ force by ramping up the phenomenological OPEP.

It is finally argued that the Breit framework almost certainly does not lend itself to an adequate description of the $N-N$ system. It *does*, however, point to novel relativistic elements which may ultimately resolve celebrated outstanding problems such as the a_t-r_m discrepancy. The triplet scattering length a_t and deuteron matter-radius r_m are tightly correlated and resistant to simultaneous fitting in conventional models. The p-wave amplitudes of the lower components of a relativistic framework offer a potential means of resolution.

Acknowledgements

It is very difficult to name all the people to whom I feel some gratitude in my graduate student years at McMaster and remain within the new 300 page limit on theses.

First of all I would like to thank McMaster University for the Desmond G. Burns Scholarship.

I thank the Ontario Government for the Ontario Graduate Scholarship awarded for two years (and abruptly discontinued when they began targetting their funds to high T_c superconductivity and the like, resulting in perhaps the strongest made-in-Ontario recession ever).

I must thank Masa Toyama, Akira Suzuki, Kaori Tanaka, Chico Coutinho, and Murthy for coffee talk whether the topic was our own personal trials and tribulations in this specialty of physics or just trials and tribulations. I feel special gratitude to Masa for generously providing me with *free* access to his DEC-alpha machine in the last year of work.

Of course, outside of my chosen specialty, there are *countless* friends I have to thank for providing much needed comradery, joy, and amusement. ...and hab fans (who, of course, *can't count*) for providing much needed amusement.

...which reminds me... I thank Brian Mulroney (a hab fan -everybody) for ensuring that whenever I felt the slightest bit gloomy, for the most part, so did everyone else.

I thank Professor Randy Dumont, of the Chemistry department, for acting as a member of my supervisory committee. His "built-in" knowledge of Quantum Mechanics sped up those committee meetings that nobody really wanted to go to anyway.

Professors Rajat Bhaduri and Witze Van Dijk were enjoyable conversation companions on every topic whether in the realm of physics or otherwise. Of course, many of those conversations took place at Rajat's home with fine food and drink offered graciously by Rajat and Manju. Those dinners I will not forget! Thank you indeed.

Professor Donald Sprung, as a member of my committee, provided a steady reliable stream of advice and background knowledge throughout the years. His very swift and utterly thorough proof-reading of the thesis was very much appreciated. His dry sense of humour helped prepare me for the upcoming years in Britain.

I would like to particularly thank my thesis advisor Professor Yuki Nogami, for infecting me with a similar pre-occupation for physics "off the beaten track". His patience and kind-heartedness will not be forgotten. Our discussions were always very fruitful. Of course, there were many dinners at the home of Yuki and Sumi at which I sampled many fine dishes so I must thank the both of them for the many invitations into their home.
(Yes, I was hungry while writing these last few paragraphs.)

I have to especially thank all the members of my family, for their very kind support and understanding. Their understanding did not extend to the details of my field of study, in which I have immersed myself but the inevitable ups and downs in the road were far more negotiable with them solidly there in the background.

Special Preface

(Original contribution to multiply authored published papers.)

Three previously published papers have been included in the body of this thesis. They each have multiple authorship and as such, the content was not entirely the sole work of the thesis author.

In the body of Chapter 3, a paper appearing in the Journal of Physics G (Nuclear and Particle Physics) forms the centerpiece of the chapter. The realization of the possible importance of relativistic reduction combined with the scalar and vector interference as a partial explanation for charge symmetry breaking *within a non-relativistic context* was Y. Nogami's. The decision to depart from a pseudoscalar one-pion-exchange potential to an axial version was carried out by Nogami and F.M. Toyama jointly. The finite-size electromagnetic interactions were the choice of the author. All numerical calculations were carried out jointly by the author and F.M. Toyama.

In the body of Chapter 4, a paper appearing in Physical Review C (Nuclear Physics) is contained as section 4.2. This was jointly authored by the same three authors above and W. van Dijk. The 1-body Dirac effective range expansion was derived jointly by Y. Nogami and the author. The author carried out the similar analysis for the 2-body Dirac (Breit) equation and supplemented the analysis with the numerical example of a singlet deuteron mentioned in the paper.

In Section 1.2 of Appendix I, a jointly authored entry by Y. Nogami and the thesis author which appeared in Euro-Physics Letters is presented. This letter offers possibly the simplest example of the phenomenon of vacuum polarization in the literature. The model was conceived by Y. Nogami and the analytical work in support of the paper was carried out jointly by both authors. The numerical example in the letter was the work of the author.

Table of Contents

List of Tables

List of Figures

Chapter 1

Introduction

1.1 AN OVERVIEW

For over half a century, much success has been achieved in the dynamical analysis of systems of nucleons by making two basic assumptions: 1.) nucleons are elementary in their own right, *i.e.*, structureless; and 2.) non-relativistic quantum mechanics, *e.g.*, the Schrödinger equation, suffices as a framework in which to describe the nuclear dynamics. These assumptions underlie the field of conventional nuclear physics. They also require a context: they have been mostly successful in the low energy range, *i.e.*, at the typical energy scale of nuclear bound systems.

Both of these assumptions are now universally viewed as only approximate at a fundamental level. Nucleons are now viewed as bound ensembles of quarks and gluons whose dynamics in turn is described by a fully relativistic quantum field theory, Quantum Chromo-dynamics (QCD). Since QCD is a

more fundamental theory than a local nonrelativistic dynamics of elementary nucleons and a host of many intermediate frameworks. we expect there to be a smaller and smaller intersection set between dynamics described by the fundamental theory and the progressively cruder frameworks. For the crudest of all such frameworks to be successful. (and it has been!). it is required that some of the more sophisticated dynamics *and kinematics* play a sparing role at low energies (T_{com}, the center of momentum frame kinetic energy, $\approx$ 0-150 MeV).

There is merit in appealing to the simpler yet cruder frameworks if the physics allows it. A clean break in the reductionist sense would be much more appealing. If we can pick the minimal "correct" number of degrees of freedom, the minimal tier of the "correct" relativistic elements and the bare essentials necessary from full blown field theory so as to bring in the "correct" amount of physics from the vacuum, then we could use that tier of explanation to describe all of the NN scattering phaseshift data. all deuteron properties and with enough computing power. the table of the nucleides. QCD could then be appealed to in order to explain why the hadron or skyrmion or soliton masses and form factors are what they are at a clearly separate level of reduction.

In a sense, it is appealing *not* to have to know quark-gluon dynamics to understand the nuclear magic numbers. It may or may not yet be the case. In complete analogy, one generally does not have to know the molecular dynamics of the organic molecules in an inclined wooden plank to understand a ball rolling down an incline under the influence of gravity. On the other hand, if the ball is heavy, the plank will bend and one must know *something* of its internal dynamics to correctly describe the equation of motion of the

rolling ball. Perhaps the quark and gluon degrees of freedom will be front and center in the ultimate nuclear force models.

Turning now to the question of relativity, the current masses of the quarks that compose the nucleon lie between 6 and 10 MeV [1]. With a characteristic energy scale for the dynamics of QCD two orders of magnitude beyond that one could surmise that physics inside the nucleon is ultra relativistic. Two such composite systems whose centers of momentum are both in a nearly simultaneous rest frame may require a full relativistic description.

Popularly, it is expressed that relativity is important only when characteristic velocities become large and the ratio (v/c) becomes appreciable. It is less often pointed out that even a relatively static physical system requires a full relativistic treatment if dynamic energy scales approach the characteristic mass scales of the particles. A relativistic description of spin-1/2 particles entails dynamic interactions which can have a rich structure in the product spinor space as well as in co-ordinate or momentum space.

The basic questions investigated in this thesis are:

1.) Does the minimal relativistic framework for two spin 1/2 particles, *i.e.*, the Breit equation (Two-Body Dirac equation, Kemmer equation alternatively) lead to a more complete description of low energy nuclear observables than that of the conventional framework? In other words, in the reductionist spirit, can we lower the bar a single notch and explain much additional physics?

2.) In the Dirac framework, extra features such as the negative energy states and Zitterbewegung appear. These are manifestations of the particle/antiparticle symmetry of the Dirac theory. A proper accounting of the transient vacuum excitations involving the antiparticle sector requires the full blown Quantum Field Theory. Does the treatment of these aspects require a

more rigorous approach more in tune with field theory? The Bethe-Salpeter equation[2] (in ladder approximation) or even the Salpeter equation[3] provide more field-theoretic rigour in this sense but are technically much more complicated. They account for physics from essentially non-static effects that perhaps may not play a large role at low energy. This in fact is the bulk of the departure from the Breit equation. It has long been known that to their detriment, ladder approximation based two body equations do not reduce in the limit of one of the two masses becoming infinite to the 1-body Dirac equation. This is a property which is evidentally tied to the absence of the crossed diagrams.

In fact, the Breit equation, which is essentially inferior in all other regards, *does* to its credit have this proper reduction characteristic. Efforts to offer both the proper mass reduction limit and account properly for the decoupling of the positive and negative energy continua have arisen recently. [4] Much of the effort is focussed on the proper accounting of particle-antiparticle interaction corresponding to Z-graphs in the perturbative language. In the two body system, the lowest order graph which has a single anti-particle leg in one of the fermion lines is of fourth order in the vertex coupling. A proper accounting of these is required if the 2-body system is brought into interaction with a third particle or an external potential either of which acts as an energy and momentum source/sink leading to the continuum dissolution problem.[5],[6],[7]

In the work which follows the two body system will be kept strictly in isolation so this problem is avoided completely. As a conciliatory acknowledgement of the Breit equation's inadequacies, a more phenomenological outlook than usual will be taken in addressing the interactions used. The machinery of ordinary Quantum Mechanics can be adopted wholesale. The other field-theoretical equations possess some non-trivial interpretive difficulties.[8] What exactly is the amplitude? Is it a proper wave-function and what is to be done with the relative time co-ordinate?

Technically, the Breit equation with local interactions offers an edge also. Local interactions (which appear non-local when reduced to a non-relativistic limit) can be introduced and treated in a straight forward co-ordinate space based system of coupled differential equations of motion - exactly as in the case of the Schrödinger equation with local interactions. To achieve this with the other choices generally requires still further layers of approximation. In their simplest form, the other equations generally offer coupled integral-differential equations which are more challenging. The motivation here is not to evade the extra rigour but to measure the gains made by adopting the Breit equation in the two nucleon system.

The Breit equation is an equal time equation for spatially separated interacting particles. It is consequently *not* fully covariant, but neither is the Schrödinger equation. The Breit equation does *not* properly account for the physics of the vacuum (negative energies) and the coupling of such states with the positive energy sector -and of course, neither does the Schrödinger equation.

The Schrödinger equation has served very well at providing us with an understanding of low energy physics with weak static potentials. Perhaps

the Breit equation is a sufficient window on moderately strong *static* interactions at low energy. What we *do* get extra is the Zitterbewegung, the p-wave amplitudes in the $^3S_1$ - $^3D_1$ system, the non-local interactions when viewed from a reduced non-relativistic framework, the proper relation between the energy and scattering state wave length at the high end of the elastic scattering energy range, and a natural richness of dynamical structure because of the spinor-dependent interaction species. For example, we gain a forum in which to view the constructive-destructive interference between scalar and vector interactions.

Other shortcomings of such a framework are the omission of internal nucleon structure (internal excitations and finite size effects) and an intrinsic breaking of Lorentz covariance due to the presence of spatially extended interactions.

The finite size of the nucleon is kept in mind however since the interactions to be discussed are regularized (smoothed) at the origin (zero separation of the two particles). These "elementary" nucleons tacitly have form factors. This smoothing performs a more important function though than merely allowing for extended particles. It also ensures that the Klein paradox can be side-stepped. If interactions are too strong, the Dirac current can leak out through the lower ("small") spinor components.

Potentials such as the bare Coulomb which blow up at $r = 0$ yield peculiar singularities at energy dependent values of finite r (and corresponding forced nodes in some of the radial amplitudes). The root of this difficulty is, once again, the improper accounting of the vacuum. In addition, recently Krowlowski[9] has pointed out that the Breit equation can reproduce the quantum electrodynamic (QED) hyperfine spectrum of para-positronium to

order α_e^2 if solved exactly but to order α_e^4 if the Breit part of the interaction is treated in first order perturbation. (Breit, himself, demonstrated this for atomic hydrogenic systems.[10])

The relativistic quantum bound state remains an open problem. In the absence of clear interpretations and empirically demonstrated superiority in the *non*-perturbative realm amongst the field-theoretic-based equations, in the following pages the simplest two-body equation for fermions available will be put to use.

In part, the motivation for this work arose out of the success of the Dirac phenomenological treatment of nucleon-nucleus scattering. [11],[12],[13] The 1-body Dirac Equation with Dirac optical potentials of Lorentz scalar and 0-th component vector types (time-like vector component only) was used to describe proton-nucleus scattering observables. The energy sensitive spin observables are more successfully fitted in the impulse approximation in this scheme than in a standard non-relativistic calculation.[14]

The other motivation is the intriguing failure of several realistic nuclear force models within the non-relativistic framework with primarily local interactions (plus spin-orbit coupling) to account for the observed inconsistencies between the (N,N) triplet scattering length a_t and the *rms* matter radius r_m of the deuteron, both of which are very low energy observables indeed. [15,16,17,18,19]

The resolution of this problem, in all likelihood, lies squarely within one or both of two augmentations of the simple nonrelativistic picture, relativity and/or non-locality associated with substructure of the nucleons. In

this work. the focus of course is on the relativistic elements in the Breit formalism. It is appropriate to provide at this point a historical perspective on the use of this equation in sub-atomic physics in particular.

1.2 HISTORICAL BACKGROUND OF THE BREIT EQUATION IN NUCLEAR SYSTEMS

Breit introduced the equation bearing his name in 1929[10] to describe the various bound two-body hydrogen-like atoms. It was adopted several years after that by N. Kemmer[20] and applied to the deuteron. Kemmer tried to preserve the covariance of the system and therefore was forced to adopt δ-function interactions for his two equal time nucleons. He found that such a form allowed no bound states.

In the decade after that, the equation was again put to the problem of the nucleon-nucleon system by Schwinger[21] and by Moller and Rosenfeld[22],[23]. At the time the nucleon was indeed thought to be elementary in its own right. With a pointlike nucleon assumed in both instances, meson exchanges involved pure Yukawa interactions with the singularity at the origin intact. This would have led to the Klein paradox related problems mentioned earlier (and a $1/r^3$ divergence in the tensor part of the interaction) unless the un-cutoff Yukawa functions of separate mesons conspired to cancel just so at the origin.

At the time, little was known of the meson species beyond the pion and the vector meson mass and coupling parameters were frozen by the regularization criterion. Since that time, the finite size nucleon and the knowledge of separate meson degrees of freedom (including 3 separate vector mesons often) has led to the cultural acceptance of smearing the interaction, often with

a common cut-off parameter, while maintaining the independance of the couplings of the different species. With a common nucleon form-factor for each meson, the parametric freedom within one-boson-exchange models (OBE's) can be reasonably minimal (8-10 parameters) and provide a reasonable fit of phase-shift data. [24]

In the mid 1960's, Green and Sawada working within the context of the Breit equation, highlighted the interference feature of relativistic interactions. [25] They considered regularized meson interactions in contrived combinations such that no large-to-large components between the nucleons were coupled. The already purely relativistic pseudo-scalar coupling, an extreme version of the $S+V$ interference theme with exact cancellation and a similar but novel combination of axial and anti-symmetric Lorentz tensor $(A+T)$ were all looked at.

They then effected a reduction to an equation with a Pauli-spinor wave function (in the large component) preserving the interaction terms to two surviving orders. A clear correspondence was set up between the obtained velocity (momentum) dependent interactions (in the reduced non-relativistic picture) and the allowed spin and momentum dependent interaction species of the two-nucleon interaction (as allowed by observed symmetries -*e.g.*, see Okubo and Marshak[26]).

The correspondence is also clear in two papers by S. Sato[27][28] in which the explicit triplet radial equations in the reduced picture illustrate the identification between the Lorentz tensor interactions of various rank (associated with the appropriate meson species) and also exhibit an explicit energy dependence. Sato merely revealed the reduction to illuminate the correspondence between conventional force models and the meson-exchange

based relativistic one. He did not *calculate* within the reduced model as did Green and Sawada. Because they eliminated lower spinor components, they had to rescale their normalization.

As will be evident in chapter 5, if the lower components are enhanced, as they inevitably are in the $S+V$-type models, a mere rescaling of the large spinor components to restore unitarity may be too crude an approximation for examining subtle relativistic effects.

The advent of 3-dimensional reductions of the Bethe-Salpeter equation such as that of Salpeter and the Blankenbecler-Sugar equation[29] or straight applications of the full Bethe-Salpeter equation in 4 dimensions with ladder approximation[30],[31],[32],[33] and the incorporation of OBE models within those formulations with much success in phase-shift fits [34] has more or less squeezed the Breit equation out of the nucleon-nucleon literature. Ironically, it fared better in application to the meson represented as a composite system, at first as bound $N\bar{N}$ pairs[35],[36], and later as quark-antiquark $q\bar{q}$ pairs.[37],[38]

As of late, it has received a small resurrection which is probably attributable in part to the fact that when it *was* in vogue, realistic calculations were computationally prohibitive for the technology of the day. When the technical advances finally came, the formal problems of the Breit equation left it in the shadow of the field-theoretically based family of two body equations.

Exact calculations with the full Breit equation with even semi-realistic interactions (beyond δ-function or square-well interactions) are quite recent in the literature [27][28] The avoidance of the Klein paradox severely restricts the parameter space available when attempting a quantitative fit of N-N data. This undoubtedly also contributed to this apparent gap in the literature.

Jumping ahead a little. we will find that the most reliable part of the N-N interaction -the one pion exchange (OPE) tail cannot be properly described in the Breit equation by either entering the interaction through an axial (devivative coupling) or pseudoscalar (direct coupling) Lorentz component. The root of the problem is that neither interaction is arrived at through the perturbative apparatus of field theory in this framework. Although a naive axial version can be devised for the $^1S_0$ sector alone, a generally acceptable pion exchange tail capable of fitting the higher partial waves must be put in by hand as in the Schrödinger equation *without* an appeal to any particular Lorentz tensor field. This will be discussed in some detail in Appendix III.

It is quite plausible that the difficulty with the bare pseudoscalar coupling alone ($G^2_{\pi N} \approx 14.7$), the Klein paradox, and the brutal nature of any regularization scheme to rectify the situation (without jeopardizing the OPEP tail in all but the farthest asymptotic region) led to disenchantment with the Breit equation in the nuclear context. In meson physics. the pseudoscalar problem is not a consideration. There, one is primarily concerned with scalar and vector interactions between the quarks which in both cases have spin-matrices diagonal in the $q\bar{q}$ spinor components. An issue of paramount importance for example, quark confinement, can be formulated nicely with a scalar interaction supplemented by its lowest order velocity-dependent corrections.[38]

1.3 SPECIFIC APPLICATIONS OF THE BREIT EQUATION

With the revived activity and interest in the Breit equation in the last decade or so, a contribution to the literature detailing the highly involved

radial decomposition of the Breit amplitudes for two unlike masses was well overdue. Leal Ferreira and Galeão present such a synopsis for a broad variety of bilinear combinations of particle-1 and particle-2 spin matrices.[39] They extended the set of possible interaction species beyond the usual 5 scalar contractions of Lorentz tensors to include a straight 0-component vector (Coulomb-type) and three velocity or retardation species as discussed by Breit[10] and Childers[38] in different contexts. This set is indeed sufficient to cover the variety of interaction combinations utilized in chapters 3 and 4 (singlet chapters) of this thesis.

In chapter 5 (the triplet chapter), the OPEP presented is entered as a combination of two spin-dependent pieces not included in their set. Further, the decomposition of Leal Ferreira and Galeão , in the case of the spin triplet, is not one which reduces in the non-relativistic limit to the Schrödinger equation. Chapter 2, therefore presents the full radial decomposition separately for singlet and triplet configurations, in both cases favouring amplitudes which contain the pure large component to ensure the proper reduction to the Schrödinger radial equations. The interaction types included in the reduction are those of Leal Ferreira and Galeão augmented by two additional aforementioned spin-dependent pieces. The increased generality necessitates a departure from their notation. The tensorial spinor basis of the two particle spinor which has passed into near universal usage is that of Moseley and Rosen.[36]

The material which follows contains three appendices the first two of which depart somewhat from the theme of this work. Appendix I comprises a self-contained study of vacuum polarization for simple models in the 1-body Dirac equation. This investigation encounters the same scalar-vector

interference theme which in two-body work leads naturally to spin-orbit interactions. In the 1-body equation, the rich structure of the vacuum when the small spinor components get enhanced by large S and V is discussed.

Appendix II addresses some of the concern about utilizing the "unrigourous" Breit equation as opposed to one of the field-theoretic offspring the Salpeter equation. A simple separable model in 1 space dimension with dialable coupling and range parameters is examined to quantify the departures of one framework from the other. The results are quite encouraging for dynamics which takes place on a length scale longer than the nucleon Compton wavelength.

The third appendix addresses the choice of OPEP as encountered in the triplet version of our equation and illuminates the trouble spots with either an axial or pseudoscalar representation of this important component of the NN-interaction in *this* framework.

Chapter 3 constitutes the first "physics" chapter. Here, a subtle interference effect between the Coulomb interaction and the combined Lorentz scalar and vector species is shown to cause an "apparent" charge symmetry breaking component when viewed naively from a non-relativistic point of view. This is the only place where the electromagnetic interaction will be addressed. The magnetic portion of the interaction (in *one* instance) is described by the retardation interaction terms of Breit.[34] No attempt is made to incorporate a consistent description that accounts for the large anomalous Pauli magnetic moments of the somewhat *un*-Dirac like nucleons.

In chapter 4, two relativistic generalizations of the effective range expansion are derived and studied. Although, the Breit version is of the

$^1S_0$ singlet form. a singlet deuteron is bound artificially to enable quantitative comparision between the two possible k^2 expansions (about threshold and about the deuteron pole) and to relate the matter radius of the singlet deuteron to the singlet-scattering length via a third related expansion and to compare the results with an exact calculation.

In the fifth chapter, attention will be diverted to the coupled triplet $^3S_1$ - $^3D_1$ channel. A local model with the alternative OPEP along with the usual scalar-vector combination will be put to use to describe the scattering data over the elastic scattering range $T_{lab} < 350MeV$ and the deuteron properties. A study of model independence is made within the framework of local dynamical interactions and Breit equation. (Model parameters are varied but the ansatzes for scalar, vector, OPEP interaction splines at small r are preserved.) Best fits catering to the deuteron and threshold data alone, the scattering data over the elastic range, and overall data are presented. For the same reasons mentioned above pertaining to the magnetic interaction, an accurate magnetic moment for the deuteron is not obtained. A crude estimate of the moment is obtained by allocating the p-wave fraction of the deuteron (from lower components of course) its equivalent nonrelativistic orbital contribution. Future work to incorporate the Pauli moments and the full relativistic current operator into the calculation is a logical next step to supplement the work of chapters 3 and 5.

Chapter 2

The 3–dimensional Breit equation and its radial decomposition

2.1 THE 3-DIMENSIONAL BREIT EQUATION

The Breit equation in 3 dimensions is considerably more sophisticated than the 4×4 spinor matrix equation of the 1-body Dirac Equation. The 2-body spinor wavefunction is expressed in the outer-product space of the 2 individual spinor spaces which each have the usual rank 4. $\Psi(\vec{r_1}, \vec{r_2})$ has 16 components. All spinor matrices become 16×16 and the 3-dimensional equation is now a 16×16 matrix equation. There is much simplicity in the structure however and we will strictly adhere to one of the most elegant choices of basis, namely that of Moseley and Rosen[36],[40]. First let us construct the equation in the $\psi_1 \otimes \psi_2$ basis. The 2 free Dirac particle Hamiltonians are simply augmented by an interaction term to yield:

$$\left\{[\vec{\alpha}_1 \cdot \vec{p_1} + \beta_1 m_1] + [\vec{\alpha}_2 \cdot \vec{p_2} + \beta_2 m_2] + \hat{H}_{int}\right\}\Psi(\vec{r_1}, \vec{r_2}) = 0 \qquad (2.1.1)$$

We take the interaction to depend on the relative coordinate $\vec{r} \equiv (\vec{r_1} - \vec{r_2})$ alone. $\vec{R} \equiv (\vec{r_1} + \vec{r_2})/2$ is a system coordinate conjugate to total momentum $\vec{P} \equiv \vec{p_1} + \vec{p_2}$. The coordinate $\vec{r}$ is conjugate to the relative momentum $\vec{p} \equiv (\vec{p_1} - \vec{p_2})/2$ which becomes $-i\vec{\nabla}/2$ in the coordinate representation. Neither this choice of $(\vec{r}, \vec{p})$ and $(\vec{R}, \vec{P})$, nor any other, can achieve the desirable separation in the Hamiltonian between the system motion and internal motion possible in the nonrelativistic system. It is, however, the simplest and most symmetric choice given that one is going to work in the $\vec{P} = 0$ frame. This is indeed a preferred frame because (2.1.1) is not covariant.

Note that Ψ is a function of 2 space points $\vec{r_1}$ and $\vec{r_2}$ at equal time. A single operation $i\frac{\partial}{\partial t} \longrightarrow W$ carried a t-dependent 2-body equation to the t-independent (2.1.1). Adherence to covariance would require the presence of t_1 and t_2 associated with the spacetime locations of 2 particles as in the case of the full Bethe-Salpeter equation (BSE) or an interaction purely of a δ-function nature. Equation (2.1.1) is much simpler to work with than the BSE however and may contain some of the essential physics which describes nuclear systems elusive in the nonrelativistic formalism. For that matter, the nonrelativistic Schrödinger equation, like the Breit equation, violates Lorentz-covariance yet has achieved great success in broad application throughout nuclear physics. It is our hope to establish whether or not the Breit equation can retain and improve on the low energy success of the Schrödinger equation.

We retain $\hat{H}_{int}$ as the 0-component of a 4-vector. Hence in the 3-space formalism it behaves as a scalar under rotation.

$$\hat{H}_{int} = \gamma_1^0\gamma_2^0\Big\{S(r) + V(r)\gamma_1^\mu\gamma_{2\mu} + T(r)\sigma_1^{\mu\nu}\sigma_{2\mu\nu} + A(r)\gamma_1^5\gamma_1^\mu\gamma_{25}\gamma_{2\mu} + P(r)\gamma_1^5\gamma_{25}\Big\}$$

is the most general interaction possible constrained to be local in $r = |\vec{r_1} - \vec{r_2}|$, symmetric in the spin indices, derivable from the bilinear scalar combinations of the Dirac Lagrangian and *not* augmented by (v/c)-correction terms as, for example, discussed by Childers.[38] As usual, the matrices above can be expressed in terms of the basic hermitean matrices such as:

$$\gamma^0 = \gamma_0 = \beta; \qquad \gamma^i = -\gamma_i = \beta\alpha^i; \qquad \sigma^{\mu\nu} = 1/2\{\gamma^\mu, \gamma^\nu\}_+; \qquad \gamma^5 = i\gamma^0\gamma^1\gamma^2\gamma^3$$

This set must be augmented to include the two species of electromagnetic interactions discussed in the Charge Symmetry Breaking work: $U_{Co}(r)$, a Coulomb-type interaction describing a purely electrostatic coupling; and $U_{Br}(r)$ a Breit interaction to describe a magnetic interaction between *Dirac* particles. It also must, unfortunately, be further augmented by two spinor combinations which also do not derive from the Lorentz transforming set above. This is because the OPEP interaction tail in the triplet case simply cannot be generated using axial or the pseudoscalar coupling. The additional species which must enter the Breit equation are simply those which are brought into the Schrödinger equation by the usual OPEP. We designate these as: $U_{\sigma\sigma}(r)$, associated with the spin-spin part of the OPEP; and $U_\Lambda(r)$ related to the tensor part. This is discussed in more detail in Appendix (III). Now we divert to the Hermitean matrices of Mosely and Rosen in writing our complete interaction encompassing both the dynamical models we will encounter in the singlet and triplet work:

$$\begin{aligned}\hat{H}_{int} =&(\beta_1\beta_2)S(r) + (1 - \vec{\alpha}_1 \cdot \vec{\alpha}_2)V(r) + (\beta_1\beta_2)(\vec{\sigma}_1 \cdot \vec{\sigma}_2 + \vec{\alpha}_1 \cdot \vec{\alpha}_2)T(r) \\ &+(\vec{\sigma}_1 \cdot \vec{\sigma}_2 - \Gamma_1\Gamma_2)A(r) + (\beta_1\beta_2)(\Gamma_1\Gamma_2)P(r) \\ &+(1)U_{Co}(r) + (\hat{\Upsilon})U_{Br}(r) + (\vec{\sigma}_1 \cdot \vec{\sigma}_2)U_{\sigma\sigma}(r) + (\hat{\Lambda})U_\Lambda(r) \qquad (2.1.2)\end{aligned}$$

where

$$\hat{\Lambda} \equiv \frac{(\vec{\sigma}_1 \cdot \vec{r})(\vec{\sigma}_2 \cdot \vec{r})}{r^2}$$

and

$$\hat{\Upsilon} \equiv \frac{(\vec{\alpha}_1 \cdot \vec{r})(\vec{\alpha}_2 \cdot \vec{r})}{r^2}$$

Here $\Sigma^i_{a(4\times4)} \equiv 1_{(2\times2)} \otimes \sigma^i_{a(2\times2)}$ and $\Gamma_{a(4\times4)} \equiv \rho^1_{a(2\times2)} \otimes 1_{(2\times2)}$ (*i.e.*, $= \gamma^5$). a is the particle label 1 or 2.

In the singlet $^1S_0$ work, which preceded the triplet $^3S_1$ work, the OPEP tail was indeed generated using an axial coupling. The ultimate irresolvability of this coupling with the tensor part of the OPEP became clear only after work on the triplet scattering began. Thus the singlet and triplet cases are examined within the context of two separate dynamical models, both within the framework of the Breit equation. Two different notations are employed in the singlet and triplet chapters that follow. We will connect them to the master $\hat{H}_{int}$ when the time comes. At the least, they will unambiguously emphasize that different models are employed.

The spinor species of $\hat{H}_{int}$ largely overlap with the rather convenient compilation of forms listed by Leal-Ferreira and Galeao [39]. Their Childers-type interactions are traded for $\vec{\sigma}_1 \cdot \vec{\sigma}_2$ and $\hat{\Lambda}$ in this work and some rescaling occurs. We prefer the overall scale factor attached to each species to enable the nonrelativistic reduction:

$$\hat{H}_{int} \longrightarrow S(r)+V(r)+U_{Co}(r)+\{T(r)+A(r)+U_{\sigma\sigma}(r)\}\vec{\sigma}_1 \cdot \vec{\sigma}_2+\{U_{Br}(r)+U_{\Lambda}(r)\}\hat{\Lambda}$$

which acts on the upper (large) spinor components.

2.2 THE EQUATIONS AND TENSORIAL SPINOR BASIS OF MOSELEY AND ROSEN

In the $\vec{P} = 0$ frame of reference, equation (2.1.1) becomes in coordinate space:

$$\left\{\frac{-i}{2}(\vec{\alpha}_1 - \vec{\alpha}_2)\cdot\vec{\nabla}_r + \beta_1 m_1 + \beta_2 m_2 + \hat{H}_{int}(r) - W\right\}\Psi(\vec{r}) = 0 \qquad (2.2.1)$$

Equation (2.2.1) amounts to a system of 16 coupled equations in the 16 spinor components of Ψ. The system is of order 4 in the differential ∂_r and its decomposition to radial equations is discussed in many places.[36]–[39] Perhaps the most elegant approach, which will be adopted in this work, involves a change of spinor basis made possible by the 2-body nature of the problem.[36],[40] The components of spinor Ψ have 2 indices associated with the 2 particles. They have the structure: $\Psi_{\alpha,\beta} = \psi_{1\alpha}\psi_{2\beta}$, a bilinear in which the 2 parts respond only to the single particle spinor matrices with the same particle label.

Now in the 1-body Dirac equation, the bilinear forms $\bar{\phi}\psi$, $\bar{\phi}\gamma^\mu\psi$, $\bar{o}\sigma^{\mu\nu}\psi$, $\bar{\phi}\gamma^5\gamma^\mu\psi$, and $\bar{\phi}\gamma^5\psi$ transform as a Lorentz scalar, vector, 2nd rank tensor, axial vector, and pseudoscalar respectively.(*e.g.*, see Messiah v.2 p.908)[42] Here ϕ and ψ are independent 1-particle spinors. ($\bar{\phi} = \phi^\dagger\gamma^0 = [\phi^{*T}]\gamma^0$). Now Moseley[40] points out that $[\phi^{*T}]$ transforms under boosts and rotations like $\phi^T Q$ where Q is $-\beta\alpha^1\alpha^3$ and that therefore the bilinear combination $(\psi_1^T Q)\psi_2$ transforms like the 0-th component of a 4-vector, and $(\psi_1^T Q\alpha_1^i)\psi_2$ like the i-th component.

One can augment the Q matrix by any of the 16 independent spinor matrices and identify a bilinear combination of the $\psi_{1\alpha}\psi_{2\beta}$ that transforms like a component of one of the 5 basic Lorentz tensors. The bilinear combinations mentioned above all have 4 terms, so a factor of 1/2 is required to fulfill

a unitary transformation between the original product basis $\Psi_{\alpha,\beta} = \psi_{1\alpha}\psi_{2\beta}$ and the tensorial spinor basis. The tensorial spinor basis components are as follows.

the scalar:

$$I = (\psi_1^T Q\beta\psi_2) \tag{2.2.2}a$$

the 4-vector:

$$A^0 = (\psi_1^T Q\psi_2) \quad , \quad \vec{A} = (\psi_1^T Q\vec{\alpha}\psi_2) \tag{2.2.2}b$$

the 2nd rank antisymmetric tensor:

$$B^{\mu\nu} = (\psi_1^T Q\beta\sigma^{\mu\nu}\psi_2)$$

whose 6 independent components can be alternatively expressed as two 3-vectors:

$$\vec{F} \quad \text{with} \quad F^k = -iB^{0k} \quad \text{and} \quad \vec{G} \quad \text{with} \quad G^k = 1/2\epsilon^{klm}B^{lm} \tag{2.2.2}c$$

the 4-axial vector:

$$U^0 = (\psi_1^T Q\Gamma\psi_2) \quad , \quad \vec{U} = (\psi_1^T Q\Gamma\vec{\alpha}\psi_2) \tag{2.2.2}d$$

and the pseudoscalar:

$$J = (\psi_1^T Q\Gamma\beta\psi_2) \tag{2.2.2}e$$

There is no formal superiority in choosing such a basis over any other which does not have the tensorial character as far as the spinor is concerned. The simplicity occurs when (2.2.1) is expressed in this basis. If only S, V, T, A, P are present, the entire interaction spinor matrix $\hat{H}_{int}$ becomes diagonal. With the extra species in our interaction, it becomes block-diagonal with mixings only between the various components of each 3-vector. We define the linear combinations encountered as follows:

$$\mathcal{Q}_1(r) \equiv S(r) + 4V(r) - 6T(r) - 4A(r) + P(r) + U_{Co}(r) - U_{Br}(r) - U_{\Lambda}(r) - 3U_{\sigma\sigma}(r) \quad (2.2.3)a$$

$$\mathcal{Q}_2(r) \equiv -S(r) + 2V(r) + 2A(r) + P(r) + U_{Co}(r) + U_{Br}(r) - U_{\Lambda}(r) + U_{\sigma\sigma}(r) \quad (2.2.3)b$$

$$\mathcal{Q}_3(r) \equiv S(r) - 2V(r) - 2A(r) - P(r) + U_{Co}(r) + U_{Br}(r) - U_{\Lambda}(r) - 3U_{\sigma\sigma}(r) \quad (2.2.3)c$$

$$\mathcal{Q}_4(r) \equiv S(r) + 2T(r) + P(r) + U_{Co}(r) - U_{Br}(r) - U_{\Lambda}(r) + U_{\sigma\sigma}(r) \quad (2.2.3)d$$

$$\mathcal{Q}_5(r) \equiv -S(r) - 2T(r) - P(r) + U_{Co}(r) - U_{Br}(r) - U_{\Lambda}(r) + U_{\sigma\sigma}(r) \quad (2.2.3)e$$

$$\mathcal{Q}_6(r) \equiv -S(r) - 2V(r) - 2A(r) + P(r) + U_{Co}(r) + U_{Br}(r) - U_{\Lambda}(r) - 3U_{\sigma\sigma}(r) \quad (2.2.3)f$$

$$\mathcal{Q}_7(r) \equiv S(r) + 2V(r) + 2A(r) - P(r) + U_{Co}(r) + U_{Br}(r) - U_{\Lambda}(r) + U_{\sigma\sigma}(r) \quad (2.2.3)g$$

$$\mathcal{Q}_8(r) \equiv -S(r) + 4V(r) + 6T(r) - 4A(r) - P(r) + U_{Co}(r) - U_{Br}(r) - U_{\Lambda}(r) - 3U_{\sigma\sigma}(r) \quad (2.2.3)h$$

$$\mathcal{X}_2(r) \equiv 2U_{Br}(r) - 2U_{\Lambda}(r) \quad (2.2.3)i$$

$$\mathcal{X}_4(r) \equiv -2U_{Br}(r) - 2U_{\Lambda}(r) \quad (2.2.3)j$$

$$\mathcal{X}_5(r) \equiv -2U_{Br}(r) - 2U_{\Lambda}(r) \quad (2.2.3)k$$

$$\mathcal{X}_7(r) \equiv 2U_{Br}(r) - 2U_{\Lambda}(r) \quad (2.2.3)l$$

Within this level of generality, the Breit equation in the center of momentum frame becomes the system:

$$(W - \mathcal{Q}_1)I + 2i\vec{\nabla} \cdot \vec{F} + 2MA^0 = 0 \quad (2.2.4)a$$

$$[(W - \mathcal{Q}_2) - \mathcal{X}_2\tilde{O}_{\times\times}]\vec{A} + 2\vec{\nabla} \times \vec{U} - 2\mu\vec{F} = 0 \quad (2.2.4)b$$

$$(W - \mathcal{Q}_3)A^0 + 2MI = 0 \quad (2.2.4)c$$

$$[(W - \mathcal{Q}_4) - \mathcal{X}_4\tilde{O}_{\times\times}]\vec{G} + 2i\vec{\nabla}J - 2M\vec{U} = 0 \quad (2.2.4)d$$

$$[(W - \mathcal{Q}_5) - \mathcal{X}_5 \check{\mathcal{O}}_{\times\times}]\vec{F} + 2i\vec{\nabla}I - 2\mu\vec{A} = 0 \qquad (2.2.4)e$$

$$(W - \mathcal{Q}_6)U^0 + 2\mu J = 0 \qquad (2.2.4)f$$

$$[(W - \mathcal{Q}_7) - \mathcal{X}_7 \check{\mathcal{O}}_{\times\times}]\vec{U} + 2\vec{\nabla} \times \vec{A} - 2M\vec{G} = 0 \qquad (2.2.4)g$$

$$(W - \mathcal{Q}_8)J + 2i\vec{\nabla} \cdot \vec{G} + 2\mu U^0 = 0 \qquad (2.2.4)h$$

We have introduced the operator $\check{\mathcal{O}}_{\times\times}$ which acts on a vector quantity $\vec{V}$:

$$\check{\mathcal{O}}_{\times\times}(\vec{V}) \equiv \vec{e}_r \times (\vec{e}_r \times \vec{V}) \qquad (2.2.5)a$$

or equivalently:

$$\check{\mathcal{O}}_{\times\times}(\vec{V}) \equiv (\vec{e}_r \cdot \vec{V})\vec{e}_r - \vec{V} \qquad (2.2.5)b$$

Two properties which prove useful in the reduction of the dynamical equations are:

$$\check{\mathcal{O}}^2_{\times\times}\vec{V} = -\check{\mathcal{O}}_{\times\times}\vec{V} \qquad (2.2.5)c$$

and

$$[a + b\check{\mathcal{O}}_{\times\times}]^{-1} = [\frac{1}{a} + \frac{b}{a(b-a)}\check{\mathcal{O}}_{\times\times}] \qquad (2.2.5)d$$

Equations $(2.2.4)a - h$ differ only slightly from equation(s) (6 a-h) of Leal-Ferreira and Galeao [39]. Consistent with their notation (and Moseley and Rosen's) are the mass parameters: $M \equiv 1/2(m_1 + m_2)$ and $\mu \equiv 1/2(m_1 - m_2)$. There is a close correspondence between our $\mathcal{Q}_{1\ldots8}(r)$ and their $V_{1\ldots8}(r)$. They differ only because of the absence of the Childers spinor species and the presence of $\hat{\Lambda}$ and $\vec{\sigma}_1 \cdot \vec{\sigma}_2$. Our quantities $\mathcal{X}_{2,4,5,7}(r)$ correspond to their $V_{9,10}$ only as far as the Breit interaction is concerned.

To gain a handle on the angular-radial separation which we wish to effect next, we take the action of the operator $\hat{\mathrm{J}}^2$ which has the explicit form: $\hat{\mathrm{J}}^2 = \frac{1}{4}(\vec{\sigma}_1 + \vec{\sigma}_2)^2 + \vec{\mathrm{L}} \cdot (\vec{\sigma}_1 + \vec{\sigma}_2) + \hat{\mathrm{L}}^2$ on each of the spinor components

in the tensorial basis. Excepting the 3-vectors. it is found that the action of $\hat{\mathrm{J}}^2$ and $\hat{\mathrm{L}}^2$ are equivalent. Therefore component $I(\vec{r})$. for example. in a state with total angular momentum $\sqrt{j(j+1)}$ can generally be expressed as: $I(\vec{r}) = \mathcal{I}(r)Y_j^{m_j}(\Omega)$.

The 3-vectors can be expressed generally as a linear combination of vector spherical harmonics within the subspace $\ell = j-1, j, j+1$. For example: $\vec{F} = f_-(r)\vec{\mathbf{Y}}_-(\Omega,\sigma)+f_0(r)\vec{\mathbf{Y}}_0(\Omega,\sigma)+f_+(r)\vec{\mathbf{Y}}_+(\Omega,\sigma)$. Here we have the introduced the definitions:

$$\vec{\mathbf{Y}}_{\mp} \equiv \vec{\mathbf{Y}}^{m_j}_{j,\ell=j\mp1}(\Omega,\sigma) \qquad (2.2.6)a$$

and

$$\vec{\mathbf{Y}}_0(\Omega,\sigma) \equiv \vec{\mathbf{Y}}^{m_j}_{j,\ell=j}(\Omega,\sigma) \qquad (2.2.6)b$$

where the harmonics obey the orthonormality convention:

$$\int d\Omega \vec{\mathbf{Y}}^{*m_j}_{j,\ell}(\Omega,\sigma)\cdot\vec{\mathbf{Y}}^{m'_j}_{j',\ell'}(\Omega,\sigma) = \delta_{j,j'}\delta_{\ell,\ell'}\delta_{m_j,m'_j} \qquad (2.2.6)c$$

These defining properties of the vector harmonics correspond to the conventions of A. R. Edmonds (p. 83)[43] The full radial decomposition can be effected with the accompanying concise list of properties within this reference.

The angular momentum considerations have restricted us to 16 independent radial amplitudes; one associated with each of the spinor components I,A^0, J,U^0; and three each associated with the 3-vectors $\vec{A}$, $\vec{F}$,$\vec{G}$, and $\vec{U}$. Let us now turn to considerations of parity. The scalars w.r.t. rotation I,A^0,J,U^0; are to be associated with spin singlets, while the 3-vectors are associated with spin triplets.

In the 1-body Dirac equation, the 4-component spinor ψ is not an eigenstate of the parity operator $\hat{\pi}$ in the naive sense: $\hat{\pi}\psi = \pm\psi$. The lower

components couple to the upper components (large in the usual sense) by an operation linear in $\vec{p}$ (or $-i\vec{\nabla}$). They are consequently of *opposite* spatial parity. The parity of the state, in the strict sense can be obtained from the operation:

$$\hat{\pi}(\beta\psi) = \pm\psi$$

In the Breit equation, $\hat{H}_{Breit}$ couples the midsized components: $\psi_{1\alpha}\psi_{2\beta}$ $\{\alpha \in (1,2)\ ,\ \beta \in (3,4)$ or *vice versa* $\}$ $(\vec{A}, \vec{F}, J, U^0$ in the tensorial basis), with the large and doubly small components through terms linear in $\vec{p}$ (or $-i\vec{\nabla}_r$). Thus the strict parity of a state is extracted by the operation:

$$\hat{\pi}(\beta_1\beta_2\Psi_{Breit}) = \pm\Psi_{Breit} \tag{2.2.7}$$

We can divide the spinor components into 2 distinct sets. The first set, $\{I, A^0, \vec{U}, \vec{G}\}$, shares the parity of Ψ as a whole. The set $\{J, U^0, \vec{A}, \vec{F}\}$ have opposite parity. We can classify the states of Ψ by designating the usual two classes: case-*i*: $\hat{\pi} = (-)^j$ and case-*ii*: $\hat{\pi} = (-)^{(j+1)}$. We are interested only in the particle-particle sector so there is no further complication due to the intrinsic parities. $\{\ ^1S_0, ^1P_1, ^3P_1, ^1D_2, ^3D_2,$ *etc.* $\}$ spectroscopic states all belong to case-*i* while $\{\ ^3S_1, ^3P_0, ^3P_2, ^3D_1, ^3D_3,$ *etc.* $\}$ belong to case-*ii*. Both classes will be subject to scrutiny in later chapters.

Parity considerations reduce the total number of allowed independent radial amplitudes from 16 to 8 for a given parity. This can be seen as follows. Take *e.g.*, case-*i*. Both I and J spinor components must have angular dependence $Y_j^{m_j}(\Omega)$ which under spatial inversion acquires a sign of $(-)^j$. The J-component, however, *must* acquire a sign of $(-)^{(j+1)}$ as dictated by the dynamical equations (2.2.4). J is forced to vanish in case-*i*. For each of the 3-vectors, one or two of the three radial amplitudes will also vanish. The

spinor components are reduced to the following structure. In case-*i*. $\hat{\pi} = (-)^j$ and we have:

$$I = \mathcal{I}(r)Y_j^{m_j}(\Omega) \quad , \quad \vec{G} = g(r)\vec{\mathbf{Y}}_0(\Omega,\sigma) \qquad (2.2.8)a,b$$

$$A^0 = a(r)Y_j^{m_j}(\Omega) \quad , \quad \vec{U} = u(r)\vec{\mathbf{Y}}_0(\Omega,\sigma) \qquad (2.2.8)c,d$$

$$J = 0 \quad , \quad \vec{A} = a_-(r)\vec{\mathbf{Y}}_-(\Omega,\sigma) + a_+(r)\vec{\mathbf{Y}}_+(\Omega,\sigma) \qquad (2.2.8)e,f$$

$$U^0 = 0 \quad , \quad \vec{F} = f_-(r)\vec{\mathbf{Y}}_-(\Omega,\sigma) + f_+(r)\vec{\mathbf{Y}}_+(\Omega,\sigma) \qquad (2.2.8)g,h$$

or in case-*ii* , $\hat{\pi} = (-)^{(j+1)}$ applies (as in the deuteron bound state) and we can write:

$$I = 0 \quad , \quad \vec{G} = g_-(r)\vec{\mathbf{Y}}_-(\Omega,\sigma) + g_+(r)\vec{\mathbf{Y}}_+(\Omega,\sigma) \qquad (2.2.9)a,b$$

$$A^0 = 0 \quad , \quad \vec{U} = u_-(r)\vec{\mathbf{Y}}_-(\Omega,\sigma) + u_+(r)\vec{\mathbf{Y}}_+(\Omega,\sigma) \qquad (2.2.9)c,d$$

$$J = \mathcal{J}(r)Y_j^{m_j}(\Omega) \quad , \quad \vec{A} = a(r)\vec{\mathbf{Y}}_0(\Omega,\sigma) \qquad (2.2.9)e,f$$

$$U^0 = u(r)Y_j^{m_j}(\Omega) \quad , \quad \vec{F} = f(r)\vec{\mathbf{Y}}_0(\Omega,\sigma) \qquad (2.2.9)g,h$$

For each case, two of the eight dynamical equations $(2.2.4)a-h$ will be satisfied trivially. Equations $(2.2.4)f,h$ in case-*i* and $(2.2.4)a,c$ in case-*ii* vanish identically yielding no dynamical information.

2.3 THE GENERAL $\hat{\pi} = (-)^J$ DECOMPOSITION

There are two motivations for reducing the Breit equation to a set of 2 coupled 2nd order differential radial equations. One is simply to express the physics concisely and in a way conducive to utilizing old standard techniques and software built around the Schrödinger equation. The other is to relate the two formalisms in the limits of low energy, small interactions, or *both*. This motivation is more concerned with physical insight. We wish to

preserve physics well described in the conventional picture, while looking for extensions to that picture which rein in some anomalous low energy features [44]–[51] which are only described in a purely nonrelativistic framework by introducing nonlocal interactions and/or finite size effects.

A priori, there is no reason why the 8 radial equations obtained simply by operating on each of equations $(2.2.4)a-h$ with $\int d\Omega \vec{Y}^{*m_j}_{j,\ell} \cdot [\ \vec{}\ ]$ or $\int d\Omega Y^{*m_j}_{j}(\Omega)[\ \ ]$ cannot be directly numerically solved for the 8 radial amplitudes given the usual boundary conditions. Four of the amplitudes can be obtained in a purely algebraic manner in terms of the others and four first order differential equations remain. Even in recasting the system in terms of two coupled 2nd-order equations in terms of two amplitudes,one is faced with a variety of choices. In case-*i* with $\tilde{\pi} = (-)^j$ one can choose *any* pair of radial amplitudes with the exceptions of pairs $\{\mathcal{I}(r), a(r)\}$ and $\{u(r), g(r)\}$ in $(2.2.8)a-h$ to which the system will reduce. The two resulting 2nd order equations will be coupled. Such a system has come to be known as a "Schrödinger-*like* equation".[39],[41]

Any such choice will concur with the first motivation. In regard to the second motivation, the choice of decomposition can dramatically affect the Schrödinger-"*likeness*" of the equations. In the non-relativistic limit, $W = 2M + \mathcal{E}$ $(\mathcal{E} \ll 2M)$ and all interactions are small. We anticipate that the dynamics of the upper spinor components reduces to the Schrödinger equation exactly after $\mathcal{O}(\mathcal{E}/M)^2$-terms are dropped. We therefore surmise that the spinor components (in the tensorial basis) I, A^0, $\vec{U}$, $\vec{G}$ will bear a more faithful resemblance to the Schrödinger-wavefunction of ordinary quantum mechanics.

Let us begin with the task of reduction by doing as much arithmetic as possible before decomposing (2.2.4)$a-h$ into the radial and angular sectors. Since, in case-i we will not pursue any analysis of the (n,p) system, we will invoke the lone simplification $\mu = (m_1 - m_2)/2 = 0$. This is a minor loss of generality but it grants us much less algebra. In essence, it decouples completely the $|\, j, j, s = 1, m_j\rangle$ and $|\, j, j, s = 0, m_j\rangle$ channels.

Recalling that in case-i, $J(\vec{r}) = U^0(\vec{r}) = 0$, from (2.2.4)$c$ and d we obtain:

$$A^0(\vec{r}) = -\frac{2M}{(W - \mathcal{Q}_3(r))} I(\vec{r}) \qquad (2.3.1)a$$

and

$$\vec{G}(\vec{r}) = +\frac{2M}{(W - \mathcal{Q}_4(r))}\{1 + \frac{\mathcal{X}_4(r)}{(W - \mathcal{Q}_4(r) + \mathcal{X}_4(r))}\tilde{\mathcal{O}}_{\times\times}\}\vec{U}(\vec{r}) \qquad (2.3.1)b$$

We can also eliminate the spinor-vectors $\vec{A}(\vec{r})$ and $\vec{F}(\vec{r})$ using (2.2.4)b and e.

$$\vec{A}(\vec{r}) = -\frac{2}{(W - \mathcal{Q}_2(r))}\{1 + \frac{\mathcal{X}_2(r)}{(W - \mathcal{Q}_2(r) + \mathcal{X}_2(r))}\tilde{\mathcal{O}}_{\times\times}\}\vec{\nabla} \times \vec{U}(\vec{r}) \qquad (2.3.1)c$$

and

$$\vec{F}(\vec{r}) = -\frac{2i}{(W - \mathcal{Q}_5(r))}\{1 + \frac{\mathcal{X}_5(r)}{(W - \mathcal{Q}_5(r) + \mathcal{X}_5(r))}\tilde{\mathcal{O}}_{\times\times}\}\vec{\nabla} I(\vec{r}) \qquad (2.3.1)d$$

We obtain the two now uncoupled 2nd order equations in $\{I(\vec{r}), \vec{U}(\vec{r})\}$ from the only remaining dynamical equations (2.2.4)a and g. They become respectively:

$$\vec{\nabla} \cdot \{\frac{1}{(W - \mathcal{Q}_5(r))}(1 + \frac{\mathcal{X}_5(r)}{(W - \mathcal{Q}_5(r) + \mathcal{X}_5(r))}\tilde{\mathcal{O}}_{\times\times})\vec{\nabla} I(\vec{r})\}$$
$$+ \{\frac{(W - \mathcal{Q}_1(r))}{4} - \frac{M^2}{(W - \mathcal{Q}_3(r))}\} I(\vec{r}) = 0 \qquad (2.3.2)a$$

and

$$
\begin{aligned}
&-\vec{\nabla}\times\{\frac{1}{(W-\mathcal{Q}_2(r))}(1+\frac{\mathcal{X}_2(r)}{(W-\mathcal{Q}_2(r)+\mathcal{X}_2(r))}\tilde{\mathcal{O}}_{\times\times})\vec{\nabla}\times\vec{U}(\vec{r})\}\\
&+\quad\{\ (\frac{(W-\mathcal{Q}_7(r))}{4}-\frac{M^2}{(W-\mathcal{Q}_4(r))})\\
&\quad-(\frac{\mathcal{X}_7(r)}{4}+\frac{M^2\mathcal{X}_4(r)}{(W-\mathcal{Q}_4(r))(W-\mathcal{Q}_4(r)+\mathcal{X}_4(r))})\tilde{\mathcal{O}}_{\times\times}\ \}\vec{U}(\vec{r})=0
\end{aligned}
\tag{2.3.2}b
$$

As will be shown shortly, the above two equations yield two independent radial equations which are quite similar to the Schrödinger radial equations. Equations (2.3.2)*a* and *b* constitute our first Schrödinger-*like* equations. Note that the decomposition could also take place by inverting (2.3.1)*a* and *b* and reducing to equations in terms of spinor components $A^0(\vec{r})$ and $\vec{G}(\vec{r})$ respectively. These take the form:

$$
\begin{aligned}
&-\vec{\nabla}\cdot\{\frac{1}{(W-\mathcal{Q}_5(r))}(1+\frac{\mathcal{X}_5(r)}{(W-\mathcal{Q}_5(r)+\mathcal{X}_5(r))}\tilde{\mathcal{O}}_{\times\times})\vec{\nabla}[\frac{2M}{(W-\mathcal{Q}_3(r))}A^0(\vec{r})]\}\\
&\qquad+\{\frac{M}{2}-\frac{(W-\mathcal{Q}_1(r))(W-\mathcal{Q}_3(r))}{8M}\}A^0(\vec{r})=0
\end{aligned}
\tag{2.3.3}a
$$

and

$$
\begin{aligned}
&-\vec{\nabla}\times\{\frac{1}{(W-\mathcal{Q}_2(r))}(1+\frac{\mathcal{X}_2(r)}{(W-\mathcal{Q}_2(r)+\mathcal{X}_2(r))}\tilde{\mathcal{O}}_{\times\times})\vec{\nabla}\times[\frac{1}{2M}((W-\mathcal{Q}_4(r))-\mathcal{X}_4(r)\tilde{\mathcal{O}}_{\times\times})\vec{G}(\vec{r})]\}\\
&+\quad\{\ (\frac{(W-\mathcal{Q}_4(r))(W-\mathcal{Q}_7(r))}{8M}-\frac{M}{2})\\
&\quad-(\frac{1}{8M}((W-\mathcal{Q}_7(r))\mathcal{X}_4(r)+(W-\mathcal{Q}_4(r))\mathcal{X}_7(r)+\mathcal{X}_4(r)\mathcal{X}_7(r)))\tilde{\mathcal{O}}_{\times\times}\ \}\vec{G}(\vec{r})=0
\end{aligned}
\tag{2.3.3}b
$$

These two separate decompositions are special in the sense that the spinor pairs $\{I(\vec{r}),\vec{U}(\vec{r})\}$ and $\{A^0(\vec{r}),\vec{G}(\vec{r})\}$ in the $\hat{\pi}=(-)^j$ case have the same structure in the $\rho_1\otimes\rho_2$ spinor space as the $\hat{\pi}=(-)^{(j+1)}$ case $\vec{U}(\vec{r})$ and $\vec{G}(\vec{r})$

components respectively. ($\gamma_{1,2}$-spinor space is $\rho_{1,2} \otimes \sigma_{1,2}$. All of our two-body spinors are built in the space $\rho_1 \otimes \sigma_1 \otimes \rho_2 \otimes \sigma_2$.) In the $\hat{\pi} = (-)^{(j+1)}$ case, $\vec{U}(\vec{r})$ and $\vec{G}(\vec{r})$ have two radial amplitudes associated with each of them. We shall find two very natural decompositions in that case involving isolated $\vec{U}(\vec{r})$ or isolated $\vec{G}(\vec{r})$.

One could select a decomposition that does not involve upper spinor components, choosing $\vec{A}(\vec{r})$ or $\vec{F}(\vec{r})$ but the nonrelativistic reduction does not correspond to the Schrödinger equation. The 2nd order (differential) equation for $\vec{A}$ is for example:

$$\vec{\nabla} \times \{(\frac{(W - \mathcal{Q}_4(r))}{(W - \mathcal{Q}_4(r))(W - \mathcal{Q}_7(r)) - 4M^2})$$
$$[1 - \frac{(W - \mathcal{Q}_4(r))(W - \mathcal{Q}_4(r) + \mathcal{X}_4(r))\mathcal{X}_7(r) + 4M^2\mathcal{X}_4(r)}{(W - \mathcal{Q}_4(r))((W - \mathcal{Q}_4(r) + \mathcal{X}_4(r))(W - \mathcal{Q}_7(r) + \mathcal{X}_7(r)) + 4M^2)}\tilde{\mathcal{O}}_{\times\times}]\vec{\nabla} \times \vec{A}(\vec{r})\}$$
$$+ \frac{1}{4}\{(W - \mathcal{Q}_2(r) - \mathcal{X}_2(r)\tilde{\mathcal{O}}_{\times\times}\}\vec{A}(\vec{r}) = 0 \qquad (2.3.4)$$

This can be decoupled into two radial equations for $a_-(r)$ and $a_+(r)$. In the limit of low energy and all interactions vanishing we find that

$$\vec{A}(\vec{r}) \longrightarrow -\frac{1}{M}\vec{\nabla} \times \vec{U}(\vec{r}) \longrightarrow \mathcal{O}(k/M)\vec{U}(\vec{r}) \longrightarrow 0.$$

The vanishing spinor component $\vec{A}(\vec{r})$ and equation (2.3.4) offer us little when the subject of nonrelativistic correspondence is central to our analysis.

There is one additional subtlety here that distinguishes the $\hat{\pi} = (-)^j$ case from the $\hat{\pi} = (-)^{(j+1)}$ case. There is a certain interchangability between the spinor components $I(\vec{r})$,$A^0(\vec{r})$, or in the one triplet scenario $\vec{U}(\vec{r})$,$\vec{G}(\vec{r})$ and the pure large spinor component: $\Psi_{\alpha,\beta}$ (with α,β running over 1,2 only) in that although slightly different dynamical equations are obeyed by each,

they all possess the identical asymptotic properties. The phase shift must be common to all as the relations (2.3.1)a, b reduce to mere constant dependencies. This does *not* hold in the $\hat{\pi} = (-)^{(j+1)}$ case between the two choices of decomposition there: $\vec{U}(\vec{r})$ and $\vec{G}(\vec{r})$.

2.4 THE $\hat{\pi} = (-)^J$ SPIN-SINGLET RADIAL EQUATION

To proceed from (2.3.2)a and b to radial equations is a small step. We will only encounter the case-i situation twice in ensuing chapters and both instances will involve the particularly simple $^1S_0$ state. In the $^1S_0$ state, equations (2.2.6)a reduces to: $I(\vec{r}) = \mathcal{I}(r)Y_0^0(\Omega)$ and of course there is no triplet configuration $^3S_0$ with this L, J combination.

From Edmonds p(84)$_{[43]}$ we have: $\vec{\nabla}I(\vec{r}) = -\frac{\partial}{\partial r}\mathcal{I}(r)\vec{\mathbf{Y}}_{0,1}^0(\Omega,\sigma)$. Equation (2.3.2)$b$ vanishes identically in the $^1S_0$ configuration. The general spin-singlet radial equation generated from (2.3.2)a reads:

$$\begin{aligned}
&\mathcal{I}''(r) + \{\frac{\mathcal{Q}_s'(r)}{(W-\mathcal{Q}_s(r))}\}\mathcal{I}'(r) \\
&+\{-\frac{j(j+1)}{r^2} + \frac{j(j+1)\mathcal{X}_s(r)}{r^2(W-\mathcal{Q}_s(r)+\mathcal{X}_s(r))} \\
&+\frac{1}{4}\frac{((W-\mathcal{Q}_3(r))(W-\mathcal{Q}_4(r)-4M^2)(W-\mathcal{Q}_5(r)}{(W-\mathcal{Q}_3(r))}\}\mathcal{I}(r) \qquad (2.4.1)
\end{aligned}$$

The presence of the dynamical quantity in the $\mathcal{I}'(r)$-term above, reflects an "apparent" momentum dependent interaction term or equivalently a non-local interaction if we were to *strictly* identify (2.4.1) with the Schrödinger radial equation for the $^1S_0$ state. This gives us some hint of the thrust of the arguments we will encounter in the forthcoming "physics" chapters. Alternatively, the radial equation for $^1S_0$ could have emanated from (2.3.3)b rather

than (2.3.3)a. $\vec{G}$ like $\vec{U}$ vanishes and we ultimately obtain for $A^0(\vec{r}) = a(r)Y_0^0(\Omega)$:

$$a''(r) + \{\frac{2}{r} + 2\frac{\mathcal{Q}_3'(r)}{(W-\mathcal{Q}_3(r))} + \frac{\mathcal{Q}_5'(r)}{(W-\mathcal{Q}_5(r))}\}a'(r)$$
$$+\{-\frac{j(j+1)}{r^2} + \frac{j(j+1)\mathcal{X}_5(r)}{r^2(W-\mathcal{Q}_5(r)+\mathcal{X}_5(r)} + \frac{(W-\mathcal{Q}_5(r))}{4}((W-\mathcal{Q}_4(r)) - \frac{4M^2}{(W-\mathcal{Q}_3(r))})$$
$$+\frac{\mathcal{Q}_3''(r)}{(W-\mathcal{Q}_3(r))} + 2(\frac{\mathcal{Q}_3'(r)}{(W-\mathcal{Q}_3(r))})^2 + \frac{\mathcal{Q}_3'(r)\mathcal{Q}_5'(r)}{(W-\mathcal{Q}_3(r))(W-\mathcal{Q}_5(r))} + 2\frac{\mathcal{Q}_3'(r)}{r(W-\mathcal{Q}_3(r))}\}a(r)$$
$$= 0 \qquad (2.4.2)$$

2.5 THE GENERAL $\hat{\pi} = (-)^{(J+1)}$ DECOMPOSITION

The Breit equation possesses much symmetry. Glancing at the dynamical equations: (2.2.4)$a-h$, one may notice that tensorial spinor components J, U^0,$\vec{A}$, and $\vec{F}$ occur symmetrically w.r.t. components I,A^0, $\vec{U}$, and $\vec{G}$ respectively if one exchanges $\mu \longleftrightarrow M$, $\mathcal{Q}_1 \longleftrightarrow \mathcal{Q}_8$, $\mathcal{Q}_2, \mathcal{X}_2 \longleftrightarrow \mathcal{Q}_7, \mathcal{X}_7$, $\mathcal{Q}_3 \longleftrightarrow \mathcal{Q}_6$, and $\mathcal{Q}_4, \mathcal{X}_4 \longleftrightarrow \mathcal{Q}_5, \mathcal{X}_5$. [36] With these exchanges, we could transform (2.3.2)a and b into two equations in components $J(\vec{r})$ and $\vec{A}(\vec{r})$. These are mid-sized components in the particle-particle sector, however, so we now look for a decomposition to the non-zero components $\vec{U}(\vec{r})$ or $\vec{G}(\vec{r})$ which contain the traditional large component.

With this, the case-*ii* decomposition will be quite similar to the coupled spin triplet state in the nonrelativistic Schrödinger equation. The mass difference between the neutron and proton is preserved in the mass parameter μ which is small but non-zero. We introduce the following definitions which entirely contain the μ-dependence:

$$\mathcal{W}_4(r) \equiv W - \mathcal{Q}_4(r)$$

$$\mathcal{W}_5(r) \equiv W - \mathcal{Q}_5(r) + \mathcal{X}_5(r)$$

$$\mathcal{W}_2(r) \equiv W - \mathcal{Q}_2(r) + \mathcal{X}_2(r) - \frac{4\mu^2}{\mathcal{W}_5(r)}$$

$$\mathcal{W}_6(r) \equiv W - \mathcal{Q}_6(r)$$

$$\mathcal{W}_7(r) \equiv W - \mathcal{Q}_7(r)$$

$$\mathcal{W}_8(r) \equiv W - \mathcal{Q}_8(r) - \frac{4\mu^2}{\mathcal{W}_6(r)}$$

Proceeding from equation set (2.2.4) with (2.2.9)$a-h$ in mind, we obtain from (2.2.4)e and f:

$$U^0(\vec{r}) = -\frac{2\mu}{\mathcal{W}_6(r)} J(\vec{r}) \qquad (2.5.1)a$$

and

$$\vec{F}(\vec{r}) = +\frac{2\mu}{\mathcal{W}_5(r)} \vec{A}(\vec{r}) \qquad (2.5.1)b$$

Equations (2.2.4)b and h then yield $J(\vec{r})$ and $\vec{A}(\vec{r})$ in terms of $\vec{U}(\vec{r})$ and $\vec{G}(\vec{r})$.

$$J(\vec{r}) = \frac{-2i}{(\mathcal{W}_8(r))} \vec{\nabla} \cdot \vec{G}(\vec{r}) \qquad (2.5.1)c$$

and

$$\vec{A}(\vec{r}) = \frac{-2}{(\mathcal{W}_2(r))} \vec{\nabla} \times \vec{U}(\vec{r}) \qquad (2.5.1)d$$

We can now choose to eliminate $\vec{U}(\vec{r})$ or $\vec{G}(\vec{r})$ in terms of the other. We will show both decompositions for completeness.

Equation (2.2.4)g yields $\vec{G}$ in terms of $\vec{U}$:

$$\vec{G}(\vec{r}) = \{\frac{\mathcal{W}_7(r) - \mathcal{X}_7(r)\tilde{\mathcal{O}}_{\times\times}}{2M}\}\vec{U}(\vec{r}) - \frac{2}{M}\vec{\nabla} \times \{\frac{1}{\mathcal{W}_2(r)}\vec{\nabla} \times \vec{U}(\vec{r})\} \qquad (2.5.2)a$$

or equation (2.2.4)d yields $\vec{U}$ in terms of $\vec{G}$:

$$\vec{U}(\vec{r}) = \{\frac{\mathcal{W}_4(r) - \mathcal{X}_4(r)\tilde{\mathcal{O}}_{\times\times}}{2M}\}\vec{G}(\vec{r}) + \frac{2}{M}\vec{\nabla}\{\frac{1}{\mathcal{W}_8(r)}\vec{\nabla} \cdot \vec{G}(\vec{r})\} \qquad (2.5.2)b$$

If we choose (2.5.2)a to eliminate $\vec{G}$, then (2.2.4)d becomes our Schrödinger-*like* equation:

$$\vec{\nabla}\{\frac{1}{\mathcal{W}_8(r)}\vec{\nabla}\cdot[(\mathcal{W}_7(r)-\mathcal{X}_7(r)\tilde{\mathcal{O}}_{\times\times})\vec{U}(\vec{r})]\}-\{(\mathcal{W}_4(r)-\mathcal{X}_4(r)\tilde{\mathcal{O}}_{\times\times})\vec{\nabla}\times[\frac{1}{\mathcal{W}_2(r)}\vec{\nabla}\times\vec{U}(\vec{r})]\}$$
$$+\quad\{\frac{1}{4}[S(r)-T(r)\tilde{\mathcal{O}}_{\times\times}]\}\vec{U}(\vec{r})=0 \qquad (2.5.3)a$$

and alternatively substituting (2.5.2)b into (2.2.4)g gives:

$$\{(\mathcal{W}_7(r)-\mathcal{X}_7(r)\tilde{\mathcal{O}}_{\times\times})\vec{\nabla}[\frac{1}{\mathcal{W}_8(r)}\vec{\nabla}\cdot\vec{G}(\vec{r})]\}-\vec{\nabla}\times\{\frac{1}{\mathcal{W}_2(r)}\vec{\nabla}\times[(\mathcal{W}_4(r)-\mathcal{X}_4(r)\tilde{\mathcal{O}}_{\times\times})\vec{G}(\vec{r})]\}$$
$$+\quad\{\frac{1}{4}[S(r)-T(r)\tilde{\mathcal{O}}_{\times\times}]\}\vec{G}(\vec{r})=0 \qquad (2.5.3)b$$

where we have introduced: $S(r)\equiv\{\mathcal{W}_4(r)\mathcal{W}_7(r)-4M^2\}$ and $T(r)\equiv\mathcal{W}_4(r)\mathcal{X}_7(r)+\mathcal{W}_7(r)\mathcal{X}_4(r)+\mathcal{X}_4(r)\mathcal{X}_7(r)$

When all interactions vanish,

$$\mathcal{W}_2(r)\to W-\frac{4\mu^2}{W}\quad,\quad \mathcal{W}_8(r)\to W-\frac{4\mu^2}{W}$$
$$\mathcal{W}_4(r)\to\quad W\qquad,\quad \mathcal{W}_7(r)\to\quad W$$

Equation (2.5.3)a reverts to the free wave equation:

$$-\nabla^2\vec{U}(\vec{r})+\{\frac{(W^2-4M^2)(W^2-4\mu^2)}{4W^2}\}\vec{U}(\vec{r})=0 \qquad (2.5.4)$$

We identify the quantity in $\{\quad\}$ with the relativistic k^2. For $W\to 2M+\mathcal{E}$ with $\mathcal{E}\ll M$ we get:

$$k^2\longrightarrow\frac{M^2-\mu^2}{M}\mathcal{E}+\mathcal{O}(\mathcal{E}^2)$$

where $\frac{(M^2-\mu^2)}{M}$ is simply $2\mathcal{M}_{red}$. Equation (2.5.4) is also the free wave equation limit of (2.5.3)b with $\vec{U}$ replaced by $\vec{G}$. With small interactions, at low energy, $\vec{G}(\vec{r})$ and $\vec{U}(\vec{r})$ which differ only linearly in the doubly-small spinor component become indistinguishable from one another.

2.6 THE GENERAL $\hat{\pi} = (-)^{(J+1)}$ BREIT RADIAL EQUATIONS

We can now proceed to decompose (2.5.3)a and b into their radial form. Acting on these expressions from the left with $\int d\Omega \vec{\mathbf{Y}}^{*m_j}_{j,\ell} \cdot [\ \vec{}\ ]$ yields nontrivial equations for the cases: $\ell = j \pm 1$ only. We then arrange the two coupled radial equations in such a way that the second derivative of a lone radial amplitude is isolated in each of them with a coefficient of 1. Equation (2.5.3)a which involves the tensorial spinor:

$$\vec{U}(\vec{r}) = u_-(r)\vec{\mathbf{Y}}_-(\Omega,\sigma) + u_+(r)\vec{\mathbf{Y}}_+(\Omega,\sigma)$$

reduces to a set of coupled equations, the first of which is:

$$\begin{aligned} & 1 \quad u''_- \quad + \quad \{\frac{2}{r} + \frac{d_1}{2} - \frac{d_2}{2\Delta} + \frac{\Delta^2-1}{\Delta r} y_2\} u'_- \\ + \{ & -\frac{(\Delta-1)(\Delta-3)}{4r^2} + \frac{\Delta^2-1}{8\Delta r^2} q_1 + \frac{\Delta^2-1}{8r^2} q_2 + \frac{\Delta b_1}{r} + \frac{b_2}{r} + \frac{b_3}{\Delta r} + c_1 - \frac{c_2}{\Delta} + (1 - \frac{1}{\Delta}) c_3 \} u_- \\ & + \quad 0 \quad u''_+ \quad + \quad \Lambda\{ -\frac{d_2}{\Delta} + \frac{y_1}{r} - \frac{2y_2}{\Delta r} \} u'_+ \\ & + \quad \Lambda\{ -\frac{2(c_2+c_3)}{\Delta} + \frac{b_4}{r} + \frac{2b_3}{\Delta r} + \frac{\Delta q_3}{r^2} + \frac{q_4}{r^2} - \frac{q_1}{4\Delta r^2} \} u_+ \quad = \quad 0 \end{aligned} \qquad (2.6.1)a$$

The second equation has the structure:

$$\begin{aligned} & 1 \quad u''_+ \quad + \quad \{\frac{2}{r} \quad + \quad \cdots \quad \} u'_+ \\ & + \quad \{ -\frac{(\Delta+1)(\Delta+3)}{4r^2} \quad + \quad \cdots \quad \} u_+ \\ & + \quad 0 \quad u''_- \quad + \quad \Lambda\{ -\frac{d_2}{\Delta} \quad + \quad \cdots \quad \} u'_- \\ & + \quad \Lambda\{ -\frac{2(c_2+c_3)}{\Delta} \quad + \quad \cdots \quad \} u_- \quad = \quad 0 \end{aligned} \qquad (2.6.1)b$$

and is fully generated from the first by making three simple interchanges: *i.)* $\Lambda \to -\Lambda$, *ii.)* $\Delta \to -\Delta$, and *iii.)* $u_\pm \to u_\mp$. The r-dependence has been suppressed above for brevity. All quantities encountered in (2.6.1)a and b

excepting Λ and Δ have a radial dependence. The notation in these radial equations is as follows: There are six dimensionless quantities defined by:

$$q_1 \equiv \left(\frac{\mathcal{W}_2(3\mathcal{W}_7 - \mathcal{X}_7)}{\mathcal{W}_8(\mathcal{W}_4 + \mathcal{X}_4)}\right) + 3\left(\frac{\mathcal{W}_4\mathcal{W}_8}{\mathcal{W}_2\mathcal{W}_7}\right) + 2\frac{\mathcal{X}_7}{\mathcal{W}_7} - 6 \qquad (2.6.2)a$$

$$q_2 \equiv 2 - \left(\frac{\mathcal{W}_2(\mathcal{W}_7 + \mathcal{X}_7)}{\mathcal{W}_8(\mathcal{W}_4 + \mathcal{X}_4)}\right) - \left(\frac{\mathcal{W}_4\mathcal{W}_8}{\mathcal{W}_2\mathcal{W}_7}\right) \qquad (2.6.2)b$$

$$q_3 \equiv \frac{1}{4}\left\{\frac{\mathcal{W}_4\mathcal{W}_8}{\mathcal{W}_2\mathcal{W}_7} - \left(\frac{\mathcal{W}_2(\mathcal{W}_7 + \mathcal{X}_7)}{\mathcal{W}_8(\mathcal{W}_4 + \mathcal{X}_4)}\right)\right\} \qquad (2.6.2)c$$

$$q_4 \equiv -\left(\frac{\mathcal{W}_2\mathcal{W}_7}{\mathcal{W}_8(\mathcal{W}_4 + \mathcal{X}_4)}\right) + \frac{1}{2}\left(\frac{\mathcal{W}_4\mathcal{W}_8}{\mathcal{W}_2\mathcal{W}_7}\right) + \frac{1}{2}\frac{\mathcal{X}_7}{\mathcal{W}_7} + \frac{1}{2} \qquad (2.6.2)d$$

$$y_1 \equiv -\frac{1}{2}\left(\frac{\mathcal{W}_2\mathcal{W}_7}{\mathcal{W}_8(\mathcal{W}_4 + \mathcal{X}_4)}\right) + \frac{1}{2}\left(\frac{\mathcal{W}_4\mathcal{W}_8}{\mathcal{W}_2\mathcal{W}_7}\right) - \frac{1}{2}\frac{\mathcal{X}_7}{\mathcal{W}_7} \qquad (2.6.2)e$$

$$y_2 \equiv \frac{1}{4}\left(\frac{\mathcal{W}_2\mathcal{W}_7}{\mathcal{W}_8(\mathcal{W}_4 + \mathcal{X}_4)}\right) + \frac{1}{4}\left(\frac{\mathcal{W}_4\mathcal{W}_8}{\mathcal{W}_2\mathcal{W}_7}\right) - \frac{1}{4}\frac{\mathcal{X}_7}{\mathcal{W}_7} - \frac{1}{2} \qquad (2.6.2)f$$

The quantities b_i and d_i have dimension length^{-1} (or equivalently energy in our natural units).

$$b_1 \equiv \frac{1}{4}\left\{\frac{\mathcal{W}_2'}{\mathcal{W}_2} - \frac{\mathcal{W}_7' + \mathcal{X}_7'}{\mathcal{W}_7} + \frac{\mathcal{W}_7'\mathcal{W}_2}{\mathcal{W}_8(\mathcal{W}_4 + \mathcal{X}_4)} + \frac{(\mathcal{W}_7 + \mathcal{X}_7)\mathcal{W}_8'}{\mathcal{W}_7\mathcal{W}_8}\right\} \qquad (2.6.2)g$$

$$b_2 \equiv -\frac{1}{2}\frac{\mathcal{W}_2'}{\mathcal{W}_2} + \frac{\mathcal{W}_7'}{\mathcal{W}_7} - \frac{\mathcal{W}_8'}{\mathcal{W}_8} \qquad (2.6.2)h$$

$$b_3 \equiv \frac{3}{4}\left\{-\frac{\mathcal{W}_2'}{\mathcal{W}_2} - \frac{\mathcal{W}_7'}{\mathcal{W}_7} + \frac{\mathcal{W}_8'}{\mathcal{W}_8}\right\} + \frac{1}{4}\left\{\frac{\mathcal{X}_7'}{\mathcal{W}_7} - \frac{\mathcal{W}'\mathcal{X}_7}{\mathcal{W}_7\mathcal{W}_8} - \frac{\mathcal{W}_7'\mathcal{W}_2}{\mathcal{W}_8(\mathcal{W}_4 + \mathcal{X}_4)}\right\} \qquad (2.6.2)i$$

$$b_4 \equiv \frac{1}{2}\left\{-\frac{\mathcal{W}_2'}{\mathcal{W}_2} - \frac{\mathcal{W}_7' + \mathcal{X}_7'}{\mathcal{W}_7} + \frac{\mathcal{W}_8'}{\mathcal{W}_8} - \frac{\mathcal{W}_7'\mathcal{W}_2}{\mathcal{W}_8(\mathcal{W}_4 + \mathcal{X}_4)} + \frac{\mathcal{X}_7\mathcal{W}_8'}{\mathcal{W}_7\mathcal{W}_8}\right\} \qquad (2.6.2)j$$

$$d_{\frac{1}{2}} \equiv 2\frac{\mathcal{W}_7'}{\mathcal{W}_7} - \frac{\mathcal{W}_8'}{\mathcal{W}_8} \mp \frac{\mathcal{W}_2'}{\mathcal{W}_2} \qquad (2.6.2)k$$

The quantities c_i have dimension length^{-2} and are defined by:

$$c_{\frac{1}{2}} \equiv \frac{S}{8}\left(\frac{\mathcal{W}_8}{\mathcal{W}_7} \pm \frac{\mathcal{W}_2}{(\mathcal{W}_4 + \mathcal{X}_4)}\right) \pm \frac{T}{8}\frac{\mathcal{W}_2}{(\mathcal{W}_4 + \mathcal{X}_4)} \qquad (2.6.2)l$$

$$c_3 \equiv \frac{1}{2}\left(\frac{\mathcal{W}_7''}{\mathcal{W}_7} - \frac{\mathcal{W}_7'}{\mathcal{W}_7}\frac{\mathcal{W}_8'}{\mathcal{W}_8}\right) \qquad (2.6.2)m$$

In the later chapters dealing with the deuteron and $^3S_1$ -scattering problem, equations (2.6.1)a and b completely determine the dynamics and will

be utilized for the numerical work associated with the exact Breit equation solution. The equations associated with $\vec{G}(\vec{r}) = g_-(r)\vec{\mathbf{Y}}_-(\Omega.\sigma) + g_+(r)\vec{\mathbf{Y}}_+(\Omega,\sigma)$ are therefore redundant for this purpose. However they, together with (2.6.1)*a* and *b*, can offer insight into the *pure* large spinor component radial equations. It is the large component: $\vec{\mathcal{L}} = \{\vec{G} + \vec{U}\}/\sqrt{2} = \ell_-(r)\vec{\mathbf{Y}}_-(\Omega,\sigma) + \ell_+(r)\vec{\mathbf{Y}}_+(\Omega,\sigma)$, and its associated radial amplitudes which are relevant in the phase-shift analysis. Each of $\vec{G}$ and $\vec{U}$ contains a doubly small spinor component contribution which asymptotically is proportional to $(\vec{\sigma}_1 \cdot \vec{\mathrm{k}})(\vec{\sigma}_2 \cdot \vec{\mathrm{k}})\vec{\mathcal{L}}$. Thus, part of the $\ell = j - 1(j+1)$-wave radial amplitude associated with *e.g.* $g_-(g_+)$ is a *kinematic* piece associated with the pure large radial component $\ell_+(\ell_-)$.

We get expressions quite similar to (2.6.1)*a* and *b*:

$$
\begin{aligned}
& 1 \quad g_-'' \quad + \quad \{\frac{2}{r} + \frac{e_1}{2} - \frac{e_2}{2\Delta} + \frac{\Delta^2 - 1}{\Delta r} z_2\} g_-' \\
+ \{ & - \frac{(\Delta-1)(\Delta-3)}{4r^2} + \frac{\Delta^2-1}{8\Delta r^2} p_1 + \frac{\Delta^2-1}{8r^2} p_2 + \frac{\Delta h_1}{r} + \frac{h_2}{r} + \frac{h_3}{\Delta r} + n_1 + \frac{n_2}{\Delta} + (1 + \frac{1}{\Delta}) n_3 \} g_- \\
& + \quad 0 \quad g_+'' \quad + \quad \Lambda\{ - \frac{e_2}{\Delta} + \frac{z_1}{r} - \frac{2z_2}{\Delta r}\} g_+' \\
& + \quad \Lambda\{\frac{2(n_2+n_3)}{\Delta} + \frac{h_4}{r} + \frac{2h_3}{\Delta r} + \frac{\Delta p_3}{r^2} + \frac{p_4}{r^2} - \frac{p_1}{4\Delta r^2}\} g_+ \quad = \quad 0 \qquad (2.6.3)a
\end{aligned}
$$

and

$$
\begin{aligned}
& 1 \quad g_+'' \quad + \quad \{\frac{2}{r} \quad + \quad \cdots \quad \} g_+' \\
& + \quad \{ - \frac{(\Delta+1)(\Delta+3)}{4r^2} \quad + \quad \cdots \quad \} g_+ \\
& + \quad 0 \quad g_-'' \quad + \quad \Lambda\{ - \frac{e_2}{\Delta} \quad + \quad \cdots \quad \} g_-' \\
& + \quad \Lambda\{\frac{2(n_2+n_3)}{\Delta} \quad + \quad \cdots \quad \} g_- \quad = \quad 0 \qquad (2.6.3)b
\end{aligned}
$$

Once again, (2.6.3)*b* is fully generated from (2.6.3)*a* by interchanging g_- and g_+ amplitudes, (and their derivatives) and negating both Λ and Δ. The six

dimensionless dynamical quantities here are:

$$p_1 \equiv 3\left(\frac{W_2(W_7+\mathcal{X}_7)}{W_8(W_4+\mathcal{X}_4)}\right)+3\left(\frac{W_4W_8}{W_2W_7}\right)+2\frac{\mathcal{X}_4W_8}{W_2W_7}-6 \qquad (2.6.4)a$$

$$p_2 \equiv 2-\left(\frac{W_2(W_7+\mathcal{X}_7)}{W_8(W_4+\mathcal{X}_4)}\right)-\left(\frac{W_4W_8}{W_2W_7}\right) \qquad (=q_2) \qquad (2.6.4)b$$

$$p_3 \equiv \frac{1}{4}\left\{\frac{W_4W_8}{W_2W_7}-\left(\frac{W_2(W_7+\mathcal{X}_7)}{W_8(W_4+\mathcal{X}_4)}\right)\right\} \qquad (=q_3) \qquad (2.6.4)c$$

$$p_4 \equiv -\left(\frac{W_2(W_7+\mathcal{X}_7)}{W_8(W_4+\mathcal{X}_4)}\right)+\frac{1}{2}\left(\frac{(W_4+\mathcal{X}_4)W_8}{W_2W_7}\right)+\frac{1}{2} \qquad (2.6.4)d$$

$$z_1 \equiv -\frac{1}{2}\left(\frac{W_2(W_7+\mathcal{X}_7)}{W_8(W_4+\mathcal{X}_4)}\right)+\frac{1}{2}\left(\frac{(W_4+\mathcal{X}_4)W_8}{W_2W_7}\right)-\frac{1}{2}\frac{\mathcal{X}_4}{W_4+\mathcal{X}_4} \qquad (2.6.4)e$$

$$z_2 \equiv \frac{1}{4}\left(\frac{W_2(W_7+\mathcal{X}_7)}{W_8(W_4+\mathcal{X}_4)}\right)+\frac{1}{4}\left(\frac{(W_4+\mathcal{X}_4)W_8}{W_2W_7}\right)+\frac{1}{4}\frac{\mathcal{X}_4}{W_4+\mathcal{X}_4}-\frac{1}{2} \qquad (2.6.4)f$$

The quantities e_i and h_i (with dimension length^{-1}) have the form:

$$h_1 \equiv \frac{1}{4}\left\{\frac{W_2'W_4}{W_2(W_4+\mathcal{X}_4)}+\frac{(W_4'+\mathcal{X}_4')W_8}{W_2W_7}-\frac{W_4'}{W_4+\mathcal{X}_4}+\frac{W_8'}{W_8}\right\} \qquad (2.6.4)g$$

$$h_2 \equiv -\frac{1}{2}\left\{\frac{W_2'}{W_2}\right\}+\frac{W_4'+\mathcal{X}_4'}{W_4+\mathcal{X}_4}-\frac{W_8'}{W_8} \qquad (2.6.4)h$$

$$h_3 \equiv \frac{1}{4}\left\{-2\frac{W_2'}{W_2}-\frac{W_2'W_4}{W_2(W_4+\mathcal{X}_4)}-\frac{(W_4'+\mathcal{X}_4')W_8}{W_2W_7}+4\frac{W_4'+\mathcal{X}_4'}{W_4+\mathcal{X}_4}+\frac{W_4'}{W_4+\mathcal{X}_4}+3\frac{W_8'}{W_8}\right\} \qquad (2.6.4)i$$

$$h_4 \equiv \frac{1}{2}\left\{-\frac{W_2'W_4}{W_2(W_4+\mathcal{X}_4)}+\frac{(W_4'+\mathcal{X}_4')W_8}{W_2W_7}+\frac{W_4'}{W_4+\mathcal{X}_4}+\frac{W_8'}{W_8}\right\} \qquad (2.6.4)j$$

$$e_{\frac{1}{2}} \equiv \pm 2\frac{W_4'+\mathcal{X}_4'}{W_4+\mathcal{X}_4}\mp\frac{W_2'}{W_2}-\frac{W_8'}{W_8} \qquad (2.6.4)k$$

Quantities of dimension length^{-2} encountered are:

$$n_{\frac{1}{2}} \equiv \pm\frac{S}{8}\left(\frac{W_8}{W_7}\pm\frac{W_2}{(W_4+\mathcal{X}_4)}\right)+\frac{T}{8}\frac{W_2}{(W_4+\mathcal{X}_4)} \qquad (=\pm c_{\frac{1}{2}}) \qquad (2.6.4)l$$

$$n_3 \equiv \frac{1}{2}\left\{\frac{W_4''+\mathcal{X}_4''}{W_4+\mathcal{X}_4}-\frac{W_2'}{W_2}\left(\frac{W_4'+\mathcal{X}_4'}{W_4+\mathcal{X}_4}\right)\right\} \qquad (2.6.4)m$$

For the sake of the numerical solution of (2.6.1)a and b we perform the usual trick of taking an auxiliary set of radial amplitudes:

$$v_{\mp}(r) \equiv r u_{\mp}(r) \qquad (2.6.5)$$

which both vanish at the origin in the case of a regular (physical) solution. This then allows (2.6.1)a,b to be recast as:

$$\begin{aligned}
&1 \quad v_-'' \quad + \quad \{\frac{d_1}{2} - \frac{d_2}{2\Delta} + \frac{\Delta^2-1}{\Delta r} y_2\} v_-' \\
&+ \{ - \frac{(\Delta-1)(\Delta-3)}{4r^2} + \frac{\Delta^2-1}{\Delta r^2}(\frac{q_1}{8} - y_2) + \frac{\Delta^2-1}{8r^2} q_2 + \frac{\Delta b_1}{r} + \frac{2b_2-d_1}{2r} + \frac{2b_3+d_2}{2\Delta r} + (c_1+c_3) - \frac{(c_2+c_3)}{\Delta} \} v_- \\
&+ \quad 0 \quad v_+'' \quad + \quad \Lambda\{ - \frac{d_2}{\Delta} + \frac{y_1}{r} - 2\frac{y_2}{\Delta r} \} v_+' \\
&+ \quad \Lambda\{ - \frac{2(c_2+c_3)}{\Delta} + \frac{b_4}{r} + \frac{(2b_3+d_2)}{\Delta r} + \frac{\Delta q_3}{r} + \frac{(q_4-y_1)}{r^2} + \frac{-q_1+8y_2}{4\Delta r^2} \} v_+ \\
&= \quad 0 \qquad (2.6.6)a
\end{aligned}$$

and

$$\begin{aligned}
&1 \quad v_+'' \quad + \quad \{\frac{d_1}{2} \quad + \quad \cdots \quad \} v_+' \\
&+ \quad \{ - \frac{(\Delta+1)(\Delta+3)}{4r^2} \quad + \quad \cdots \quad \} v_+ \\
&+ \quad 0 \quad v_-'' \quad + \quad \Lambda\{ - \frac{d_2}{\Delta} \quad + \quad \cdots \quad \} v_-' \\
&+ \quad \Lambda\{ - \frac{2(c_2+c_3)}{\Delta} \quad + \quad \cdots \quad \} v_- \quad = \quad 0 \qquad (2.6.6)b
\end{aligned}$$

Equations (2.6.6)a and b are in the form in which they are encoded in the FORTRAN code brtrip.f and all related routines which are used in the $(^3S_1)$-$(^3D_1)$ nucleon-nucleon scattering and deuteron related calculations of chapters 8 and 9 respectively.

2.7 MATRIX ELEMENTS

The focus of this chapter up to now was on the systematic casting of the Breit equation into forms which bear much similarity to the Schrödinger equation in its 3-dimensional (and 3-dimensional-radial) forms. This enables us to take advantage of existing algorithms to obtain solutions to the Breit equation . The only apparent complication is that we must maintain a more

sophisticated definition of the matrix elements which in the tensorial basis is:

$$\langle\Phi|\hat{\mathcal{O}}|\Psi\rangle \equiv$$

$$\begin{bmatrix} I^* & A^{0*} & \vec{A}^* & U^{0*} & \vec{U}^* & \vec{F}^* & \vec{G}^* & J^* \end{bmatrix} \begin{bmatrix} \hat{\mathcal{O}}_{II} & \hat{\mathcal{O}}_{IA^0} & \cdots & & \cdots & \hat{\mathcal{O}}_{IJ} \\ \hat{\mathcal{O}}_{A^0I} & \hat{\mathcal{O}}_{A^0A^0} & \cdots & & & \hat{\mathcal{O}}_{A^0J} \\ \vdots & & \ddots & & & \\ & & & & & \\ & & & & & \\ \vdots & & & & \ddots & \\ \hat{\mathcal{O}}_{JI} & & & & & \hat{\mathcal{O}}_{JJ} \end{bmatrix} \begin{bmatrix} I \\ A^0 \\ \vec{A} \\ U^0 \\ \vec{U} \\ \vec{F} \\ \vec{G} \\ J \end{bmatrix}$$

(2.7.1)

$\hat{\mathcal{O}}$ necessarily leaves rotational scalars and vectors unmixed. This matrix element involves rotational scalars in the form: $(I_\Phi|\hat{\mathcal{O}}_{\alpha\beta}|A^0_\Psi)$ and rotational vectors in the form: $(\vec{A}_\Phi \cdot |\hat{\mathcal{O}}_{\gamma\delta}|\vec{F}_\Psi)$. With this, we are finished with the preliminary mathematical details associated with the 3-dimensional Breit equation 's decomposition. In the next chapters we will turn to the interesting physics which it contains.

Chapter 3

Nonrelativistic charge symmetry breaking of relativistic origin

3.1 SPECIFICS OF THE MODEL USED FOR THE CHARGE-ASYMMETRY PROBLEM

In the last chapter, the formalism for the Breit equation was developed. The variety of interaction types included in the development of the various systems of equations encompassed the physical models of this and all following chapters. Any one of the models, taken alone, obeys a much simpler dynamics than the apparent complexity of the last chapter would indicate.

In the following section, which is a reprint of a paper appearing in the Journal of Physics G: Nuclear and Particle Physics, we examine the troublesome problem of the asymmetry between the $^1S_0$ nucleon-nucleon scattering lengths of the $n-n$ and $p-p$ systems (with isospin: 1). The two systems have very different dynamics due to the obvious Coulomb repulsion in the $p-p$ system, but the nuclear component of the dynamics is believed to be largely

the same. The extent to which it may not be is a subject of some debate. For a broad discussion. see Henley in reference [52] for example.

Chronologically. the general algebra of the preceeding chapter was done after this work on the Breit singlet state. The change of notation between the last chapter and the published paper of the next section was mainly to enable the model's simplicity to carry over into the notation of a stand-alone paper. It is necessary, therefore, to provide some transitional commentary to relate the two.

We consider a Breit equation Hamiltonian (2.1.2), in which the nuclear portion is comprised of a large attractive scalar interaction $S(r)$, a large repulsive vector interaction $V(r)$, both of which are taken to be Gaussian. and an axial version of the one-pion-exchange-potential (OPEP) $A(r) = -\frac{1}{3}V_\pi(r)$. This $V_\pi(r)$ is chosen such that it is regularized at the origin and reproduces the *singlet state* OPEP tail asymptotically.

Two descriptions of the electromagnetic interaction are to be employed. In the first instance, (form I), a purely electrostatic interaction between the two particles is present, $U_{Co}(r) = V_C(r)$ where $V_C(r)$ asymptotically is the Coulomb interaction. $U_{Co}(r)$ fulfills this role alone. In the second case, (form II), we wish to treat the magnetic part of the interaction a little less lightly. We want the electromagnetic part of the Hamiltonian to be: $V_{EM}(r) = \{1 - \frac{1}{2}[\alpha_1 \cdot \alpha_2 + \frac{(\alpha_1 \cdot \mathbf{r})(\alpha_2 \cdot \mathbf{r})}{r^2}]\}V_C(r)$ This Hamiltonian does not include Pauli-type interactions coupling to the anomalous magnetic moments so it

is still a simplified model. This combination can be generated by the assignments:

$$V_{Co}(r) \longrightarrow +\frac{1}{2}V_C(r)$$

$$V(r) \longrightarrow V_{Nuclear} + \frac{1}{2}V_C(r)$$

$$V_{Br}(r) \longrightarrow -\frac{1}{2}V_C(r)$$

The nonrelativistic reduction of equation (2.1.2) *in the singlet case* is of course: $S(r) + V(r) + V_\pi(r) + V_{Co}(r)$ for either of the two electromagnetic prescriptions applied between the two protons.

3.2

J Phys. G: Nucl. Part. Phys. 18 (1992) 1039–1049. Printed in the UK

Charge asymmetry in non-relativistic nucleon–nucleon potential derived from charge symmetric relativistic interaction

D J Beachey†, Y Nogami† and F M Toyama‡

† Department of Physics and Astronomy, McMaster University, Hamilton, Ontario, Canada L8S 4M1

‡ Institute of Computer Sciences, Kyoto Sangyo University, Kyoto 603, Japan

Received 20 May 1991, in final form 27 November 1991

Abstract. Consider a relativistic model of the nucleon–nucleon (NN) system subject to an interaction which is a sum of a charge symmetric NN interaction and the Coulomb potential. When the model is rewritten in the form of a non-relativistic model, the resulting effective non-relativistic potential obtains a charge-symmetry-breaking (CSB) component. We illustrate this by means of the Breit equation. If the relativistic NN interaction contains a combination of a strongly attractive Lorentz scalar and a strongly repulsive vector, the non-relativistic potential obtains a large CSB component. When the magnetic interaction is included, however, the CSB effect may be reduced. This and other aspects, in which relativistic and non-relativistic models may exhibit significant differences, are discussed.

1. Introduction

It is believed that the nuclear interaction itself is charge independent (and charge symmetric), and electromagnetic effects are responsible for any observed charge dependence. A sensitive test of charge dependence of the nucleon–nucleon (NN) interaction is provided by measurements of the low-energy scattering parameters in the ^{1}S state, in particular the scattering lengths. In this paper, we focus on charge symmetry and compare the scattering length for proton–proton (pp) with that for neutron–neutron (nn).

Let us quote relevant experimental data and the analysis of the ^{1}S scattering lengths. The experimental value of the nn scattering length a_{nn}, determined from the reaction $\pi^-\mathrm{d}\rightarrow\gamma$nn, is [1]

$$a_{nn} = -18.5 \pm 0.4\ \mathrm{fm}. \tag{1.1}$$

The a_{nn} has also been extracted from the reactions nd→nnp, dt→nn ^{3}He, tt→nn ^{4}He, and n ^{9}Be→nn ^{8}Be. These data lead to a value of a_{nn} about 2 fm smaller in magnitude than that of (1.1) [2]. For example, $a_{nn} = -16.5 \pm 1.0$ fm has been deduced from n ^{9}Be→n ^{8}Be by Bodek *et al.* [3]. The discrepancy between the value based on $\pi^-\mathrm{d}\rightarrow\gamma$nn and those based on nd→nnp, etc, has been a subject of controversy. However, we take the value of a_{nn} of (1.1) rather than that of [3]. Slaus *et al* argue that the discrepancy is due to certain three-body forces acting in the final

0954-3899/92/061039 + 11 $04.50

states of nd→nnp, etc, and recommend $a_{nn} = -18.5 \pm 0.3$ fm; see section 6 of [2]. There is another reason for choosing (1.1); this is concerned with the Coulomb energy of ^{3}He as stated at the end of the next paragraph.

For the pp system, we have to distinguish the 'nuclear' scattering length and the 'Coulomb-corrected' or 'non-Coulombic' scattering length [4]. Let us denote the former by a'_{pp} and the latter by a_{pp}. The a'_{pp} is the pp scattering length due to the nuclear interaction in the presence of the Coulomb potential e^2/r. The a_{pp} is the scattering length in the absence of the Coulomb potential. The experimental value is $a'_{pp} = -7.823 \pm 0.011$ fm; see, e.g. [5]. The a_{pp} cannot be measured directly; rather it is estimated as follows. Assume a 'non-Coulombic potential' for pp, V_{NC}. Solve the Schrödinger equation for pp scattering with the (total) potential $V_{NC} + e^2/r$. Adjust V_{NC} such that the experimental phaseshift, in particular $a'_{pp} = -7.823$ fm, is fitted. Then, switch off the Coulomb potential, i.e., use V_{NC} alone, and solve the Schrödinger equation again to determine the scattering length; this is a_{pp}. A widely accepted value of a_{pp} is [6, 7]

$$a_{pp} = -17.1 \pm 0.2 \text{ fm}. \tag{1.2}$$

Actually the above value of a_{pp} was obtained by removing the effects of e^2/r and vacuum polarization. For the degree of accuracy which we are concerned with in this paper, the vacuum polarization effect is unimportant. Combining (1.1) and (1.2), we obtain

$$\Delta a \equiv a_{pp} - a_{nn} = 1.4 \pm 0.6 \text{ fm}. \tag{1.3}$$

If the point Coulomb potential e^2/r were the only difference between the potentials for pp and nn, then one would find that V_{NC} of pp is equal to V_{nn} and hence $a_{pp} = a_{nn}$. Here V_{nn} is the nn potential. The Δa of (1.3) implies that V_{NC} is less attractive than V_{nn}; charge symmetry is broken. This feature is consistent with the results of the binding energy calculations of the mirror nuclei ^{3}H and ^{3}He. The calculated Coulomb energy of ^{3}He is about 10% smaller than the empirical mass difference between ^{3}He and ^{3}H. This discrepancy can be removed by assuming a charge-symmetry-breaking (CSB) component in the NN interaction which is consistent with (1.3) [7, 8].

Various CSB effects, which are responsible for $V_{NC} \neq V_{nn}$, have been examined so far. They can be classified into two types: direct and indirect [4]. The direct effects include those of the vacuum polarization, the magnetic interaction and the finite size of the nucleon. These are characterized by no meson exchange between nucleons. The indirect effects include any process in which the electromagnetic interaction modifies the nuclear force. Those considered so far include the ρ–ω mixing and the γ–π exchange.

The main purpose of this paper is to examine yet another type of the CSB effect which seems to have escaped attention so far. This effect emerges when a relativistic model is rewritten in the form of an effective non-relativistic model. Recall that the analysis of the ^{1}S scattering lengths in relation to charge symmetry has been done always within the framework of non-relativistic quantum mechanics using the Schrödinger equation. As noted above, in determining a_{pp} which can be compared with a_{nn}, the Coulomb effect in pp has been removed by using the non-relativistic Schrödinger equation. We emphasize this point because the definition of 'CSB' does depend on the framework in which one chooses to work. Throughout this paper, we are interested in CSB effects which appear in the non-relativistic framework.

One usually expects that relativistic effects are negligible in low energy quantities; the scattering length is the scattering amplitude for zero kinetic energy. When the relativistic interaction contains a combination of a strongly attractive Lorentz scalar S and a strongly repulsive vector V, however, relativistic effects can be appreciable even at very low energies [9]. For the model of the relativistic NN system, let us consider the Breit equation (two-body Dirac equation) with an instantaneous potential; there are many references regarding the Breit equation which can be traced through [10, 11]. We are aware of some shortcomings of the Breit equation, but the equation will serve the purpose of illustrating some remarkable differences that can arise between relativistic and non-relativistic approaches. For the interaction we assume that it is a sum of charge-symmetric nuclear part and an electromagnetic (EM) potential V_{EM}. The V_{EM} acts only in the pp system. For the nuclear part, which we call the NN interaction, we assume that it contains a combination of S and V as we mentioned above. For V_{EM} we consider two forms. One is just the Coulomb potential V_C, while the other consists of V_C and the so called Breit potential which takes care of the magnetic interaction. The Breit equation can be reduced to a Schrödinger-like equation without any approximation. The interaction W that emerges in the latter equation then exhibits a CSB effect. This is in the sense that $W_{pp} - V_{EM} \neq W_{nn}$ where W_{pp} and W_{nn} are the W for pp and nn, respectively. This CSB effect can be significant if the S and V of the NN interaction are very strong as we assume. A similar aspect of the nucleon in a relativistic shell model has been discussed recently [12].

Besides the novel CSB effect outlined above, the effect due to the finite size of the proton (one of the direct effects) becomes more important in our relativistic model. The proton of radius $\simeq 0.9$ fm can hardly be considered as a point. When this finite size is taken into account, the pp Coulomb potential is suppressed as compared with e^2/r. On the other hand, the effective potential W of our model is much softer than the NN potentials in the conventional non-relativistic models. Thus the nucleons can approach each other more easily. As a consequence the finite-size effect is enhanced.

In section 2, we set up a model of the relativistic interaction (for the Breit equation). Then we reduce the Breit equation for the ^1S state to a Schrödinger-like equation. In section 3, we examine the CSB effect on the scattering lengths. The results are discussed in section 4.

2. Model

We start with the Breit equation

$$[(\boldsymbol{\alpha}_1 - \boldsymbol{\alpha}_2)\cdot\boldsymbol{p} + (\beta_1 + \beta_2)m + U]\psi = E\psi \tag{2.1}$$

where suffixes 1 and 2 refer to the two nucleons. The units are such that $c = \hbar = 1$, and $m = 939$ MeV is the nucleon mass. We have taken the centre-of-mass system; $\boldsymbol{p} = \boldsymbol{p}_1 - \boldsymbol{p}_2$ is the relative momentum. The potential U consists of nuclear and Coulomb parts. The nuclear part consists of Lorentz scalar $S(r)$, vector $V(r)$, and pseudovector $V_\pi(r)$;

$$U = \beta_1\beta_2 S(r) + (1 - \boldsymbol{\alpha}_1\cdot\boldsymbol{\alpha}_2)V(r) - \tfrac{1}{3}(\boldsymbol{\sigma}_1\cdot\boldsymbol{\sigma}_2 - \Gamma_1\Gamma_2)V_\pi(r) + V_{EM}(r) \tag{2.2}$$

where $r = |\boldsymbol{r}_1 - \boldsymbol{r}_2|$, $\Gamma = -i\alpha_x\alpha_y\alpha_z$ [10].

For $V_\pi(r)$, we take the following cut-off Yukawa potential,

$$V_\pi(r) = -g^2[\exp(-\mu r) - \exp(-\Lambda_\pi r)]/r, \tag{2.3}$$

where $g^2 = 0.08$ is the usual pion–nucleon coupling constant and $\mu = 135$ MeV is the mass of the neutral pion π^0. For the cut-off parameter Λ_π, we try $\Lambda_\pi = m/2$. This cut-off is *ad hoc*, but we need some cut-off so that $V_\pi(r)$ does not become too strong at short distances. Otherwise the effective non-relativistic potential W that we obtain later may develop an unwelcome singularity (not in the ^{1}S state but in some other states). We also tried $\Lambda_\pi = m$, but without any significant difference in the final results. We will set up U, in the spirit of phenomenology, such that the empirical ^{1}S phaseshift is well fitted. When we change the value for any of the parameters involved in U, it is of course understood that other parameters are readjusted such that the phaseshift fit is restored. In any case the short-range part of the one-pion-exchange potential (OPEP) is not known. We take the attitude that, apart from the long-range part of the OPEP which is represented by $V_\pi(r)$ of (2.3), we determine the NN interaction U phenomenologically. For the rest of the interaction, $S(r)$ and $V(r)$, we assume the Gaussian form;

$$S(r) = -g_s \exp[-(r/a_s)^2] \tag{2.4}$$

$$V(r) = g_v \exp[-(r/a_v)^2]. \tag{2.5}$$

We have also tried a cut-off Yukawa form for $S(r)$ and $V(r)$, but again with no essential difference in the final results. We prefer the Gaussian form rather than the cut-off Yukawa form. This is because we found that, although the two forms yield equally good phaseshift fits, the former requires fewer parameters. This aspect is related to a complication with $S(r)$ and $V(r)$ of the cut-off Yukawa form, which we will explain towards the end of this section. We will determine the parameters in S and V in section 3.

For potential $V_{EM}(r)$ of (2.2), we consider two forms:

$$V_{EM}(r) = \begin{cases} V_C(r) \\ \{1 - \frac{1}{2}[\boldsymbol{\alpha}_1 \cdot \boldsymbol{\alpha}_2 + (\boldsymbol{\alpha}_1 \cdot \mathbf{r})(\boldsymbol{\alpha}_2 \cdot \mathbf{r})/r^2]\} V_C(r) \end{cases} \tag{2.6}$$

We refer to the above two as forms I and II, respectively. For point protons, $V_C(r)$ is of course e^2/r. However, we take the $V_C(r)$ for finite-size protons, given in the next paragraph. The V_{EM} of form II can be derived from the one-photon-exchange process in a certain approximation [11]. The reason why it contains the $\boldsymbol{\alpha}$ of that particular form rather than $(1 - \boldsymbol{\alpha}_1 \cdot \boldsymbol{\alpha}_2)$ can be traced to the transverse nature of the photon. The part that contains the $\boldsymbol{\alpha}$ is often called the Breit potential in the literature. This part represents the magnetic interaction associated with the (normal) magnetic moment of the proton. The anomalous magnetic moment is not included here.

For $V_C(r)$ we take

$$V_C(r) = (2\pi^2)^{-1} e^2 \int \mathrm{d}\mathbf{q} F^2(q^2) \mathrm{e}^{\mathrm{i}\mathbf{q}\cdot\mathbf{r}}/q^2 \tag{2.7}$$

where $F(q^2)$ is an appropriate form factor which takes account of the finite size of the proton. This $V_C(r)$ is more realistic than e^2/r, but there is another reason for taking this instead of e^2/r which we will explain at the end of this section. For $F(q^2)$

let us assume the standard dipole form (see, e.g. [13]),

$$F(q^2) = 1/[1 + (q/\Lambda)^2]^2 \qquad \Lambda^2 = 0.71\ \mathrm{GeV}^2. \tag{2.8}$$

Then $V_C(r)$ becomes

$$V_C(r) = \frac{e^2}{r}\left[(1 - e^{-s}) - \frac{se^{-s}}{16}\left(11 + 3s + \frac{s^2}{3}\right)\right] \tag{2.9}$$

where $s = \Lambda r$.

Having decided about the form of the interaction, we now reduce (2.1) to a Schrödinger-like equation. The two-body wavefunction ψ of (2.1) has 16 components. According to Moseley and Rosen [10], however, the components that are relevant to the ^{1}S state are the following:

$$I = f_1(r) \qquad A_4 = f_2(r) \qquad F = f_3(r)r/r. \tag{2.10}$$

The interaction U is diagonal with respect to the above components, and (2.1) can be reduced to

$$(E - U_1)f_1 + 2i\left(r\frac{d}{dr} + 3\right)\frac{f_3}{r} + 2mf_2 = 0 \tag{2.11}$$

$$(E - U_2)f_2 + 2mf_1 = 0 \tag{2.12}$$

$$(E - U_3)f_3 + 2i\frac{df_1}{dr} = 0. \tag{2.13}$$

The U_i are given by

$$U_1 = S + 4V + \tfrac{4}{3}V_\pi + \binom{1}{3}V_C \tag{2.14}$$

$$U_2 = S - 2V + \tfrac{2}{3}V_\pi + \binom{1}{-1}V_C \tag{2.15}$$

$$U_3 = -S + \binom{1}{1}V_C \tag{2.16}$$

where the upper and lower elements of the column matrices correspond to forms I and II of (2.6), respectively. It is understood that $V_C = 0$ for nn.

It is straightforward to eliminate f_2 and f_3 in favour of f_1. If we define $u(r)$ by

$$u(r) = (E - U_3)^{-1/2}rf_1 \tag{2.17}$$

we arrive at

$$-\frac{1}{m}\frac{d^2u}{dr^2} + Wu = \frac{E^2 - 4m^2}{4m}u \tag{2.18}$$

where E is the relativistic energy including the rest mass 2m. The effective potential W is defined by

$$W = \frac{E - U_3}{4m}\left(U_1 - E + \frac{4m^2}{E - U_2}\right) + \frac{1}{m(E - U_3)}\left(\frac{U_3'}{r} + \frac{U_3''}{2}\right) + \frac{3U_3'^2}{4m(E - U_3)^2} + \frac{E^2 - 4m^2}{4m} \tag{2.19}$$

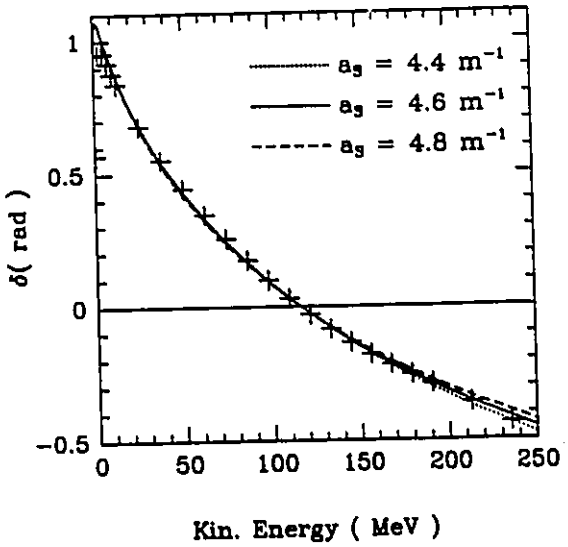

Figure 1. The ^{1}S phaseshift in degrees versus the centre of mass energy in MeV, for three sets of values of the parameters ($a_s = 4.4/m$, $4.6/m$, and $4.8/m$, with a_t kept constant at $3.0/m$) listed in table 1. They all go through zero at $E = 2.123m$ (centre-of-mass kinetic energy of 116 MeV). The crosses are for the empirical phaseshift.

where $U_3' = dU_3/dr$ and $U_3'' = d^2U_3/dr^2$. Note that W is a function of r and E. If the U were much smaller in magnitude than m and if $E \simeq m$, then W would approximately be given by

$$W \simeq (U_1 + U_2)/2 = S + V + V_\pi + V_C. \tag{2.20}$$

Let us add that we could have taken the pseudoscalar interaction for V_π in (2.2). We opted for the pseudovector interaction because we found its non-relativistic reduction more straightforward.

At this point let us explain the complication with the S and V of the cut-off Yukawa form which we mentioned after equation (2.5). If we adopt the cut-off Yukawa form like (2.3) for $S(r)$ and $V(r)$, $S'(r)$ and $V'(r)$ become non-zero at $r = 0$. Then, because of the term with U_3'/r, W of (2.19) behaves like $1/r$ around the origin. We found that such S and V do not fit the phaseshift very well. By further regularizing the potential we were able to obtain a fit as good as that obtained with the Gaussian form. Obviously such a regularized potential needs more parameters than those for the Gaussian form. We find it quite remarkable that the simple Gaussian form that we have chosen works so well (as shown in figure 1). The V_π of (2.3) does not lead to such a problem, because U_3 does not contain V_π.

If we were working entirely in the usual non-relativistic way, the W for pp and nn, W_{pp} and W_{nn}, would simply be related by $W_{pp} = W_{nn} + V_C$. This is not the case for W of (2.19), which is not linear with respect to V_C. In order to have a feel for this, let us expand W for $E \simeq 2m$ in powers of U/m. Then we find

$$W_{pp} \simeq W_{nn} + V_C\left[1 + \frac{1}{2m}\begin{pmatrix} S - 3V - \frac{1}{3}V_\pi \\ -S + V + \frac{5}{3}V_\pi \end{pmatrix}\right] \tag{2.21}$$

where we have ignored terms with the derivatives of the U. The presence of the Coulomb–nuclear interference term is evident in (2.21). Since $S<0$, $V>0$ and V_π is much weaker than S and V, the interference term for form I is negative (attractive), and counteracts the repulsive Coulomb potential. This is similar to what was found for the one-body Dirac equation [12]. For form II, the Coulomb–nuclear interference term is positive. We should add that the expansion in powers of U/m is useful only for $r \gtrsim 1$ fm. We do not use this expansion in the actual calculations.

If we use e^2/r in place of V_C in W_{pp} of (2.19), the denominators $E-U_2$ and $E-U_3$ vanish at (very small) values of r, resulting in a singular behaviour of W_{pp}. This does not happen with V_C of (2.9). A similar situation will be encountered (in a state in which the V_π becomes repulsive) if we do not introduce a cut-off in V_π.

3. CSB effect on the singlet scattering length

We first determine the parameters in our model potential. We have already decided about V_C and V_π. For S and V, we assume certain values for the ranges a_s and a_v, and determine the strength parameters g_s and g_v such that $a_{nn}=-18.5$ fm and the ^{1}S nn phaseshift vanishes at $E=2.123\,m$, i.e., for the centre-of-mass kinetic energy of $0.123m=116$ MeV. The empirical phaseshift is the one for pp rather than for nn [14], but the phaseshifts for nn and pp should be indistinguishable except at very low energies. For a_v, we arbitrarily fix it to $a_v=3/m=0.63$ fm, while we try three different values for a_s, $4.4/m$, $4.6/m$ and $4.8/m$. Table 1 lists three sets of values of the parameters. Figure 1 compares the calculated ^{1}S phaseshift with the experimental one. The agreement is very good. There is a small disagreement near the threshold; this is because the calculated phaseshift is for nn, while the empirical one is for pp.

Figure 2 shows W_{nn} (with $a_s=4.6/m$) for three different energies in the centre-of-mass system. The phaseshift changes sign at 116 MeV. Below (above) that energy W_{nn} is effectively attractive (repulsive). In the same figure the Reid soft-core potential is also shown [15]. Note that W is much softer than the Reid potential. With the Reid potential, which is energy independent, the sign change in the phaseshift (at 116 MeV) is caused by the strong short-range repulsion, whereas, with W the sign change is due to the energy dependence of the potential. The difference in the softness between the two potentials results in the differences between the corresponding wavefunctions at short distances, which are displayed in figure 3. Figure 4 shows the Coulomb–nuclear interference potential defined by

Table 1. The parameters in $S(r)$ and $V(r)$: a_s and a_v are in units of the nucleon Compton wavelength $1/m=0.2101$ fm, and g_s and g_v are in units of $m=939$ MeV. The non-Coulombic scattering lengths a_{pp} in fm, calculated for V_{EM} of form I, are listed together with $\Delta a=a_{pp}-a_{nn}$ where $a_{nn}=-18.5$ fm. The values for V_{EM} of form II are shown in brackets.

a_s	a_v	g_s	g_v	a_{pp}	Δa
4.4	3.0	0.3515	0.5370	−20.47 (−19.43)	−1.97 (−0.93)
4.6	3.0	0.2855	0.4808	−20.34 (−19.41)	−1.84 (−0.91)
4.8	3.0	0.2365	0.4345	−20.24 (−19.38)	−1.74 (−0.88)

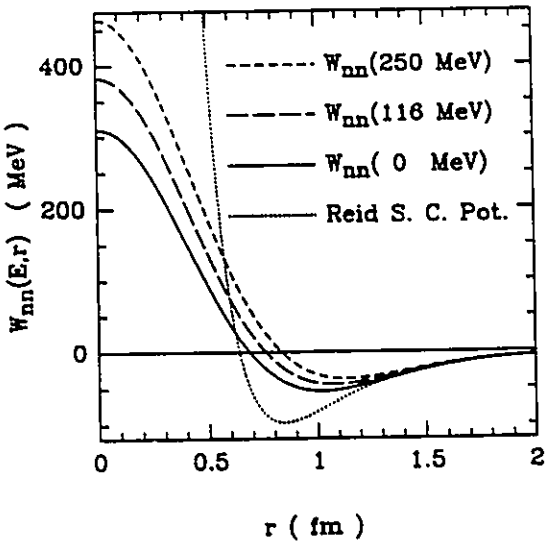

Figure 2. The effective potential W of (2.18) for $a_s = 4.6/m$ and $a_t = 3.0/m$ is plotted for three values of the centre-of-mass kinetic energy of 0, 116 and 250 MeV. The phaseshift changes from positive to negative at 116 MeV. The Reid soft-core potential, which is energy independent, is also shown for comparison.

$W_{pp} - W_{nn} - V_C$, for forms I and II. Note that the signs of the long-range part ($r \gtrsim 1$ fm) of the two interference potentials are consistent with (2.21). In addition, $V_C(r) - e^2/r$ is shown in the same figure; this difference in the Coulomb potential is due to the finite size of the proton.

We calculate the non-Coulombic scattering length a_{pp} by solving the Schrödinger-like equation (2.19), but replacing W_{pp} with $W_{pp} - e^2/r$. Table 1 lists the

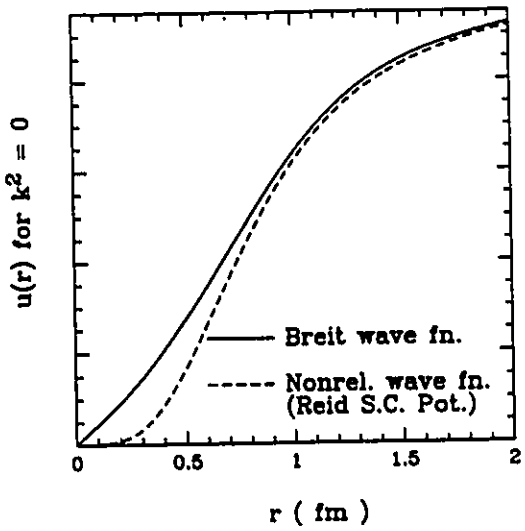

Figure 3. The relativistic wavefunction (in an arbitrary scale) determined by (2.18) for nn is compared with the corresponding non-relativistic wavefunction due to the Reid soft-core potential. For the relativistic potential, the parameter set with $a_s = 4.6/m$ has been used.

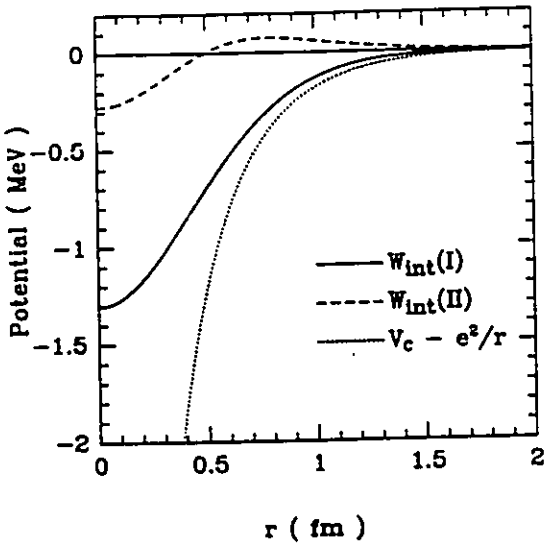

Figure 4. The Coulomb–nuclear interference potential $W_{pp} - W_{nn} - V_C$ and the potential for the finite-size effect $V_C - e^2/r$ are shown. The W are for the parameter set with $a_s = 4.6/m$.

values of a_{pp} for the three sets of the parameters of S and V, and for V_{EM} of forms I and II. Table 1 also lists the calculated values of $\Delta a \equiv a_{pp} - a_{nn}$, where $a_{nn} = -18.5$ fm. The Δa ranges from -1.80 to -2.04 fm for form I, and from -0.93 to -0.98 fm for form II. The calculated values of Δa are large in magnitude (and unfortunately negative). Compare these with the effect of the ρ–ω mixing on Δa, which has been estimated to be $\lesssim 0.6$ fm [4].

Since we calculated a_{pp} by using $W_{pp} - e^2/r$ rather than $W_{pp} - V_C$, part of Δa is due to the finite-size effect in the Coulomb potential. Actually more than a half of the large Δa that we have found is due to the finite-size effect in the Coulomb potential. We calculated the scattering length for $W_{nn} + (V_C - e^2/r)$, and found (for $a_s = 4.6/m$) $a = -19.62$ fm. Hence the Δa due to the finite-size effect alone is -1.12 fm. This is very large, but is not really surprising. We repeated the same calculation, but replacing W_{nn} with the Reid soft-core potential and found $\Delta a = -0.71$ fm. This can be compared with the result of the old calculation by Schneider and Thaler who used a hard-core potential [16]; the corresponding value that they obtained is -0.68 fm. In this connection see also [17]. The large value of $\Delta a = -1.17$ fm with W_{nn} is understandable in view of the large difference between the relativistic and non-relativistic wavefunctions shown in figure 3.

4. Discussion

We started with the Breit equation (2.1) for the NN system in the ^1S state and reduced it to the Schrödinger-like equation (2.18) with the effective potential W of (2.19). Although the nuclear part of the relativistic interaction, consisting of S, V and V_π, is exactly charge symmetric, the non-Coulombic part of W exhibits charge asymmetry: $W_{pp} - W_{nn} \neq e^2/r$. As we emphasized in section 1, whether or not the interaction is charge symmetric depends on the framework in which one chooses to

work. When we talk about charge symmetry regarding the low energy NN interaction, it is conventional to choose the non-relativistic framework with the Schrödinger equation. By 'CSB' we mean the CSB in this conventional language throughout this paper.

We assumed that the (charge symmetric) NN interaction and the EM potential are additive in the relativistic model. This is an assumption which is not exactly correct. There are CSB effects like the ρ–ω mixing and the γ–π exchange in the relativistic model as well as in the non-relativistic model. By assuming the additivity of the NN interaction and the EM potential in the relativistic model, we did not mean that the ρ–ω mixing, etc, are absent; rather we wanted to single out the specific effect that we have examined. For the potentials S and V in the relativistic model we simply assumed that they are some given functions of r. They should be taken as phenomenological potentials. However, if S and V are associated with meson exchanges, then the effect that we have discussed could be related to the γ–ρ and γ-σ (scalar meson) exchanges. In that case, however, the relativistic effects must be carefully retained in deriving the potential. In addition to the Coulomb–nuclear interference effect of the relativistic origin, we found that the finite-size effect in the Coulomb potential becomes much larger than in the conventional non-relativistic models. This is because the effective potential W is much softer at short distances than the conventional non-relativistic potentials.

Since the non-Coulombic (Coulomb-subtracted) part of the pp interaction $W_{pp} - e^2/r$ is more attractive than the nn interaction W_{nn} in our model, the calculated value Δa is negative. This is contrary to the experimental result of (1.3). This would mean that other CSB effects such as that of the ρ–ω mixing must be greater in magnitude and opposite in sign to the relativistic effect that we have found. They must be greater than so far estimated [4].

Although the model interaction that we have used reproduces the ^{1}S phaseshift well, as seen in figure 1, there is still some arbitrariness regarding the details of the interaction. Ideally, one should determine the interaction by examining other partial wave states also, in particular, the triplet state. However, we expect that a more sophisticated model interaction will lead to similar results. The Breit equation which we have used is only 'semi-relativistic'; it is not fully covariant. It would be interesting to repeat the analysis by means of some other relativistic two-body equations.

For V_{EM}, we considered two forms, I and II. The results were quite different between the two. As Bethe and Salpeter argued, perhaps form II should not have been used beyond first order perturbation [11]. Also, we have not included anomalous magnetic moments of the nucleons. There is an extended form of the Breit interaction, given by Schwinger [18], which includes anomalous magnetic moments, but it may also be subject to Bethe and Salpeter's criticism. Despite such uncertainties, however, we believe that, with the combination of strong S and V in the relativistic interaction, the mechanism of the NN interaction is very different from that of the conventional non-relativistic models, and the difference may well manifest itself in low-energy nuclear phenomena.

Acknowledgments

We would like to thank Tatsuya Saskawa, Souichi Ishikawa and Akira Suzuki for helpful discussions. This work was supported by the Natural Sciences and

Engineering Research Council of Canada and the Japan Society for the Promotion of Science.

References

[1] Gabioud B *et al* 1979 *Phys. Rev. Lett.* **42** 1508; 1981 *Phys. Lett.* **103B** 9; 1984 *Nucl. Phys.* A **420** 496
de Téramond G F and Gabioud B 1987 *Phys. Rev.* C **36** 691
Schori O *et al* 1987 *Phys. Rev.* C **35** 2252
[2] Slaus I, Akaishi Y and Tanaka H 1989 *Phys. Rep.* **173** 257
[3] Bodeck K *et al* 1990 *Few-Body Syst.* **8** 23
[4] Henley E M 1966 *Isospin in Nuclear Physics* ed J D Fox and D Robson (New York: Academic) p 3; 1969 *Isospin in Nuclear Physics* ed D H Wilkinson (Amsterdam: North-Holland) p 17
[5] Henley E M and Miller G A 1979 *Mesons in Nuclei* vol I, ed M Rho and D H Wilkinson (Amsterdam: North-Holland) p 405
[6] Wilkinson D H 1972 *Few Particles Problems in the Nuclear Interaction* ed I Slaus *et al* (Amsterdam: North-Holland) p 191
de Téramond G F 1989 *Proc. Symp./Workshop on Spin and Symmetries* (*TRIUMF, Vancouver*) ed W D Ramsay and W T H van Oers (Vancouver: TRIUMF) p 235
[7] Gerstein A, Greeniaus L G, Niskanen J A, Ishikawa S, Sasakawa T and Thomas A W 1988 *Few-Body Syst.* **3** 171
[8] Wu Y, Ishikawa S and Sasakawa T 1990 *Phys. Rev. Lett.* **64** 1875
[9] Nogami Y and Toyama F M 1988 *Phys. Rev.* C **38** 1578
[10] Breit G 1929 *Phys. Rev.* **34** 533
Kemmer N 1937 *Helv. Phys. Acta* **10** 48
Fermi E and Yang C N 1949 *Phys. Rev.* **76** 1739
Moseley H M and Rosen N 1950 *Phys. Rev.* **80** 177
Morishita H, Kawaguchi M and Morii T 1988 *Phys. Rev.* D **37** 159
Ferreira P L 1988 *Phys. Rev.* D **38** 2648
Cheung C Y and Li S P 1990 *Phys Lett.* **234B** 444
Ferreira P L and Galeao A P 1990 *Mod. Phys. Lett.* A **5** 2523
[11] Bethe H A and Salpeter E E 1957 *Quantum Mechanics of One- and Two-Electron Atoms* (Berlin: Springer) section 38
[12] Nogami Y and Toyama F M 1990 *Phys. Rev.* C **42** 2449
[13] Halzen F and Martin A D 1984 *Quarks and Leptons* (New York: Wiley) pp 178–9
[14] Arndt R A, Roper L D, Bryan R A, Clark R B, VerWest B J and Signell P 1983 *Phys. Rev.* D **28** 97
[15] Reid R V 1968 *Ann. Phys., NY* **50** 411
[16] Schneider R E and Thaler R M 1965 *Phys. Rev.* **137B** 874
[17] Kiang D, Machida S and Nogami Y 1973 *Can. J. Phys.* **51** 1120
[18] Schwinger J 1950 *Phys. Rev.* **78** 135

Chapter 4

Relation between the bound state and the scattering length: Relativistic effects

4.1 SPECIFICS OF THE MODEL USED FOR THE EFFECTIVE RANGE EXPANSION PROBLEM

The effective range expansion[53],[54], is an optimal means of bridging theoretical dynamical models and raw experimental scattering data. The expansion relates the quantity $k\cot\delta$ to a Taylor series in k^2 or $(k^2+\alpha^2)$ where α is the inverse decay length of a bound state. The coefficients of the expansion are progressively more dependent on details of the model, such as potential shape parameters as one takes higher and higher orders. Fitting the lowest two coefficients, essentially shape-independent, is almost a minimal requirement to be satisfied by any successful model. As will be shown in the following section, the expansion's coefficients can be derived from fundamental considerations and are found to be dependent on both dynamic (model) properties and kinematic properties (relativistic or non-relativistic choice of framework). We examine the kinematic differences between the

expansions in these two frameworks. To enable a test of the expansion about $k^2 = -\alpha^2$ for the Breit equation, the ${}^1S_0$ model of the last chapter is used. We dial up the attraction of the interaction to create a bound state which we casually equate with the deuteron. We *simulate* a singlet deuteron because the complexity of the true triplet Breit equation probably does not offer any further illumination of the point. The triplet also requires a great deal of extraneous discussion pertaining to the choice of spinor amplitudes involved in the expansion, choice of phase convention *etc.*, which are not central here.

Once again, where the discussion turns to the two-body Dirac equation (*a.k.a.* Breit equation, in *sub*sections IV and V of the following section, the notation is different from that of chapter 2. We borrow the dynamic model of chapter 3 with the electromagnetic components of the interaction turned off. (Our simulated deuteron will still contain an electrically neutral neutron.)

At this point, the reprint of a self-contained paper, as it appeared published in Physical Review C., can best be used to present a detailed discussion of the ideas.

4.2

PHYSICAL REVIEW C VOLUME 44, NUMBER 1 JULY 1991

Relation between the bound state radius and the scattering length: Relativistic effects

F. M. Toyama
Institute of Computer Sciences, Kyoto Sangyo University, Kyoto 603, Japan

D. J. Beachey, Y. Nogami, and W. van Dijk*
Department of Physics, McMaster University, Hamilton, Ontario, Canada L8S 4M1
(Received 8 February 1991)

Relativistic effects on the relation between the root-mean-square radius r_D of the bound state and the scattering length a are examined for models which simulate the triplet S state of the two-nucleon system. Two models are considered; one is based on the one-body Dirac equation and the other on the two-body Dirac equation. The relation is expressed as $(r_D/a)^2=(c_0+c_1x^1+c_2x^2+\cdots)/8$, where $x\equiv\alpha r_0$; α is related to the binding energy and r_0 is the effective range. This expansion is compared with the corresponding expansion of the nonrelativistic Schrödinger case. The first three terms are shape independent. The c_0 ($=1$) and c_1 ($=0$) are the same as those of the nonrelativistic case but a relativistic correction appears in c_2.

I. INTRODUCTION

Recently several papers have appeared examining the relation between the root-mean-square (rms) radius of the deuteron r_D and the scattering length a (commonly denoted by a_t) of the triplet S state of the two-nucleon system [1–7]. The interest in this problem was inspired by the remark by Klarsfeld *et al.* [1] that the values of r_D and a, calculated on the basis of a number of realistic nucleon-nucleon potentials, exhibit a linear relation; when a is plotted against r_D one obtains a straight line. It is interesting that the experimental (r_D,a) point lies distinctly off the calculated line. The discrepancy, although only about 1%, is believed to be significant.

When the relativistic interaction consists of a strongly attractive Lorentz scalar and a strongly repulsive (zeroth component of) Lorentz vector, there could be significant relativistic effects even at low energies [8,9]. This observation motivated the analysis of relativistic effects on the r_D/a ratio [2]. Within limited one-dimensional model calculations, however, relativistic effects were found to be too small to remedy the discrepancy. Incidentally it was then conjectured that the discrepancy is a signature of nonlocality of the nucleon-nucleon interaction. Later analyses support this conjecture [3,4,6].

Through nonrelativistic (NR) model calculations Bhaduri *et al.* [4] found that, when r_D/a is expressed in the form of the expansion,

$$(r_D/a)^2=(c_0+c_1x^1+c_2x^2+\cdots)/8\ , \tag{1.1}$$

where $x=r_0/a$ and r_0 is the effective range, the first three coefficients are shape independent:

$$c_0=1,\ \ c_1=0,\ \ c_2=\tfrac{1}{4}\ . \tag{1.2}$$

The dependence on the shape of the potential begins to appear through c_3. Since $x\simeq 0.36$, Eq. (1.1) together with Eq. (1.2) explains why r_D/a is almost shape independent. The expansion has been further elucidated by Sprung *et al.* [5] and by Kermode *et al.* [6].

The purpose of this paper is to obtain relativistic versions of the expansion (1.1). Unlike Ref. [2] we consider three-dimensional models in this paper. However, we will point out an interesting difference between one and three dimensions. We consider two models, I and II. In model I we use the one-body Dirac equation with an external central potential. Model II is based on the two-body Dirac equation with an instantaneous interaction. Unlike in NR quantum mechanics, relativistic two-body problem cannot simply be reduced to a one-body problem; hence the one-body Dirac equation of model I can only simulate the two-nucleon system. The two-body Dirac equation of model II does describe the two-body system but the equation is not exactly covariant. Nevertheless, we hope to be able to get a feel for relativistic effects through these models.

II. THE rms RADIUS VERSUS SCATTERING LENGTH: NONRELATIVISTIC CASE

Before discussing the relativistic models, let us review the relation between r_D and a in the NR case. We consider an S state which contains only one bound state (which simulates the deuteron). The S matrix has a pole at $k=i\alpha$, which corresponds to the bound state. The binding energy is $\alpha^2/2\mu$, where $\mu=m/2$ is the reduced mass; m is the nucleon mass. The effective range expansion for the scattering phase shift δ can be done in two ways:

$$k\cot\delta=-\frac{1}{a}+\frac{1}{2}r_0k^2-Pr_0^3k^4+\cdots \tag{2.1}$$

$$=-\alpha+\tfrac{1}{2}r_d(k^2+\alpha^2)-\cdots\ . \tag{2.2}$$

The parameters in the two expansions are related by

$$\alpha=\frac{1}{a}+\frac{1}{2}\alpha^2r_0+P\alpha^4r_0^3+\cdots\ , \tag{2.3}$$

$$r_d=r_0+4P\alpha^2r_0^3+\cdots\ . \tag{2.4}$$

Following Ref. [6], we put the rms radius of the bound state into the form

$$\left|\frac{r_D}{a}\right|^2=\frac{\int_0^\infty \rho(\alpha,r)(r/2)^2dr}{a^2\int_0^\infty \rho(\alpha,r)dr}$$
$$=\frac{1-4\alpha^3 I_2(\alpha)}{8(\alpha a)^2[1-2\alpha I_0(\alpha)]}, \quad (2.5)$$

where

$$I_0(\alpha)=\int_0^\infty [e^{-2\alpha r}-\rho(\alpha,r)]dr, \quad (2.6)$$

$$I_2(\alpha)=\int_0^\infty [e^{-2\alpha r}-\rho(\alpha,r)]r^2dr. \quad (2.7)$$

The $\rho(\alpha,r)$ is related to the bound state wave function $u(\alpha,r)/r$ by

$$\rho(\alpha,r)=u^2(\alpha,r), \quad (2.8)$$

where $u(\alpha,r)$ is such that $u(\alpha,r)\to e^{-\alpha r}$ as $r\to\infty$, and $\int_0^\infty \rho(\alpha,r)dr=1$.

Kermode *et al.* [6] derived the expansion

$$\left|\frac{r_D}{a}\right|^2=\tfrac{1}{8}[1+\tfrac{1}{4}(\alpha r_0)^2+c_3(\alpha r_0)^3+\cdots], \quad (2.9)$$

where

$$c_3=(1-2J+8P)/4, \quad (2.10)$$

$$J=I_2(0)/I_0(0)^3. \quad (2.11)$$

Obviously c_3 is shape dependent. Actually, Kermode *et al.* [6] gave an expression for r_D/a rather than for $(r_D/a)^2$; moreover, their expansion is with respect to $\alpha r_0/2$. Their a_3 is related to our c_3 by $a_3=4c_3$. Note that Eq. (2.9) is an expansion in terms of αr_0 rather than r_0/a which Bhaduri *et al.* [4] adopted; the c_3's of Eqs. (1.1) and (2.9) are slightly different, but their relation can easily be obtained by using Eq. (2.4).

In arriving at Eq. (2.9) there were two important steps, namely,

$$I_0(\alpha)=r_d/2, \quad (2.12)$$

and that $I_2(\alpha)$ is finite when $\alpha\to 0$ as implied by Eq. (2.10). Equation (2.12) arises in the derivation of expansion (2.2). For the behavior of $I_2(\alpha)$ when $\alpha\to 0$, we know of no example of the bound S state such that $I_2(\alpha)$ diverges. We point out in Sec. III that relativistic corrections appear in these two steps, resulting in a correction of order α^2 in Eq. (2.9).

III. ONE-BODY DIRAC EQUATION

We consider the Dirac equation (in natural units $c=\hbar=1$)

$$[\alpha\cdot\mathbf{p}+\beta(\mu+S)+V]\psi=E\psi, \quad (3.1)$$

where S and V are a Lorentz scalar and the zeroth component of a Lorentz vector, respectively. The S and V are both central potentials, and can be local or nonlocal. For the mass we take $\mu=m/2$ so that the NR reduction of Eq. (3.1) becomes the two-body Schrödinger equation. The angular part of Eq. (3.1) can be separated, and the ψ is reduced to a two-component form [10]. We denote the radial part of ψ by $g(r)/r$ and $f(r)/r$, which are the upper and lower components, respectively.

Let us examine the effective range expression for scattering. We introduce auxiliary functions $\varphi(r)$ and $\mathcal{f}(r)$ which are defined by

$$\varphi(r)=\frac{\sin(kr+\delta)}{\sin\delta}, \quad \mathcal{f}(r)=\frac{k\cos(kr+\delta)}{(\mu+E)\sin\delta}, \quad (3.2)$$

where $E=(\mu^2+k^2)^{1/2}$. The φ/r and $\mathcal{f}/r$ satisfy the Dirac equation in the absence of the interaction and the centrifugal terms. When $k\to 0$, φ and $\mathcal{f}$, respectively, become

$$\varphi_0(r)=1-r/a, \quad \mathcal{f}_0(r)=-1/2\mu a. \quad (3.3)$$

We also choose the phase and normalization of $g(r)$ and $f(r)$ such that, when $r\to\infty$, they approach $\varphi(r)$ and $\mathcal{f}(r)$, respectively. Using a trick similar to that of the nonrelativistic case [11] we obtain

$$k\cot\delta=(\mu+E)\left[-\frac{1}{2\mu a}+(E-\mu)\int_0^\infty(\varphi\varphi_0+\mathcal{f}\mathcal{f}_0-gg_0-ff_0)dr\right], \quad (3.4)$$

where g_0 and f_0 are for $k=0$. This leads to the expansion around $k=0$. However, note that, for r greater than the interaction range, $g=\varphi$ but $f=\mathcal{f}+O(1/r)$. Hence the integral in Eq. (3.4) gets a contribution from beyond the interaction range.

Next let us consider the expansion around $k=i\alpha$. To this end we introduce $\varphi_\alpha(r)$ and $\mathcal{f}_\alpha(r)$, defined by

$$\varphi_\alpha(r)=e^{-\alpha r}, \quad \mathcal{f}_\alpha(r)=\frac{-\alpha}{\mu+E_\alpha}e^{-\alpha r}, \quad (3.5)$$

and obtain

$$k\cot\delta=(\mu+E)\left[-\frac{\alpha}{\mu+E_\alpha}+(E-E_\alpha)\int_0^\infty(\varphi\varphi_\alpha+\mathcal{f}\mathcal{f}_\alpha-gg_\alpha-ff_\alpha)dr\right]. \quad (3.6)$$

where $g_\alpha(r)$ and $f_\alpha(r)$ form the exact wave function for the bound state. When $k \simeq i\alpha$, the integral on the right-hand side of Eq. (3.6) can be approximated by

$$\int_0^\infty (\varphi_\alpha^2+\mathcal{f}_\alpha^2-g_\alpha^2-f_\alpha^2)dr = \int_0^\infty \left| \frac{2\mu}{\mu+E_\alpha} e^{-2\alpha r}-(g_\alpha^2+f_\alpha^2) \right| dr = \frac{2\mu}{\mu+E_\alpha} I_0(\alpha) , \tag{3.7}$$

where $I_0(\alpha)$ is defined by Eq. (2.6), together with

$$\rho(\alpha,r)=\frac{\mu+E_\alpha}{2\mu}(g_\alpha^2+f_\alpha^2) . \tag{3.8}$$

This $\rho(\alpha,r)$ replaces $u^2(\alpha,r)$ of the NR case. Note that $\rho(\alpha,r)\to e^{-2\alpha r}$ as $r\to\infty$; see Eq. (3.12). Putting Eq. (3.7) in Eq. (3.6), expanding around $k^2=-\alpha^2$, and comparing the result with Eq. (2.2), we obtain

$$r_d=-\frac{\alpha}{E_\alpha(\mu+E_\alpha)}+\frac{2\mu}{E_\alpha} I_0(\alpha) , \tag{3.9}$$

which leads to

$$I_0(\alpha)=\frac{1}{2}r_d+\frac{\alpha}{4\mu^2}-\frac{\alpha^2}{4\mu^2}r_d+O(\alpha^3) . \tag{3.10}$$

Next let us examine $I_2(\alpha)$ which is defined by Eq. (2.7) together with the $\rho(\alpha,r)$ of Eq. (3.8). This requires a closer look at the asymptotic form of g_α and f_α. Beyond the range of the interaction they are given by

$$g_\alpha \simeq e^{-\alpha r}, \quad f_\alpha \simeq -\frac{\alpha}{\mu+E_\alpha}\left(1+\frac{1}{\alpha r}\right)e^{-\alpha r} , \tag{3.11}$$

and hence

$$e^{-2\alpha r}-\rho(\alpha,r) \simeq -\frac{\alpha^2}{2\mu(\mu+E_\alpha)}\left[\left|1+\frac{1}{\alpha r}\right|^2-1\right]e^{-2\alpha r} . \tag{3.12}$$

For R greater than the interaction range we obtain

$$\int_R^\infty [e^{-2\alpha r}-\rho(\alpha,r)]r^2dr \simeq -\frac{1}{2\mu\alpha(\mu+E_\alpha)}(1+\alpha R)e^{-2\alpha R} , \tag{3.13}$$

which diverges as $\alpha\to 0$. Consequently, $I_2(\alpha)$ behaves like $-1/(4\mu^2\alpha)$ as $\alpha\to 0$ [12]. We therefore define J by

$$I_2(\alpha)\equiv -\frac{1}{4\mu^2\alpha}+\frac{1}{8}r_d^2 J+O(\alpha) . \tag{3.14}$$

Taking account of the relativistic corrections of Eqs. (3.10) and (3.14) we obtain the Dirac version of Eq. (2.8),

$$\left|\frac{r_D}{a}\right|^2=\frac{1}{8}\left[1+\frac{3\alpha^2}{2\mu^2}+\frac{1}{4}(\alpha r_0)^2+c_3(\alpha r_0)^3+\cdots\right] , \tag{3.15}$$

$$c_3=(1-2J+8P)/4 . \tag{3.16}$$

The c_3 is shape dependent. The term $3\alpha^2/2\mu^2$ in Eq. (3.15) is a relativistic correction. For the deuteron, $(\alpha r_0)^2/4\simeq 0.041$ and $3\alpha^2/(2\mu^2)\simeq 0.014$. This relativistic correction on r_D is only 0.7%, but the discrepancy regarding r_D/a that we are concerned with is about 1%.

If one considers a fictitious one-dimensional model with the one-dimensional Dirac equation, the correction due to Eq. (3.14) does not appear; this is because the $1/\alpha r$ term does not appear in the one-dimensional counterpart of f_α. Then the J is defined by Eq. (2.11). The one-dimensional version of Eq. (3.15) is obtained by replacing $3\alpha^2/2\mu^2$ in Eq. (3.15) with $\alpha^2/(2\mu^2)$.

IV. TWO-BODY DIRAC EQUATION

By the "two-body Dirac equation" we mean

$$[(\alpha_1-\alpha_2)\cdot\mathbf{p}+(\beta_1+\beta_2)m+U]\psi=E\psi , \tag{4.1}$$

where subscripts 1 and 2 refer to the two nucleons [13, 14]. We have taken the center-of-mass system; $\mathbf{p}=\mathbf{p}_1-\mathbf{p}_2$ is the relative momentum. The potential U can be any linear combination of Lorentz scalar, vector, etc., but we need not specify it until we consider an explicit example later.

There are various configurations of the two-nucleon system, but let us consider the simplest one which corresponds to the ^1S state. Of course the deuteron is the ^3S state, but Eq. (4.1) is very complicated for the ^3S state. To use the ^1S state to simulate the ^3S state is like dropping the tensor force in the NR case. This is admittedly crude; nevertheless, let us try. We assume that the potential is such that there is a bound state (in the ^1S state) which simulates the deuteron.

According to Moseley and Rosen [14], the relevant components of the wave function for the ^1S state are those of the form

$$I=f_1(r), \quad A_4=f_2(r), \quad i\mathbf{F}=f_3(r)\mathbf{r}/r . \tag{4.2}$$

There is a departure from Moseley and Rosen's notation; our $i\mathbf{F}$ corresponds to their $\mathbf{F}$, i.e., our f_3 is equal to their if_3. In this way all the f_i's can be taken as real functions. Equation (4.1) becomes

$$(E-U_1)f_1+2\left(r\frac{d}{dr}+3\right)\frac{f_3}{r}+2mf_2=0 , \tag{4.3}$$

$$(E-U_2)f_2+2mf_1=0 , \tag{4.4}$$

$$(E-U_3)f_3-2\frac{df_1}{dr}=0 , \tag{4.5}$$

where U_1, etc., are certain linear combinations of the Lorentz scalar part, vector part, etc., of U.

On the basis of Eqs. (4.3)–(4.5) we can derive effective range formulas similar to those for the one-body Dirac equation. Let us define $\mathcal{f}_i(r)$'s by

$$r\mathcal{f}_1=-\frac{2m}{E}r\mathcal{f}_2=\frac{\sin(kr+\delta)}{\sin\delta} , \qquad r\mathcal{f}_3=\frac{2k\cos(kr+\delta)}{E\sin\delta} , \tag{4.6}$$

where $E=2(m^2+k^2)^{1/2}$. When $k\to 0$, the $\mathcal{f}_i$'s become

$$r\mathcal{f}_{10}=-r\mathcal{f}_{20}=1-\frac{r}{a},\quad r\mathcal{f}_{30}=-\frac{1}{ma}\ . \tag{4.7}$$

We choose the phase and normalization of the f_i's such that they have the same asymptotic form as the $\mathcal{f}_i$'s. The effective range expansion around $k=0$ can be obtained from

$$k\cot\delta=E\left[-\frac{1}{2ma}+\frac{1}{4}(E-2m)\sum_i\int_0^\infty(\mathcal{f}_i\mathcal{f}_{i0}-f_if_{i0})r^2dr\right], \tag{4.8}$$

where the f_{i0}'s are for $k=0$, and the $\sum_i$ is for $i=1$, 2, and 3.

For the expansion around $k=i\alpha$ we introduce

$$r\mathcal{f}_{1\alpha}=-\frac{2m}{E_\alpha}r\mathcal{f}_{2\alpha}=e^{-\alpha r},\quad r\mathcal{f}_{3}(r)=\frac{-2\alpha}{E_\alpha}e^{-\alpha r}, \tag{4.9}$$

where $E_\alpha=2(m^2-\alpha^2)^{1/2}$, and arrive at

$$k\cot\delta=E\left[-\frac{\alpha}{E_\alpha}+\frac{1}{4}(E-E_\alpha)\sum_i\int_0^\infty(\mathcal{f}_i\mathcal{f}_{i\alpha}-f_if_{i\alpha})r^2dr\right], \tag{4.10}$$

where the $f_{i\alpha}$'s are the f_i's for the bound state.

We now define the two-body version of $\rho(\alpha,r)$ by

$$\rho(\alpha,r)=(E_\alpha^2/8m^2)r^2\sum_i f_{i\alpha}^2\ , \tag{4.11}$$

which behaves like $e^{-2\alpha r}$ as $r\to\infty$. This $\rho(\alpha,r)$ enters into $I_0(\alpha)$ and $I_2(\alpha)$. The two-body counterpart of Eq. (3.10) reads

$$I_0(\alpha)=\frac{1}{2}r_d+\frac{\alpha}{2m^2}-\frac{\alpha^2}{2m^2}r_d+O(\alpha^3)\ . \tag{4.12}$$

For r greater than the interaction range,

$$\begin{aligned} rf_{1\alpha}&\simeq-\frac{2m}{E_\alpha}rf_{2\alpha}\simeq e^{-\alpha r}\ ,\\ rf_{3\alpha}&\simeq-\frac{2\alpha}{E_\alpha}\left[1+\frac{1}{\alpha r}\right]e^{-\alpha r}\ , \end{aligned} \tag{4.13}$$

which leads to

$$I_2(\alpha)\cong-\frac{1}{2m^2\alpha}+\frac{1}{8}r_d^3J+O(\alpha)\ . \tag{4.14}$$

Combining the above results we obtain

$$\left[\frac{r_D}{a}\right]^2=\frac{1}{8}\left[1+\frac{3\alpha^2}{m^2}+\frac{1}{4}(\alpha r_0)^2+c_3(\alpha r_0)^3+\cdots\right], \tag{4.15}$$

$$c_3=\tfrac{1}{4}(1-2J+8P)-\frac{1}{2(mr_0)^2}\ . \tag{4.16}$$

The correction $3\alpha^2/m^2$ in Eq. (4.15) is $\frac{1}{4}$ of the corresponding term of Eq. (3.15). The relativistic correction in $c_3(\alpha r_0)^3$ is $-\alpha^3 r_0/(2m^2)\simeq-5\times10^{-5}$, which is negligible. For a fictitious one-dimensional model, the term $3\alpha^2/m^2$ of Eq. (4.15) is replaced by α^2/m^2.

V. MODEL CALCULATIONS

Let us consider two models. The first one is the nonlocal separable potential model of Ref. [12]. This model uses the one-body Dirac equation. The relation between r_D and a of this model has been examined recently [7]. In order to see the relativistic effects, the results are compared with those of a phase-equivalent NR model. The NR model is constructed by means of the inverse scattering method. Also the NR model has a bound state of the same binding energy as that of the relativistic model.

When a is plotted against r_D, the (r_D,a) lines of the relativistic and NR models lie close to each other, but the relativistic one is slightly shifted to the right (such that r_D is larger for the same value of a); see Fig. 1 of Ref. [7]. The increase in r_D (for the same value of a) is (0.2–0.3)%. The term $3\alpha^2/2\mu^2$ of Eq. (3.15) increases r_D by 0.7%. On the other hand, the J of the relativistic models is larger than the J of the phase-equivalent NR models. This tends to compensate for the $3\alpha^2/2\mu^2$ term. In fact, $I_2(\alpha)$ for the relativistic and NR models are nearly equal. This is because the density distribution $\rho(r,\alpha)$ differs very little between the two models. We should add that, the phase shift in these models does not become negative at high energies; so it does not simulate the empirical phase shift very well. The NR separable potential has no short-range repulsion.

The second model is based on the two-body Dirac equation of Sec. IV. For the potential U we assume a combination of Lorentz scalar $S(r)$, vector $V(r)$, and pseudovector $V_\pi(r)$;

$$U=\beta_1\beta_2S(r)+(1-\alpha_1\cdot\alpha_2)V(r)-\tfrac{1}{3}(\sigma_1\cdot\sigma_2-\Gamma_1\Gamma_2)V_\pi(r)\ , \tag{5.1}$$

where $r=|\mathbf{r}_1-\mathbf{r}_2|$ and $\Gamma=-i\alpha_x\alpha_y\alpha_z(=\gamma^5)$ [14]. Then U_1, U_2, and U_3 of Eqs. (4.3)–(4.5) are given by

$$U_1=S+4V+\tfrac{4}{3}V_\pi\ , \tag{5.2}$$

$$U_2=S-2V+\tfrac{1}{3}V_\pi\ , \tag{5.3}$$

$$U_3=-S\ . \tag{5.4}$$

For the radial dependence of the potential we assume [15]

$$S(r)=-g_s\exp[-(r/a_s)^2]\ , \tag{5.5}$$

$$V(r)=g_v\exp[-(r/a_v)^2]\ , \tag{5.6}$$

$$V_\pi(r)=-g^2[\exp(-m_\pi r)-\exp(-\Lambda r)]/r\ . \tag{5.7}$$

The V_π with $g^2=0.08$ and $m_\pi=138$ MeV is a cutoff one-pion-exchange potential. For the cutoff parameter Λ we

arbitrarily assume $\Lambda = m/2$.

We solve the two-body Dirac equation without any approximation. The parameters in S and V are fixed such that there is a bound state of the deuteron binding energy 2.225 MeV ($\alpha = 0.04866m$), and that the ^3S scattering phase shift is well fitted as shown in Fig. 1. The values of the parameters of S and V, i.e., a_s, a_v, g_s, g_v, together with the calculated values of a, r_D, r_0, P, J, and c_3 are listed in Table I. The potential is similar to that of model $R1$ of Ref. [2] (which is the same as model A of Ref. [8]) in which $a_s = 5/m$, $a_v = 3/m$, $g_s = 0.37m$, $g_v = 0.46487$ [16]. The two-body Dirac equation can be rewritten into the form of a Schrödinger-like equation [15]. The effective potential W that appears in the Schrödinger-like equation of the present model is similar to the W of the one-dimensional model shown in Fig. 2 of Ref. [8]. The W is energy dependent. At low energies, W is almost entirely attractive, and is much softer than the nucleon-nucleon potential of the usual NR models.

In expansion (4.15), if we retain the terms up to $c_3(\alpha r_0)^3$, we find $8(r_D/a)^2 = 1.0300$, which can be compared with the exact calculated value of $8(r_D/a)^2 = 1.0305$. Hence the truncation error is 0.0005. Let us look into some details of the term in the square brackets of expansion (4.15). The relativistic terms of order α^2 is $3\alpha^2/m^2 = 0.0071$. The shape-dependent part of $c_3(\alpha r_0)^3$ is $-(J/2)(\alpha r_0)^3 = -0.0287$, which is not much smaller than the shape-independent term of order α^2, i.e., $(\alpha r_0)^2/4 = 0.0381$.

In Ref. [2] a variety of one-dimensional models, relativistic as well as NR, were examined. It was found that relativistic corrections on r_D/a were altogether negligible. This was surprising in the following sense. In contrast to the usual NR models in which the potential has a strong short-range repulsion, the effective potential W of the Schrödinger-like equation of the relativistic models of Ref. [2] is very soft. It was thought that the absence of the strong repulsion at short distances would result in a smaller size of the bound state as compared with the NR models. What actually happens is this. The value of J is larger in relativistic models than in the NR models; this indeed results in a smaller radius of the bound state. For r_D/a, however, the relativistic correction α^2/m^2 (in one dimension) nearly compensates for the increase in J. As we noted earlier, the relativistic correction of order α^2 is $3\alpha^2/m^2$ in three dimensions. This correction in three dimensions tends to overcompensate for the change in J, and shifts the (r_D, a) slightly to the right.

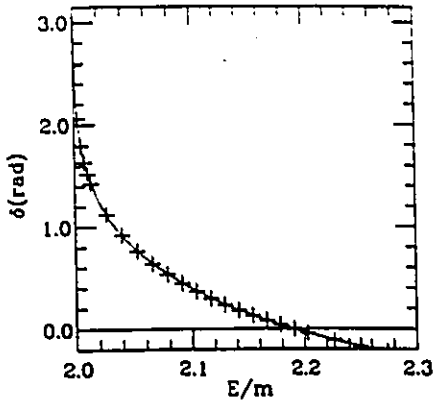

FIG. 1. The triplet S phase shift δ in radians versus the center-of-mass energy (including the rest mass) in units of $m = 939$ MeV. The experimental phase shift is indicated by the crosses. The line represents the calculated phase shift.

VI. SUMMARY

We examined the ratio $(r_D/a)^2$ for two relativistic models, I and II. Model I is based on the one-body Dirac equation and model II on the two-body Dirac equation. We obtained Eqs. (3.15) and (4.15) for models I and II, respectively. In both cases relativistic corrections begin to appear in order α^2; $3\alpha^2/2\mu^2$ and $3\alpha^2/m^2$ in the square brackets of Eqs. (3.15) and (4.15), respectively Since $\mu = m/2$, this correction term for I is twice as large as that of II. We also pointed out that, if one uses one-dimensional models as those of Ref. [2], the correction terms of order α^2 are reduced by a factor of 3 in both models.

The expansions we obtained are relativistic generalizations of Eq. (1.1). These formulas explain why the ratio r_D/a is not very sensitive to the details of the potential. In Sec. V we examined an explicit model based on the three-dimensional two-body Dirac equation. We discussed the mechanism which underlies the negligible relativistic effects on r_D/a found in the one-dimensional models of Ref [2]. In the three-dimensional model, the relativistic effects on r_D/a are slightly larger. We should

TABLE I. The parameters of the potential a_s, a_v, g_s, g_v, and various calculated quantities of the two-body model of Sec.. V. The values of a_s, a_v, a, r_D, and r_0 are in units of the nucleon Compton wavelength $1/m = 0.2101$ fm, and g_s, g_v, and α are in units of the nucleon mass $m = 939$ MeV. The parameters P, J, and c_3 are dimensionless.

a_s	a_v	g_s	g_v	$10^2\alpha$	a
4.6	3.0	0.35662	0.43902	4.866	25.54
r_D	r_0	10^3P	J		c_3
9.168	8.024	−7.600	0.9626		−0.2543

add that the two-body calculation of Sec. V is only a simulation of the deuteron; we used the singlet state for simplicity. It would be interesting to do calculations for the triplet state.

ACKNOWLEDGMENTS

This work was supported by the Natural Sciences and Engineering Research Council of Canada.

---

*Also at Redeemer College, Ancaster, Ontario, Canada L9G 3N6.

[1] S. Klarsfeld, J. Martorell, J. A. Oteo, M. Nishimura, and D. W. L. Sprung, Nucl. Phys. A456, 373 (1986).
[2] F. M. Toyama and Y. Nogami, Phys. Rev. C 38, 2881 (1988).
[3] W. van Dijk, Phys. Rev. C 40, 1437 (1989).
[4] R. K. Bhaduri, W. Leidemann, G. Orlandini, and E. L. Tomusiak, Phys. Rev. C 42, 1867 (1990).
[5] D. W. L. Sprung, H. Wu, and J. Martorell, Phys. Rev. C 42, 863 (1990).
[6] M. Kermode, S. A. Moszkowski, M. M. Mustafa, and W. van Dijk, Phys. Rev. C 43, 416 (1991).
[7] W. van Dijk (unpublished).
[8] Y. Nogami and F. M. Toyama, Phys. Rev. C 38, 1578 (1988).
[9] Y. Nogami and F. M. Toyama, Phys. Rev. C 42, 2449 (1990).
[10] See, e.g., L. I. Schiff, *Quantum Mechanics*, 3rd ed. (McGraw-Hill, New York, 1955), Chap. 13.
[11] J. M. Blatt and V. F. Weisskopf, *Theoretical Nuclear Physics* (Wiley, New York, 1952), Chap. II.
[12] We have confirmed this behavior of $I_2(\alpha)$ for two exactly solvable models. One is the δ-shell potential, and the other is the nonlocal separable potential; Y. Nogami and W. van Dijk, Phys. Rev. C 34, 1855 (1986); 36, 1648(E) (1987).
[13] G. Breit, Phys. Rev. 51, 248 (1937); N. Kemmer, Helv. Phys. Acta 10, 48 (1937); E. Fermi and C. N. Yang, Phys. Rev. 76, 1739 (1949). This two-body Dirac equation should be distinguished from the more sophisticated two-body Dirac equation of H. W. Carter and P. Van Alstine, Ann. Phys. (N.Y.) 148, 57 (1983); P. Van Alstine and H. W. Carter, Phys. Rev. D 34, 1932 (1986).
[14] H. M. Moseley and N. Rosen, Phys. Rev. 80, 177 (1950).
[15] D. J. Beachey, Y. Nogami, and F. M. Toyama (unpublished).
[16] In addition to the dimensional difference, there are the following differences between the models of Ref. [2] and the present one. (i) The potential in the relativistic models of Ref. [2] consists of S and V, while the present one has S, V, and V_μ. (ii) In Ref. [2], $m=1$ GeV and the binding energy of the simulated deuteron is $0.002m$, whereas we use $m=939$ MeV and the deuteron binding energy 2.225 MeV in the present paper.

Chapter 5

Breit treatment of the j=1 triplet nucleon-nucleon sector

5.1 BACKGROUND AND MOTIVATION

The non-relativistic wave function in the locally interacting two-nucleon system is essentially in a "straight jacket" at very low energy. All length scales in the system are commensurate. The centrifugal barrier which affects the D-component of the $j = 1$ triplet configuration forces the D-wave radial amplitude to rise as r^2 (while the S-component is finite at the origin) The characteristic length scale at which the D-wave can depart from this form is the Compton wavelength of the nucleon. This is a familiar kinematic restriction on the partial waves. The dynamics in the wave equation takes over and determines the topology (nodes and asymptotic wave function phases or exponential tails).

The nuclear *dynamics* however also take place on a length scale that, no matter what physics underlies it, it is essentially defined by M_N quite

in contrast to atomic physics where the Coulomb interaction has infinite range. QCD's characteristic scale Λ: is $\approx$ 240MeV $\approx 0.25M_N$; constituent quark masses are $\approx 0.33M_N$, alternatively in a purely hadrodynamic scheme we have meson masses -hence inverse ranges: $\pi \approx 0.15, \rho \approx 0.82, \omega \approx 0.83, \phi \approx 1.09M_N$ and the fictitious $\sigma \approx 0.5M_N$.[55] Consequently, it would be expected that the amplitudes should both vary quite smoothly over these length scales.

The nonrelativistic deuteron S-wave and D-wave amplitudes must abandon their r^0 and r^2 behaviour and descend exponentially on a short distance scale with no nodes and with little room to maneuver because of the rapidly weakening short range potentials. In all realistic local models which correctly match the value of the triplet scattering length a_t there is a $\approx 3\sigma$ overestimate[48] of the deuteron mean-square matter radius. The characteristic range and strength parameters of such models are used up in fitting the deuteron binding and a_t.

The wave functions of the threshold scattering state and the bound deuteron cannot be very different from one another in the near region because of their proximity in energy (a mere $0.0024M_N$.) A useful expansion relating the radius r_m to the scattering length a_t was devised by Bhaduri *et al.* [18] using the expansion parameter $x = (r_o/a_t)$ Here, r_o is the effective range for the given potential model. Alternatively, Sprung *et al.* [48] suggest $x = (\alpha r_i)$ as an appropriate expansion parameter where r_i is one of three mildly different effective ranges. The quantity α is the inverse decay length of the deuteron wave-function tail. As α vanishes the threshold state and bound state must converge. The two quantities at odds are associated with these two only slightly different wave-functions.

In either expansion, it is clearly indicated that potential shape effects enter only in the third order. Profound shape effects are called for in local models to bring about agreement with the quoted values for the matter radius: 1.9643 ± 0.0038 fm. (a weighted mean of the two values quoted in Table 3 of Machleidt's review article on the Bonn model[58] -specifically Bérard *et al.* [59] and Simon *et al.* [60] This is the value and error estimate used in the various χ^2 fits of the next sections. A very recent reanalysis of past data quotes a value consistent with this: 1.961 ± 0.007 fm.[61]. The Machleidt aggregate value with its more stringent error estimate weighted the matter radius more heavily in the fitting criteria so it was retained.)

Non-locality as a result of internal nucleon excitations $(\Delta - \Delta)$[18] or explicit quark degrees of freedom[57] are widely suggested as a remedy to this problem. (*e.g.*, six constituent quarks can interact locally at a distance removed from the physical centers of both nucleons which mark the end points of the relative co-ordinate in the Schrödinger equation. An accounting of their influence through a potential would appear *non*-local in that particular co-ordinate.) Hence, there is a realistic expectation for explicit non-locality in an interaction.

Alternatively, when a two-elementary-nucleon wavefunction is projected out of a parton one, the projected wavefunction can have features which are counter-intuitive for a ground-state configuration. The recently presented version of the Moscow potential[62] which is entirely *local* has a node in the S-wave amplitude for example. The amplitude's radial dependence is not particularly misbehaved for a $2S$-state. The model includes a very deep bound $1S$-state however which the authors argue must be projected out of calculations.

Non-local interactions can resolve the problem by essentially creating a pathological spline between the $r << M_N^{-1}$ and $r >> M_N^{-1}$ regions without appealing to an equally pathologically shaped potential to accomplish the task.[50]

For a relativistic framework to resolve this problem, the additional spinor components, perhaps only nominally small, are required to save the day. The features which intuition would lead us to expect of the mid-sized spinor components would include the following:

i.) There are important structural differences to the radial amplitudes attached to S, P, and D wave components of the spinor wave-function which are solely related to kinematic considerations. For example, the P-wave dependence arises from the 4 mid-sized radial amplitudes which characteristically rise as r^1. The P-wave is pushed away from the origin by a centrifugal barrier 1/3 as strong as that of the D-wave. If P-wave strength is drawn away from the even further pushed out D-wave, we might expect the matter radius to be drawn inward. In fact, the opposite will be found. The tails of the amplitudes, also dictated by pure kinematics, fall exponentially at large r as: S-wave $\rightarrow A_s e^{-\alpha r}$; P-wave $\rightarrow \eta_{p_s} A_s \{1 + \frac{1}{\alpha r}\} e^{-\alpha r}$; and D-wave $\rightarrow \eta_{d_s} A_s \{1 + \frac{3}{\alpha r} + \frac{3}{\alpha^2 r^2}\} e^{-\alpha r}$; So, it is the S-wave whose tail pulls out the deuteron radius more than that of the others -all other things being equal. The point is, that these intrinsic differences in addition to the dynamics may provide an opportunity for simple resolution of the a_t-r_m puzzle. Dynamics still plays the lead role in deciding both the tensor strength (for the D-state component) and the level of enhancement in the lower spinor components.

ii.) The P-wave amplitudes experience a vastly different potential from the large component amplitudes. In the large attractive scalar and repulsive

vector scheme, these radial amplitudes, $(a(r),\mathcal{J}(r),u(r),f(r))$ of equations (2.2.9)$e-h$, experience a deep attraction and should be pulled inward. This effect would be over and above a mere P-amplitude enhancement as that could also be accomplished if these amplitudes saw a large repulsion also.

In the following, a resolution of this longstanding problem will be sought within these two hypothetical mechanisms. In a similar vein to Kukulin and Pomerantsev's argument to dismiss their deep lying bound state artifact, one could argue that anomalous bound states arising from the $\bar{N}\bar{N}$ and $\bar{N}N$-sectors of *this* model are artifacts of the incorrect vacuum and $+E,-E$ continua coupling. As long as such artifacts remain distant in energy from our $+E$ NN sector, we can reliably argue that our picture is viable. (A comforting glance at Figure A2.3 of Appendix II will help assure the reader that departures from a more rigorous field theoretic picture are likely to be negligible for the problem at hand. The deuteron weighs in at an energy of $1.997630M_N$ with $\log(1/\beta) \approx 0.5 - 0.8M_N^{-1}$ for the various interactions for the purpose of comparison with this figure.) In addition, if a lone deuteron bound state is pulled out of the positive energy continuum, the energy dependence of the phaseshifts reflects a single drop in π, consistent with Levinson's theorem[63].

Of course, a clear bound on this minimal relativistic framework exists as the NN-scattering energy rises. A departure from the picture of elementary nucleons is necessary for NN-scattering near and above the pion production threshold ($T_{lab} \approx 270$ MeV) As a comparible upperbound, the energy at which the $^3S_1$ phaseshift crosses 0 is taken as the upperbound of the energy range for which an attempted fit of scattering phase parameters is to be made.

5.2 THE DYNAMICAL MODEL

A distinct preference has developed in the literature for Yukawa type interactions modulated by form factors to smear the singular behaviour at the origin. Here, the approach will be to take Gaussian ansatzes for both S and V as was the case in the previous two singlet chapters. This has the advantage of allowing extended ranges for these two Lorentz species *inside* 1 fm. capturing some of the flavour of the large extended nucleon without penalizing the physics outside this radius by attaching to Yukawa-tails associated with too low a meson mass. The only tail in the asymptotic region is that of OPEP. The Gaussian ranges can seem uncharacteristically large in comparison to the usual cut-off Yukawa ansatzes.

Indeed, a spline onto a Yukawa-tail where the decay length asymptotically remained faithful to the meson exchange mechanism would have been more realistic but the Gaussian can be viewed as the first order term in a unique expansion of oscillator eigen functions of whatever cut-off Yukawa species one prefers. Further shape embellishments can be implemented systematically if one wants to go beyond the zeroth order description. That will not be done here however. An additional benefit of the Gaussian is that the radial equations possess a reduced number of dynamically-dependent divergent terms of the $1/r$ and $1/r^2$ sort.

The scalar and vector interactions adopted are therefore simply:

$$S(r) = g_s e^{-(r/b_s)^2} \qquad (5.2.1)a$$

and

$$V(r) = g_v e^{-(r/b_v)^2} \qquad (5.2.1)b$$

The pion tail however is a sacrosanct part of any model should higher partial wave phaseshifts be fitted. If treated as a dialable parameter in such fits, the pion-nucleon coupling G^2 falls into quantitative agreement with the directly measured value: $G^2/4\pi \approx 14.5$ [64] (observed in pion nucleon scattering). The higher partial waves are not a subject of study here but a faithful reproduction of the OPEP tail should bring about convergence between this model and others which have successfully described these channels.

The pion exchange interaction in the near region is a question mark however. If a pseudoscalar coupling is used,$P(r) \approx G^2 e^{-m_\pi r}/r$, the interaction assures Klein paradox singularities at finite r. The differentiated quantities $P'(r)$ and $P''(r)$ occur in the precise combinations in the numerators of the potential-like terms of the large component radial equations required to have the proper spin dependence. It is the bare $P(r)$ that presents difficulty.

To curtail the interaction by damping it severely at < 1 fm. but not beyond introduces wild transients in the 1st and 2nd radial derivatives of the interaction -both of which show up prominently in the dynamical equations. If a long tempered damping factor is used to tame the pseudoscalar at low r, then the OPEP tail is not reproduced well until out beyond several fm.

In the case of an axial coupling, $A(r) \approx g^2 e^{-m_\pi r}/r$, the direct interaction, its 1st and 2nd derivatives also appear explicitly in the radial equations but $A(r)$ alone does not have the proper spin dependence. Once again,the 1st and 2nd derivatives occur in the exact spin-dependent combination required but the $g^2 \approx 0.08$ coupling of the bare axial interaction is severely reduced by a factor $\approx (m_\pi/2M_N)^2$ in these terms. There is an order of magnitude less tensor coupling between the S and D waves.

The above two paragraphs, the subject matter of which is expounded in Appendix III, would be highly discouraging *if* we chose to preserve the mesonic identification of the OPEP simply because the Breit equation offers a straightforward interpretation and recipe for its inclusion. Ask instead, how is the OPEP "derived" in its incorporation into the non-relativistic Schrödinger equation. It is lifted from field theory in 1st order perturbation and then written into the non-relativistic framework..

What is called for in the Breit equation is an abandonment of the apparently natural pseudoscalar or axial form and a similar putting in of OPEP by hand. We have the following co-ordinate-space ansatz:

$$V_{OPEP} = \vec{\sigma}_1 \cdot \vec{\sigma}_2 U_{\sigma\sigma}(r) + \frac{(\vec{\sigma}_1 \cdot \vec{r})(\vec{\sigma}_2 \cdot \vec{r})}{r^2} U_\Lambda(r)$$

The radial potentials $U_{\sigma\sigma}$ and U_Λ are attached to the large spinor component in the lowest order in exactly the way they appear in the Schrödinger equation. There are residual contributions to the OPEP from reducing the small and doubly-small spinor components but they are of an order $(m_\pi/2M_N)^2 \approx$ 1/200 smaller still and are inconsequential.

The specific radial dependence of $U_{\sigma\sigma}(r)$ and $U_\Lambda(r)$ is dictated by the traditional Yukawa tail from a distance of the pion Compton wavelength and outward ($\approx$ 1.43 fm.) Inside that length, they are governed by independent polynomial splines which match the asymptotic pieces to four radial derivatives. More specific details are relegated to Appendix III.

The net interaction in the model is therefore:

$$U_{total} = (\beta_1\beta_2)S(r) + (1 - \vec{\alpha}_1 \cdot \vec{\alpha}_2)V(r) + (\vec{\sigma}_1 \cdot \vec{\sigma}_2)U_{\sigma\sigma}(r) + (\frac{(\vec{\sigma}_1 \cdot \vec{r})(\vec{\sigma}_2 \cdot \vec{r})}{r^2})U_\Lambda(r) \tag{5.2.2}$$

where $U_{\sigma\sigma}(r)$ and $U_{\Lambda}(r)$ are as given by equations (A3.1)a, b with $\vec{\tau}_1 \cdot \vec{\tau}_2 = 1$ or by the spline expressions which follow shortly thereafter.

Referring back to equation (2.1.2) it is clear that the spin-spin part of the co-ordinate space OPEP does indeed resemble an axial coupling. The absence of a *S-D* coupling tensor part in the previous singlet chapters enabled the OPEP to be described in this way. An all encompassing model should have a consistent definition of this interaction across all channels.

In Sato's approach[27], the pseudoscalar identity of the OPEP is preserved. A particular conspiracy with an additional ficticious scalar meson (isovector) interaction is called upon to cancel the small r strength thus sidestepping the Klein paradox problem. The additional scalar is specifically designed to address this framework dependent problem. This is not an ideal circumstance. On the other hand here it will be found that if the phenomenological OPEP spin-spin and tensor potential splines at small r are allowed to become strong, then χ^2 fits of deuteron and scattering data tend to force the scalar and vector interactions into parametric forms where their identification with appropriate meson exchange also becomes dubious. This blurring of identity with meson-exchange must be viewed in the context of our utilitarian approach to the Breit equation. We essentially want a Schrödinger equation with a *P*-wave small component! The only connection between the identification of a particular interaction in the non-relativistic formalism and a meson-exchange mechanism is that established by a reduction from a rigourous relativistic framework.

This blurring is not such a loss for ficticious scalar mesons but the vector meson presence is a well established feature of more rigourous frameworks [58] and there are of course real vector mesons!

Here there is parametric freedom in the OPEP splines that could be viewed as extraneous parametric freedom akin to Sato's extra scalar meson. This is not quite accurate. The extra parametric freedom (2 parameters namely: $U_{\sigma\sigma}(r=0)$ and $U_{\Lambda}(r=0)$ ($or\ U'_{\Lambda}(r=0)$) are associated with the inner most unknown part of the $N-N$ interaction where undoubtedly many mechanisms *i.e.*, many degrees of freedom contribute. There is nothing contrived about them to cancel divergent terms brought about by other unrelated interaction species.

The model as established above provides a window on dynamics with basic ingredients:

i.) mid-sized spinor components with P-wave radial dependence

ii.) a rich variety of possible interference mechanisms of which $S \pm V$ is merely one. The phenomenological OPEP at small r also has a hand in the interference behaviour. The richness of possibility can be seen at a glance by examining the linear combinations $\mathcal{Q}_i(r)$, and $\mathcal{X}_i(r)$ of equations (2.2.3)*a-l*. In the triplet, only $\mathcal{Q}_1$ and $\mathcal{Q}_3$ do not appear.

The following section (5.3) details a quasi-model-independent study of the Breit framework, in particular as it applies to the a_t-r_m problem. An empirical relation between these two lengths akin to that of Klarsfeld *et al.* [15] is undertaken.

After that, the best fits obtained for the deuteron and low energy scattering data alone will be detailed (section 5.4). An attempt to further encompass the triplet scattering data will be made in section 5.5.

To generate the broad survey necessary for section 5.2, the 5-parameter space of $\{g_v, b_v, b_s, C_{\sigma\sigma 0}, C_{\Lambda 0}\}$ (where $U_{\sigma\sigma}(r=0) = g_\pi^2 C_{\sigma\sigma 0}$ and $U_{\Lambda}(r=0) =$

$g_\pi^2 C_{\Lambda 0}$) was randomly sampled within the bounds:

Vector coupling	g_v	$\subset \{0.0, 0.6\}M_N$	$= \{0.0, 563\}$MeV
Vector range:	b_v	$\subset \{1.0, 5.0\}M_N^{-1}$	$= \{0.210, 1.051\}$fm.
Scalar range:	b_s	$\subset \{3.0, 8.0\}M_N^{-1}$	$= \{0.630, 1.681\}$fm.
OPEP spin-spin @ $r = 0$:	$C_{\sigma\sigma 0}$	$\subset \{-5.0, 10.0\}M_N$	$= \{-4.695, 9.389\}$GeV
OPEP Λ-piece: @ $r = 0$:	$C_{\Lambda 0}$	$\subset \{-10.0, 5.0\}M_N$	$= \{-9.389, 4.695\}$GeV

For every point within this sample, a range of the scalar coupling g_s such that the Klein paradox was avoided was determined. Within this range, g_s was varied to bring about, if possible, a single isolated bound state at the deuteron binding. Such a state would also have to be from the particle-particle sector (as determined by an adiabatic turning off of all couplings). Singular interactions for finite r were allowed to creep up as high as $1.90M_N$ in energy (or ≈ 100 MeV below the deuteron bound state). This is also a rough bound on the encroachment of spurious states from the vacuum sector.

The alternative parameter varying choice for the OPEP tensor related interaction $U_\Lambda(r)$ is to bend its first radial derivative as opposed to the spline function value itself at $r = 0$. This leads to a tapered tensor OPEP (*i.e.*, tapered at both ends). A more limited survey of this parameter space was undertaken. The quantity $C_{\Lambda 1}$ controlling the spline, $(U'_\Lambda(r = 0) = g^2 C_{\Lambda 1})$ was allowed to fall within the bounds: $(-10, 0)$.

The random element to the survey was introduced to meet several objectives simultaneously. A uniform spread over the entire sample space could be achieved. In addition, a large number of points would ensure that many interference combinations would occur at random also. A simple grid

survey pattern of managable size tended to skip over narrow topological features in the χ^2 function on the space.

The lowest χ^2 for collective scattering and deuteron data were followed up with the simplex minimization algorithm amoeba from the Numerical Recipes software package.[65]. The results of these searchs form the content of sections 5.4 and 5.5.

The random survey allowed favourable configurations for the best overall fit, best low energy fit and best elastic scattering fit to appear quite quickly whereas a grid survey would have to have a serendipidous starting point to generate such points right away.

5.3 BROAD SURVEY OF MODEL INDEPENDENCE IN THE BREIT FRAMEWORK

As mentioned earlier, an intriguing aspect of the a_t-r_m discrepancy is the model independence of their linear relationship that is exhibited within the scope of realistic nonrelativistic local potential models. The reasons for the relationship were tied in the last section to the extreme light binding of the deuteron. As suggested by the singlet case of chapter 4, the relativistic framework also yields a nearly linear relationship between the two albeit slightly shifted from that of the non-relativistic one. There appears to be no corresponding derivation in the literature as of yet for the triplet effective range expansion with a relativistic equation. The presence of a D-state component in the non-relativistic case shifted the a_t-r_m line further to the right, away from the experimental datum, in one analysis.[47]

The numerical example of an artificial singlet deuteron of chapter 4 actually generates a a_t-r_m value to the left of the empirical non-relativistic

line. One might be misled to believe in the possibility of a resolution of this celebrated discrepancy. It must be kept in mind that comparing singlet to singlet, the relativistic corrections all direct the a_t-r_m relation *further* to the right.

Despite the lack of an analytic a_t-r_m relation for the relativistic triplet, we obtain, as a by-product of an extensive parameter search within the space discussed earlier, a set of 981 configurations (out of an attempted total of 1494) which produce an isolated particle-particle bound state at deuteron binding. The a_t and r_m data are plotted on two scales in Figure 5.3.1. Clearly, the relativistic triplet relation is shifted right, to larger r_m away from the accepted value. The small deviations below and above the line are due, in all likelihood, to the interaction shape dependent effects manifesting themselves at third order and beyond in the quantity (αr_o). Indeed, we see that the Breit triplet, with its typical D-state component of 5-6%, leads to an empirical relation *further* to the right than the empirical *non*-relativistic relation.

Taken at face value, this fact seems to be a striking indication that explicit nonlocality is required to resolve the discrepancy *and* that nonlocality must be even more drastic in a relativistic framework. There are several open ended questions however that require closer examination and through which the relativistic resolution hypothesis remains viable.

Firstly, the typical P-wave contribution to the overall normalization is 1%.(This is from the lower midsized components -of course.) Figure 5.3.1 supports the suggestion that the P-wave draws out and away from the S-state and/or D-state strength. Qualitatively, the results as illustrated indicate that dramatic shape effects are required in the Breit case. Pathological shapes are

required to resolve the problem in the nonrelativistic case but perhaps here another avenue remains open. It is possible that the P-wave components can be pulled in even further by a particular interaction interference configuration that must be precisely tuned and consequently was overlooked in the hit-and-miss scheme used to generate the data set. In fact the best overall χ^2_{loW} points (χ^2 over low energy W: experimental deuteron data and effective range parameters) from the random search were followed up. The best result (it appears there are several local χ^2 minima) is discussed in the next section.

A second possible opening lies in a re-analysis of the physics associated with the very *indirect* determination of r_m.[66] The quantity obtained from electron-deuteron scattering is the electromagnetic form factor $F(q^2)$. To two orders in momentum transfer, we have the equation:

$$F(q^2) = 1 - \frac{1}{6} r_{Ch}^2 q^2 + \mathcal{O}((q^2)^2) \tag{5.3.1}$$

From this quantity, the deuteron *charge* radius r_{Ch} is determined.

This quantity (r_{Ch}^2) must be further pared by finite size charge distributions of the proton and neutron components. Meson exchange corrections yield another uncertain but very likely small deduction.[67] More importantly, a subtraction commonly associated with the *relativistic* Zitterbewegung is present.[68] This can be concisely written:

$$r_m^2 = r_{Ch}^2 - r_p^2 - r_n^2 - \Delta r_m^2 \quad - \quad \left\{ \frac{3}{4m^2} \right\} \tag{5.3.2}$$

Now the r_m refers, in a non-relativistic state, to the quantity:

$$r_m^2 = \frac{1}{4} \int dr r^2 \{ u_{NR}(r)^2 + w_{NR}(r)^2 \}.$$

(Here $u_{NR}(r)$ and $w_{NR}(r)$ are the auxiliary radial amplitudes associated with S and D parts of the nonrelativistic wave function.) Clearly, referring back

to section 2.4 (chapter 2), the relativistic version of r_m involves P-wave contributions from $\vec{A}$,$\mathcal{J}$ *etc.* . so there is a question now, of overcorrection. The Zitterbewegung is a natural consequence of coupling upper and lower components which are automatically present in the Breit amplitude.

Further, an ambiguity in choosing the "proper" relativistic form factor $F(q^2)$ exists. A relation between the directly observable form factor and the rest frame Fourier transform of the density $\Psi^\dagger\Psi$ is in question at present.(The two are equivalent non-relativistically.) This will be addressed in an upcoming paper.[66] The question is unsettled as of now but there are compelling arguments to offer in support of a subtraction of $\frac{3}{8m^2}$ as a correction in the reduction of $r_{Ch}^2 \rightarrow r_m^2$ in place of the $\frac{3}{4m^2}$ correction when relating to the *rms* radius as determined in the *relativistic* system's *rest* frame.

The dotted $\pm 1\sigma$ box in the second panel of Figure (5.3.1) shifts to larger r_m and is to be compared with the relativistic data of that figure only. The shift would return the a_t-r_m discrepancy to the status quo *vis à vie* the Breit framework data of this work. One must note that the full sophisticated Bonn model in the Blankenbecler-Sugar reduction of the full relativistic Bethe-Salpeter equation falls dead center. If the $\frac{3}{8m^2}$ correction holds, this would indicate that a relativistic framework is indeed sufficient to resolve the problem but that the framework apparently lies above the tier of the Breit equation. Off shell effects accounted for in the field-theoretically based Bonn model could be responsible.

It remains to be determined however, whether or not shape dependence effects can be "tuned" by a sufficiently strong interference mechanism so as to greatly enhance the P-wave part *within* the Breit framework and model space of this work. That will be the subject investigated next.

By enhancement of the P-wave part, it is not meant that the contribution to the overall normalization from the lower mid-sized P-wave components should necessarily rise to meet the experimental data. The most resistant datum, by far, remains the matter radius r_m. A shift inward in these amplitudes may be all that is required. Indeed, Figure (5.3.2) seems to indicate that over the entire survey, rising P-wave representation beyond 1 % carries the fit *away* from the r_m-a_t point quite sharply.

Figure 5.3.1 Breit $^3S_1$ a_t and deuteron r_m: Broad survey results

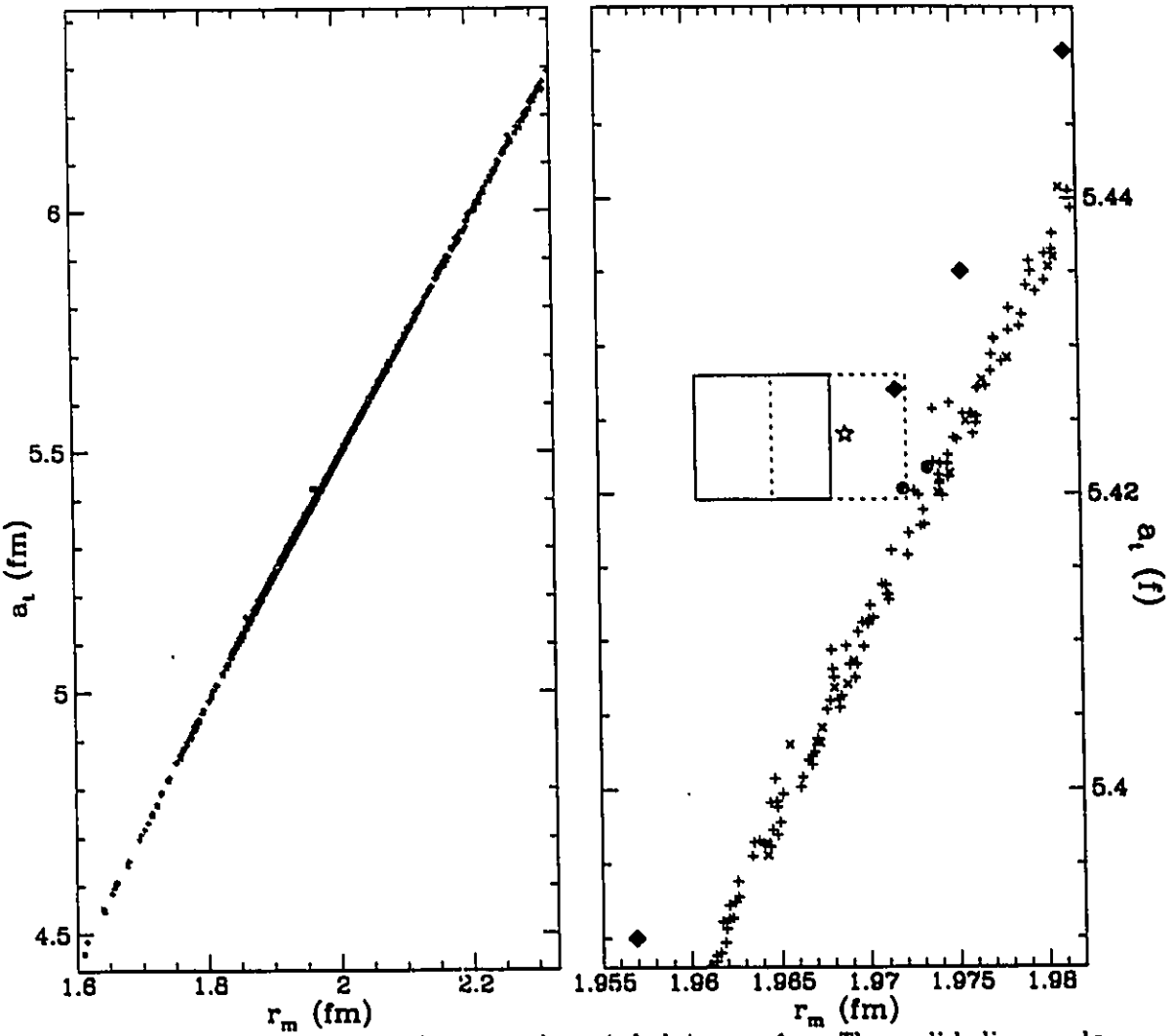

The solid line box marks the experimental datum ±1 σ. The solid diamonds from bottom left to top right are the nonrelativistic potentials: RSC, Paris, TRS, V_{14} (see Bhaduri *et al*[18]). The star is the full Bonn model[48] from the Blankenbecler–Sugar equation. The dotted box is that of the proposed relativistic model r_m for comparison with full Bonn model and broad Breit model survey: (+: untapered OPEP tensor part; ×: tapered OPEP tensor part) ⊕: Breit model A (untapered OPEP tensor); ⊗Breit model B (tapered OPEP tensor)

Figure 5.3.2 Relationship of $\chi^2_{\{a_t, r_m\}}$ and % p−wave (from broad survey)

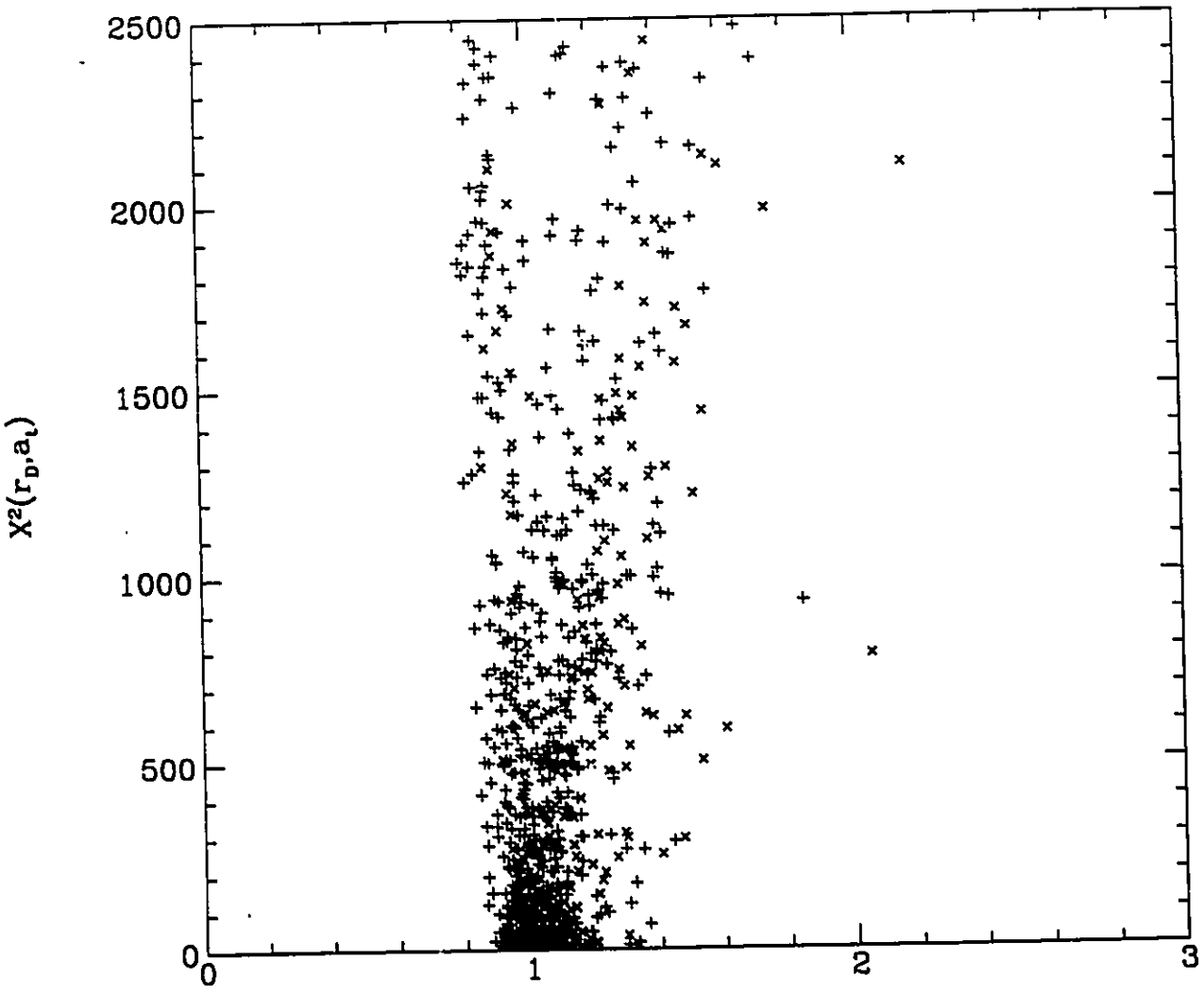

+ : Untapered OPEP survey configurations.
× : Tapered OPEP survey configurations.

% p−wave component

5.4 BREIT MODEL OF THE DEUTERON AND THRESHOLD SCATTERING.

The pursuit of a best fit to the deuteron and low energy scattering observables is implemented here with the following experimental data to serve as targets. All values are taken (or derived) as compiled in Table 3 in a 1987 paper by Machleidt *et al.* [58] The tabulated values are repeated here for easy reference but can be tracked from reference [58] and the experimental references therein. The deuteron binding of 2.224575 has an uncertainty of ±0.000009 MeV. Never-the-less, it is fitted exactly every time, thus eliminating the binding from the χ^2 function. This was done for technical reasons. (It is easier to fix the energy at the right binding and vary dynamical parameters to fix the radial amplitude continuity conditions than to scan for the binding energy for each configuration. The dynamical parameter varied each time to bring about the exact binding is the scalar coupling g_s. The quantity M_N is the average nucleon mass: 938.91897 MeV.

As noted in chapter 3, the magnetic properties are casually treated in this model. The magnetic moments of the proton and neutron are perhaps the most glaring signal of compositeness. The anomalous (Pauli) moments can probably be treated consistently in this framework by following a procedure outlined by Schwinger[69] but it would require a considerable leap in the sophistication of this model. The deuteron magnetic moment is not one of the prime targets to be fitted here consequently. We can generate a quasirelativistic value by simply weighting the orbital contribution of the lower P-wave components by the P-wave percentage but using the nonrelativistic formula.

This is not quite correct since the Schrödinger and Breit current operators are different but the magnetic moment is *not* included in the χ^2

fitting scheme but is calculated for completeness and at least a rough estimate of the P-wave contribution. The calculation of the non-relativistic moment:

$$\mu_{deut\,non-rel} = \mu_p + \mu_n - \frac{3}{2}(\mu_p + \mu_n - \frac{1}{2})P_D \qquad (5.4.1)a$$

(*e.g.*, see DeBenedetti[70] p.51,52) is supplemented by a contribution

$$\delta\mu_{deut} = -\frac{1}{2}(\mu_p + \mu_n - \frac{1}{2})P_P \qquad (5.4.1)b$$

by a straight forward extension of the discussion within those pages. Here, the individual moments for the proton and neutron are respectively: $\mu_p = 2.792847386\mu_N$ and $\mu_n = -1.91304275\mu_N$. [56] No meson exchange corrections are included in this formula either -so a lot of precision here is unexpected.

Table 5.4.1 DEUTERON AND EFFECTIVE RANGE DATA

Property	Symbol	Value / (Uncertainty)
Deuteron rest energy:	W_{deut}	1.997630725(49) M_N
D-state probability:	P_D	5(2) %
quadrupole moment:	Q_{deut}	0.2860(15) fm^2
magnetic dipole moment:	μ_{deut}	0.857406(1) μ_N
asymptotic S-state:	A_S	0.8846(16) fm$^{(-1/2)}$
asymptotic D/S ratio:	η	0.0271(8)
deuteron matter radius:	r_m	1.9643(38) fm
$^3S_1$ scattering length:	a_t	5.424(4) fm
$^3S_1$ effective range:	r_t	1.759(5) fm

Turning now to the quadrupole moment of the deuteron, nonrelativistically, the quadrupole operator: $\hat{Q} \equiv (\frac{r}{2})^2(3\cos^2\theta - 1)$ disappears (of course) in the pure S-state, mixes S and D parts as well as well as picking up a contribution from the D-component. This operator will not mix the odd P-part with the even S or D parts of the relativistic generalization but a direct P-P contribution will occur. A further subtlety is that the pure spatial operator $\hat{Q}$ will not intermix different spinor components even if they occur in the required S-D, P-P, or D-D combinations. In the tensorial spinor basis, we have:

$$\begin{aligned} Q_{deut} = \Big\{ & \langle \vec{Y}^1_{0,1}(\Omega,\sigma)|\frac{1}{4}(3\cos^2\theta - 1)|\vec{Y}^1_{0,1}(\Omega,\sigma)\rangle_\Omega \{\langle r^2\rangle_{u_-} + \langle r^2\rangle_{g_-}\} \\ & + \langle \vec{Y}^1_{2,1}(\Omega,\sigma)|\frac{1}{4}(3\cos^2\theta - 1)|\vec{Y}^1_{2,1}(\Omega,\sigma)\rangle_\Omega \{\langle r^2\rangle_{u_+} + \langle r^2\rangle_{g_+}\} \\ & + \langle \vec{Y}^1_{0,1}(\Omega,\sigma)|\frac{1}{4}(3\cos^2\theta - 1)|\vec{Y}^1_{2,1}(\Omega,\sigma)\rangle_\Omega \{\langle r^2\rangle_{u_-u_+} + \langle r^2\rangle_{g_-g_+}\} \\ & + \langle \vec{Y}^1_{1,1}(\Omega,\sigma)|\frac{1}{4}(3\cos^2\theta - 1)|\vec{Y}^1_{1,1}(\Omega,\sigma)\rangle_\Omega \{\langle r^2\rangle_a + \langle r^2\rangle_f + \langle r^2\rangle_\mathcal{J} + \langle r^2\rangle_{u_o}\} \Big\} \end{aligned} \tag{5.4.2}$$

The four angular pieces in order are 0, $-\frac{1}{20}$, $+\frac{1}{2\sqrt{50}}$, and the new P-contribution: $+\frac{1}{20}$.

To obtain relativistic analogs of A_s and η, we substitute the following quantities in place of the usual expressions:

$$A_s = \lim_{r\to\infty} \sqrt{u_-^2(r) + g_-^2(r)}re^{\alpha r} \tag{5.4.3}$$

and

$$\eta_{D/S} \equiv \frac{1}{A_s} \lim_{r\to\infty} \sqrt{u_+^2(r) + g_+^2(r)}re^{\alpha r}\{1 + \frac{3}{\alpha r} + \frac{3}{(\alpha r)^2}\}^{-1} \tag{5.4.4}$$

with

$$\alpha \equiv \sqrt{\frac{(W_{deut}^2 - 4\mu^2)(4M^2 - W_{deut}^2)}{4W_{deut}^2}}$$

Of course, the much focussed on quantity r_m is also obtained with a straightforward extension of its non-relativistic version.

$$r_m \equiv \left\{ \sum_{\alpha_i = \begin{smallmatrix} u_- \\ g_- \end{smallmatrix} ; \begin{smallmatrix} a \\ f \end{smallmatrix} \begin{smallmatrix} \mathcal{J} \\ u_0 \end{smallmatrix} ; \begin{smallmatrix} u_+ \\ g_+ \end{smallmatrix}} \langle r^2 \rangle_{\alpha_i} \right\}^{1/2} \tag{5.4.5}$$

Many of these relativistically altered expressions clearly offer a possible mechanism to provide interesting physics through the participation of the P-wave amplitudes.

With the aforementioned $\{S, V, U_{\sigma\sigma}, U_\Lambda\}$ model-ansatz calculated at many points in the space $\{g_v, b_v, b_s, C_{\sigma\sigma 0}, C_{\Lambda 0}\}$ the top five random fits were seeded as the starting points of several minimization threads. The best fit within the model with independent $U_{\sigma\sigma}$ and U_Λ splines, with both quantities finite at $r = 0$, certainly does well in fitting the deuteron and effective range quantities: $\{W_{deut}, Q_{deut}, A_s, \eta_{D/S}, r_m; a_t, r_t\}$ with a total $\chi^2_{low} = 5.32$, (or 0.76 per datum with 6 dynamical parameters in all excluding the pion tail which is taken as given). This will be referred to as Model-A.

The parametric freedom of the two OPEP generating species $U_{\sigma\sigma}(r)$ and $U_\Lambda(r)$ at *small* r however leads to several unnatural consequences. The fit is obtained when the simplex algorithm ramps up both $C_{\sigma\sigma 0}$ and $C_{\Lambda 0}$ controlling parameters of the OPEP strength at the origin. The phenomenological OPEP takes over as a dominant influence at small r. The long range nature of these interactions does not allow that unduly large influence to dissipate away very quickly as r becomes larger. The response of the scalar and vector interaction ranges then is to stretch out considerably so that the large powerful OPEP part can be countered somewhat.

Although Gaussian ranges b_s and b_v are somewhat naturally larger than characteristic cut-off Yukawa ranges for crudely equivalent fits, those

encountered here depart significantly from the characteristic meson ranges we associate with the vector and scalar (all be it ficticious) fields in more rigourous and successful relativistic frameworks. Table 5.4.2 lists the dynamical parameters and evaluated physical quantities as they occur in model-A.

The choice of shape of ansatz for $S(r)$ and $V(r)$ could perhaps have a detrimental effect that causes the χ^2 function to minimize with a push towards a $U_{\sigma\sigma}(r)$-$U_{\text{A}}(r)$ interference mechanism that drives the lower component P-wave amplitudes to become large and influential. A presumably better approach may have been to include more parametric freedom associated with the vector. There are indeed more than one vector meson playing a role in the microscopic process, we presume.

One of the reasons for allowing the one parametric freedom in $U_{\text{A}}(r)$ to be its value at the origin was to enable it to affect the fit of $\bar{\epsilon}_1$ (the $^3S_1$-$^3D_1$ mixing angle) near the elastic/inelastic scattering threshold. An attempt to fit the scattering data accompanied model selections in subsequent sections but here it was not a fitting criterion. Still as an artifact of those attempts to fit the entire $^3S_1$-$^3D_1$ channel over the body of deuteron and elastic scattering data, this freedom allowed for a better fit than the model-B with the tapered OPEP. The fact that the χ^2_{low} function at the end point in the parameter space is dominated by the same "sore thumb", r_m, as in the non-relativistic models may well be the sole reason for this excursion into a nonintuitive region of parameter space.

From a purely phenomenological perspective, however, Model-A provides us with enhanced P-wave amplitudes at small r and smooth interactions which lead to short range structure and important energy-dependence in the *effective* potentials of the Schrödinger-like equation (as represented in radial

Table 5.4.2 MODEL-*A*: PARAMETERS AND LOW ENERGY DATA

Dynamical model parameters			
Scalar coupling g_s:	$-0.19039\ M_N$	range b_s:	$6.47870\ M_N^{-1}$
Vector coupling g_v:	$+0.11040\ M_N$	range b_v:	$7.25557\ M_N^{-1}$
OPEP splines $U_{\sigma\sigma}\|_{r=0}$:	$+0.84604\ M_N$	$U_\Lambda\|_{r=0}$:	$-0.65352\ M_N$

Quantity	Numeric value	$\Delta\chi^2_{low}$ contribution
W_{deut}:	1,875.6134 MeV	0.000
Q_{deut}:	0.28587 fm^2	0.007
μ_{deut}:	0.82718 μ_N	*n.a.*
A_s:	0.88456 fm$^{-\frac{1}{2}}$	0.006
$\eta_{D/S}$:	0.02665	0.321
$\eta_{P/S}$:	0.03444	*n.a.*
r_m:	1.97198 fm	4.085
% D-state:	5.98083 %	0.241
% P-part:	1.16945 %	*n.a.*
a_t:	5.42028 fm	0.865
r_o:	1.75935 fm	0.005
P: (shape parameter)	-0.02066	*n.a.*
	total χ^2_{low}:	5.323

Figure 5.4.1a Breit low energy model solution A dynamic components (A = untapered OPEP tensor)

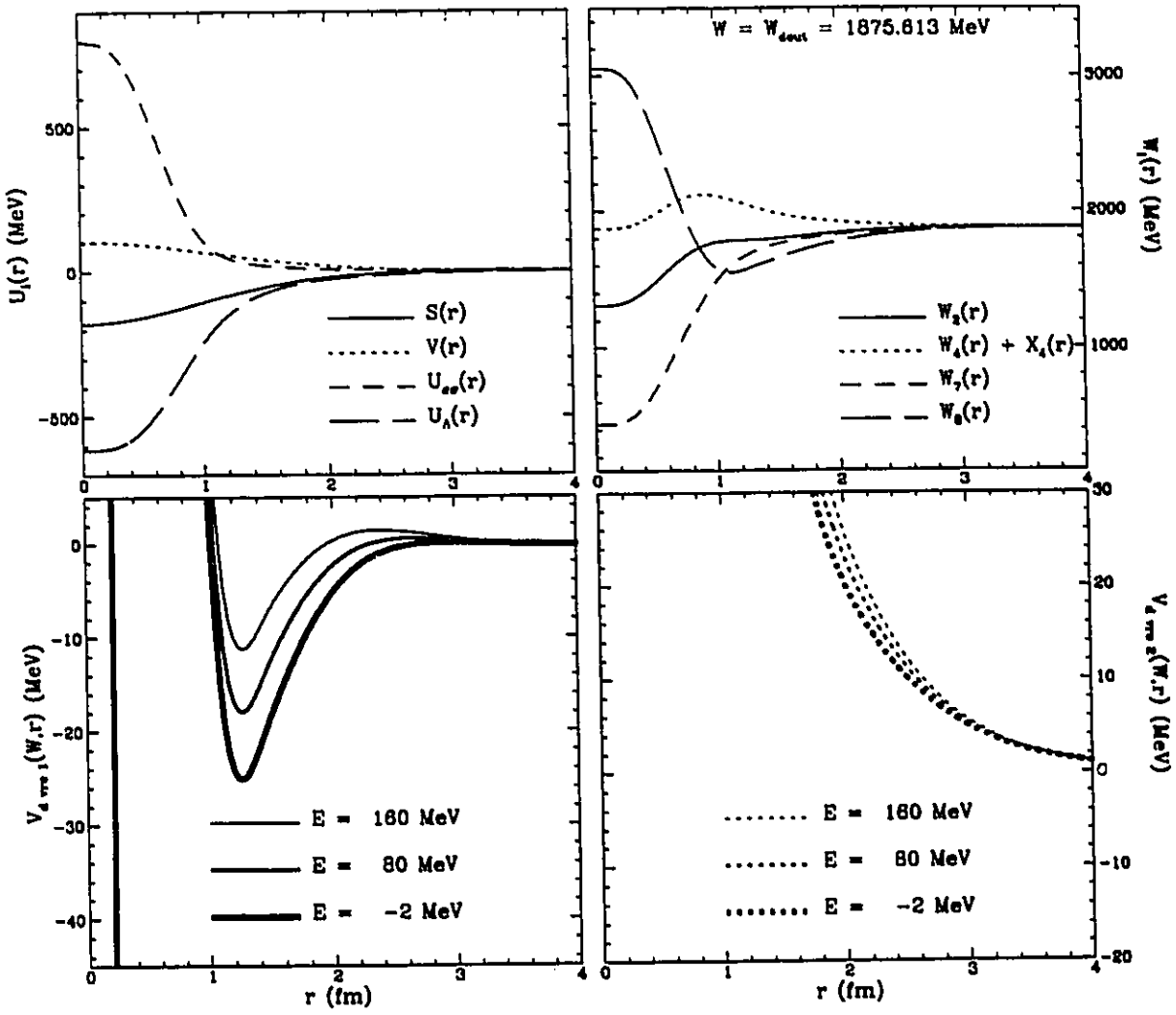

Top-left: The four simple dynamic model components
Top-right: The four crucial linear combinations which occur in denominators of equations (2.6.6)a & b (Zeroes of these quantities lead to the Klein paradox.)
Bottom-left/right: Energy dependent effective direct interactions of radial equations (2.6.6)a (solid lines) & (2.6.6)b (dotted lines). (E =W − $2M_n$)

Figure 5.4.1b Breit low energy model solution A dynamic components (continued)

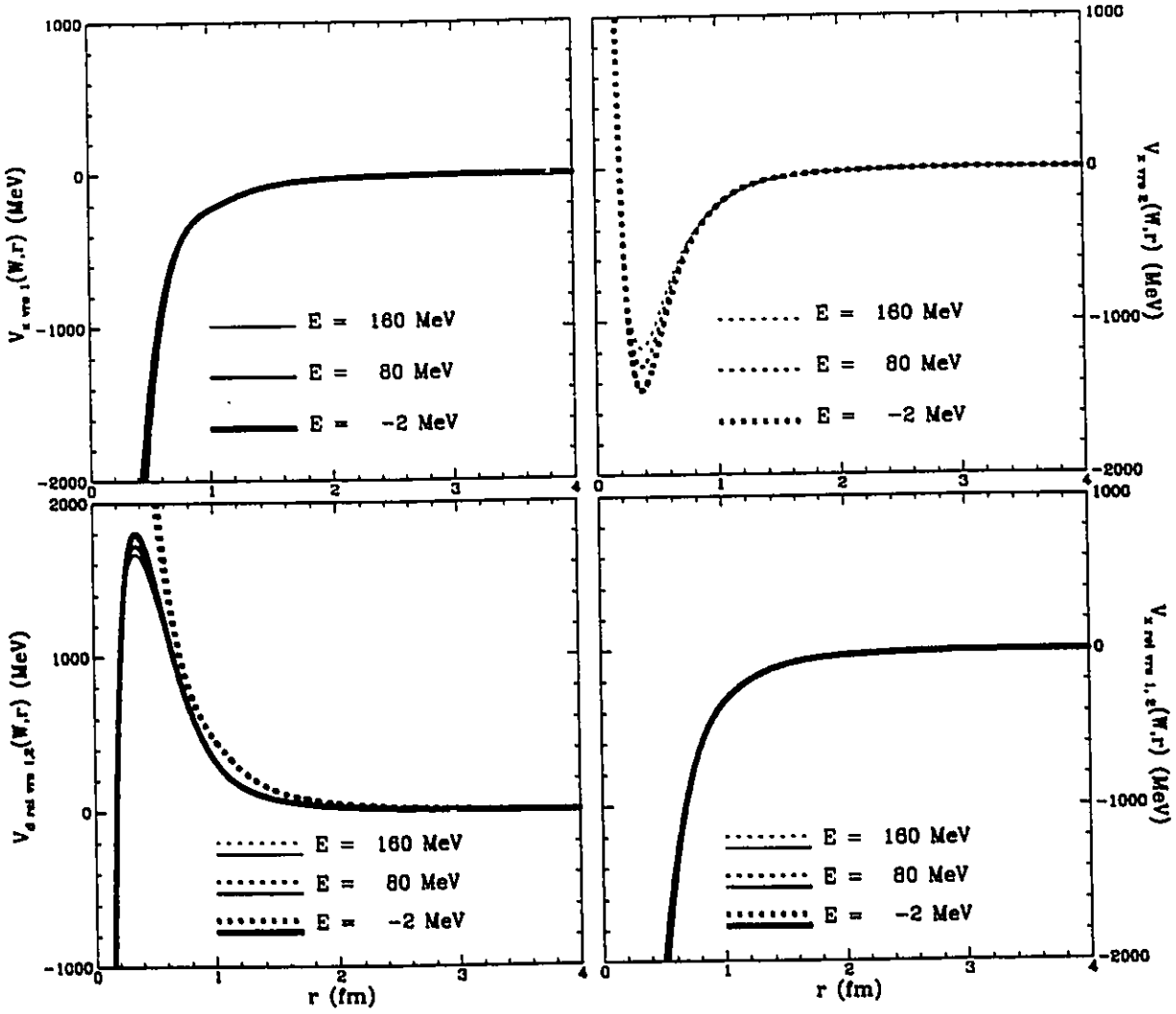

Top-left/right: Energy dependent effective S-D crossterm interactions of radial equations (2.6.6)a (solid lines) & (2.6.6)b (dotted lines).
Bottom-right/left: Purely relativistic interaction after subtraction of non-relativistic reduction in the direct and cross channels.

Figure 5.4.2 Breit radial amplitudes for Model A

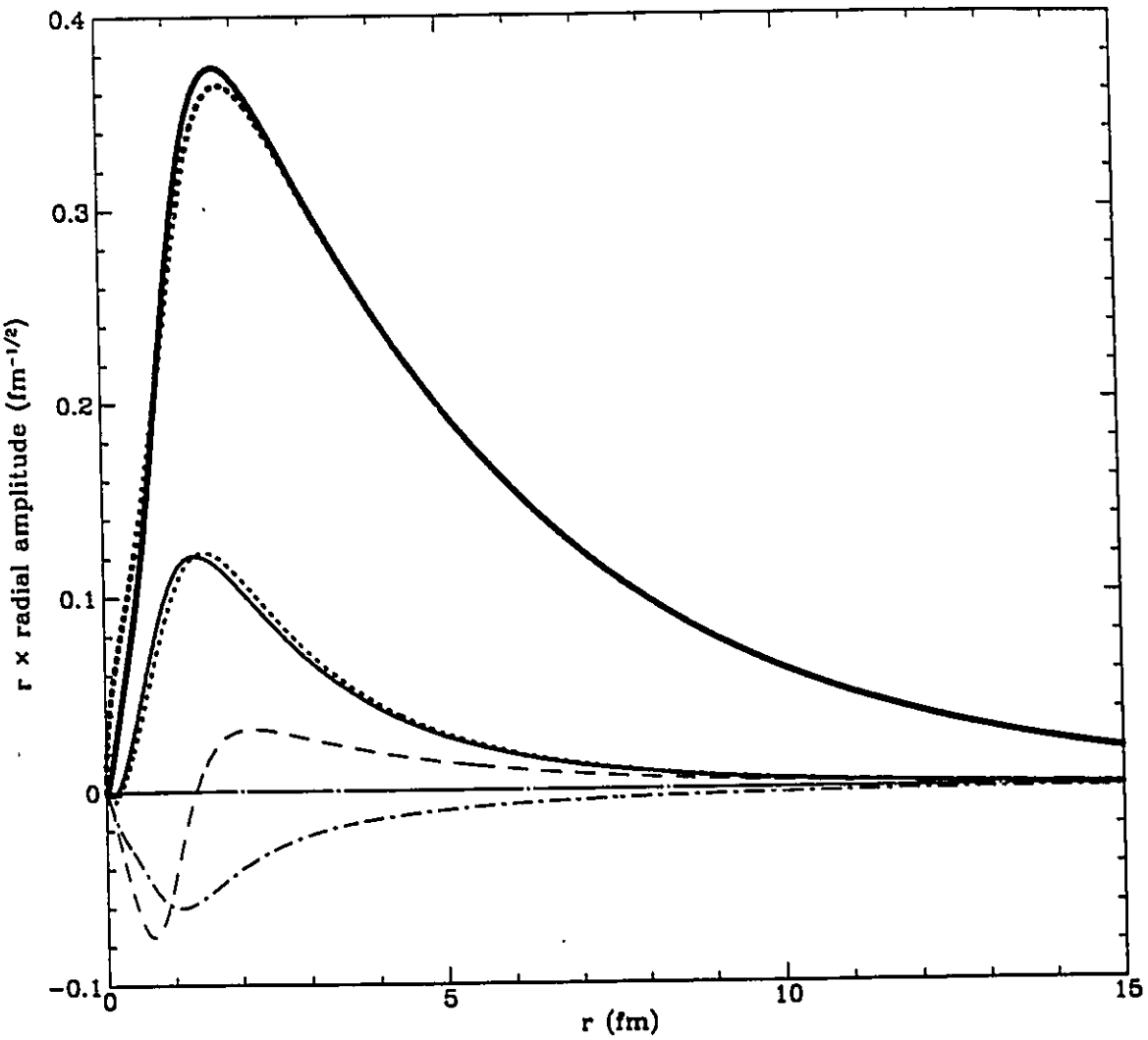

S–wave: ——— r $u_-(r)$, ····· r $g_-(r)$.
D–wave: ——— r $u_+(r)$, ····· r $g_+(r)$.
P–wave: – – – – –i r a(r), —— —— - –i r J(r).
.–.–.–.– –i r f(r), —.—.— –i r $u_o(r)$.

f and u_o hug the axis. (They would vanish identically for $m_n=m_p$).

form by equation (2.6.6)a and b.). It clearly hints at an interference mechanism. (See the top-left frame of Figure 5.4.1*a*.)

Since, in this section, the emphasis is purely to seek out a low energy fit of deuteron and effective range data, another attempt is called for which pays more homage to the consideration that $U_{\sigma\sigma}(r)$ and $U_{\Lambda}(r)$ are really dependent. Strictly speaking a single function, the Fourier transform of the nucleon-pion form-factor modulus squared $\mathcal{Z}_{\pi}(r)$ dictates entirely the spin-spin and tensor portions of the OPEP. Refer to equation (*A*3.1)*a* and *b*. The dependent relation for $r < m_{\pi}^{-1}$ was lifted to enable short range phenomenological part of the interaction to have a spin-spin and tensor portion not necessarily connected with the pion alone.

With the strict dependence between $U_{\sigma\sigma}(r)$ and $U_{\Lambda}(r)$ in place, it can be seen (Appendix 3) that finite $U_{\sigma\sigma}(r=0)$ implies $U_{\Lambda}(r=0)=0$. If the first radial derivative vanishes for $U_{c\sigma}(r)$ as it does for either OPEP ansatz here, then *both* $U_{\Lambda}(r=0)$ and $U'_{\Lambda}(r=0)$ would vanish.

The tapered tensor OPEP model, maintains the first restriction while flaunting the second. Hence, a flavour of extra short range phenomenology associated with direct spin-spin and direct tensor parts remains.

The tapered OPEP parameter search led to Model-B. Here, it is evident that the fit is slightly worse than with untapered OPEP but that once again, the χ^2_{low} is dominated by r_m. The dominant interference mechanism to enhance the *P*-amplitudes is indeed scalar/vector however. This bodes well for any followup study that utilizes additional vector degrees of freedom which may then have the ability to *tune* this interference to resolve the r_m-a_t discrepancy. The model dynamics is described in Table 5.4.3 and illustrated in Figures (5.4.3)*a* and *b*, with the solution illustrated in Figure (5.4.4).

Table 5.4.3 MODEL-B: PARAMETERS AND LOW ENERGY DATA

Dynamical model parameters			
Scalar coupling g_s:	$-0.33527\ M_N$	range b_s:	$4.08399\ M_N^{-1}$
Vector coupling g_v:	$+0.47501\ M_N$	range b_v:	$3.44266\ M_N^{-1}$
OPEP splines $U_{\sigma\sigma}\|_{r=0}$:	$+0.18511\ M_N$	$U'_\Lambda\|_{r=0}$:	$-0.11747\ M_N$

Quantity	Numeric value	$\Delta\chi^2_{low}$ contribution
W_{deut}:	1,875.6134 MeV	0.000
Q_{deut}:	0.28585 fm^2	0.009
μ_{deut}:	0.83256 μ_N	*n.a.*
A_s:	0.88601 fm$^{-\frac{1}{2}}$	0.780
$\eta_{D/S}$:	0.02670	0.253
$\eta_{P/S}$:	0.01399	*n.a.*
r_m:	1.97336 fm	5.687
% D-state:	5.36937 %	0.034
% P-part:	1.11153 %	*n.a.*
a_t:	5.42174 fm	0.319
r_o:	1.75489 fm	0.674
P: (shape parameter)	-0.00941	*n.a.*
	total χ^2_{low}:	7.771

Figure 5.4.3a Breit low energy model solution B dynamic components (B = tapered OPEP tensor)

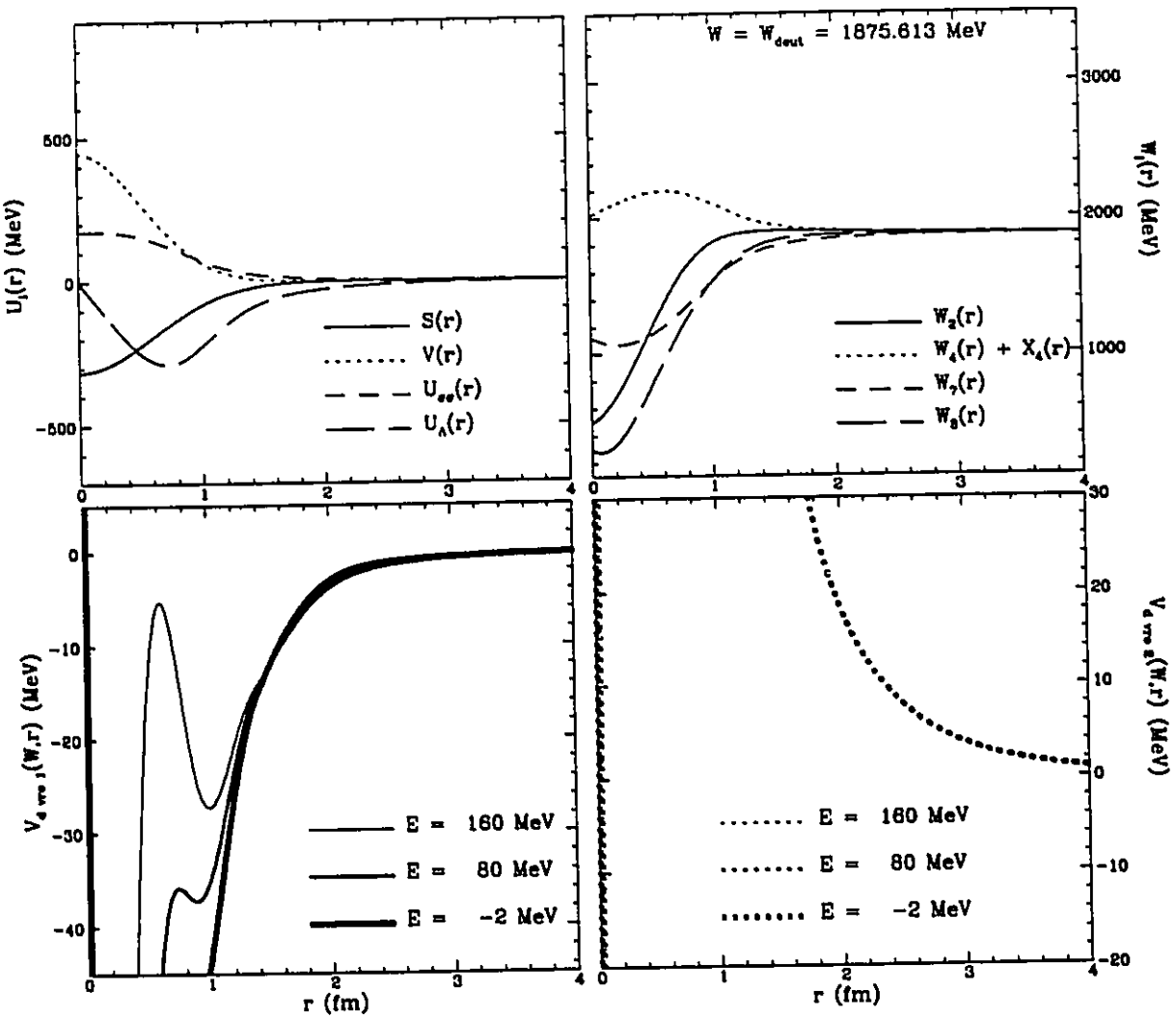

Top-left: The four simple dynamic model components
Top-right: The four crucial linear combinations which occur in denominators of equations (2.6.6)a & b (Zeroes of these quantities lead to the Klein paradox.)
Bottom-left/right: Energy dependent effective direct interactions of radial equations (2.6.6)a (solid lines) & (2.6.6)b (dotted lines). (E =W − $2M_n$)

Figure 5.4.3b Breit low energy model solution B dynamic components (continued)

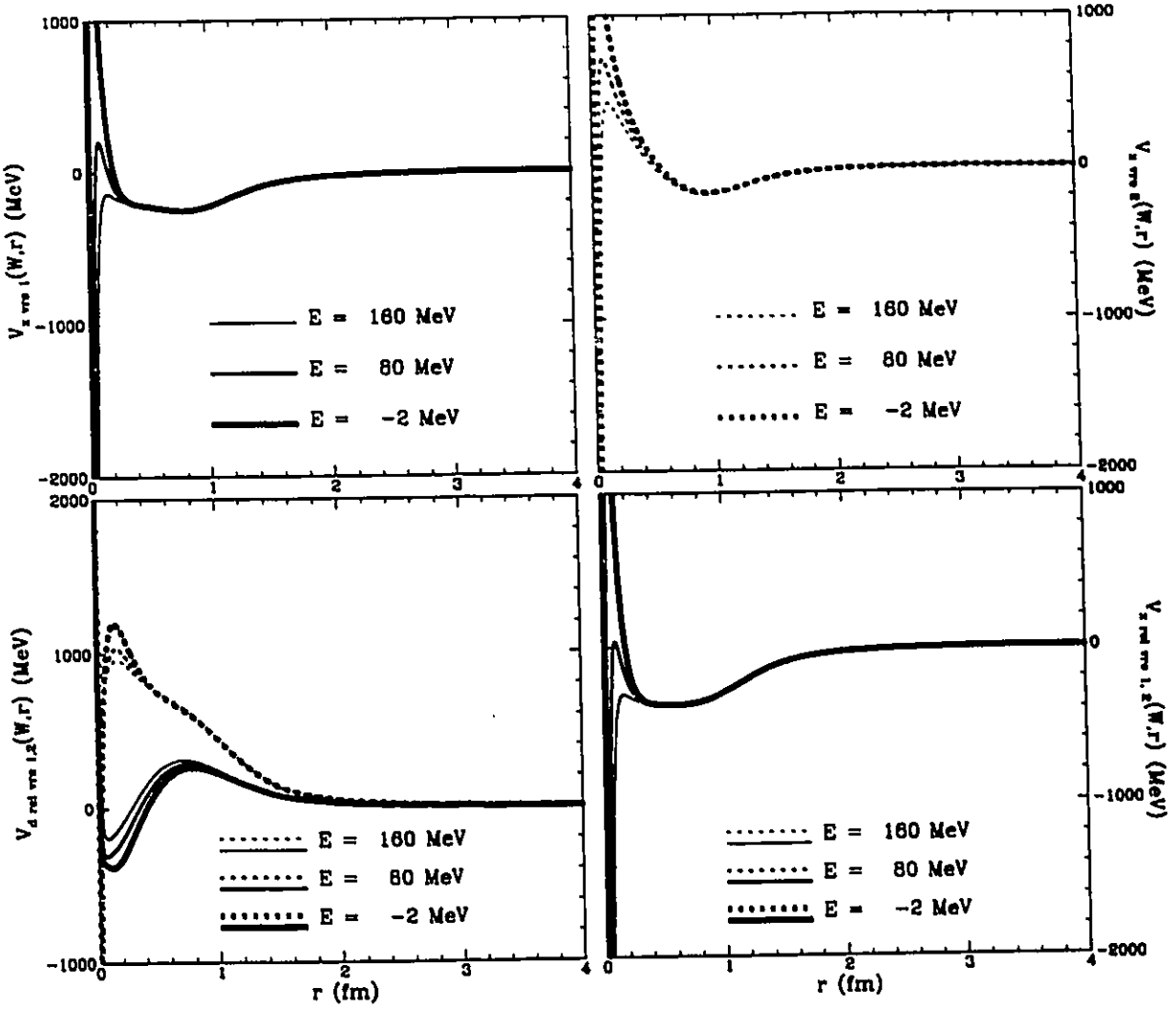

Top-left/right: Energy dependent effective S-D crossterm interactions of radial equations (2.6.6)a (solid lines) & (2.6.6)b (dotted lines).
Bottom-right/left: Purely relativistic interaction after subtraction of non-relativistic reduction in the direct and cross channels.

Figure 5.4.4 Breit radial amplitudes for Model B

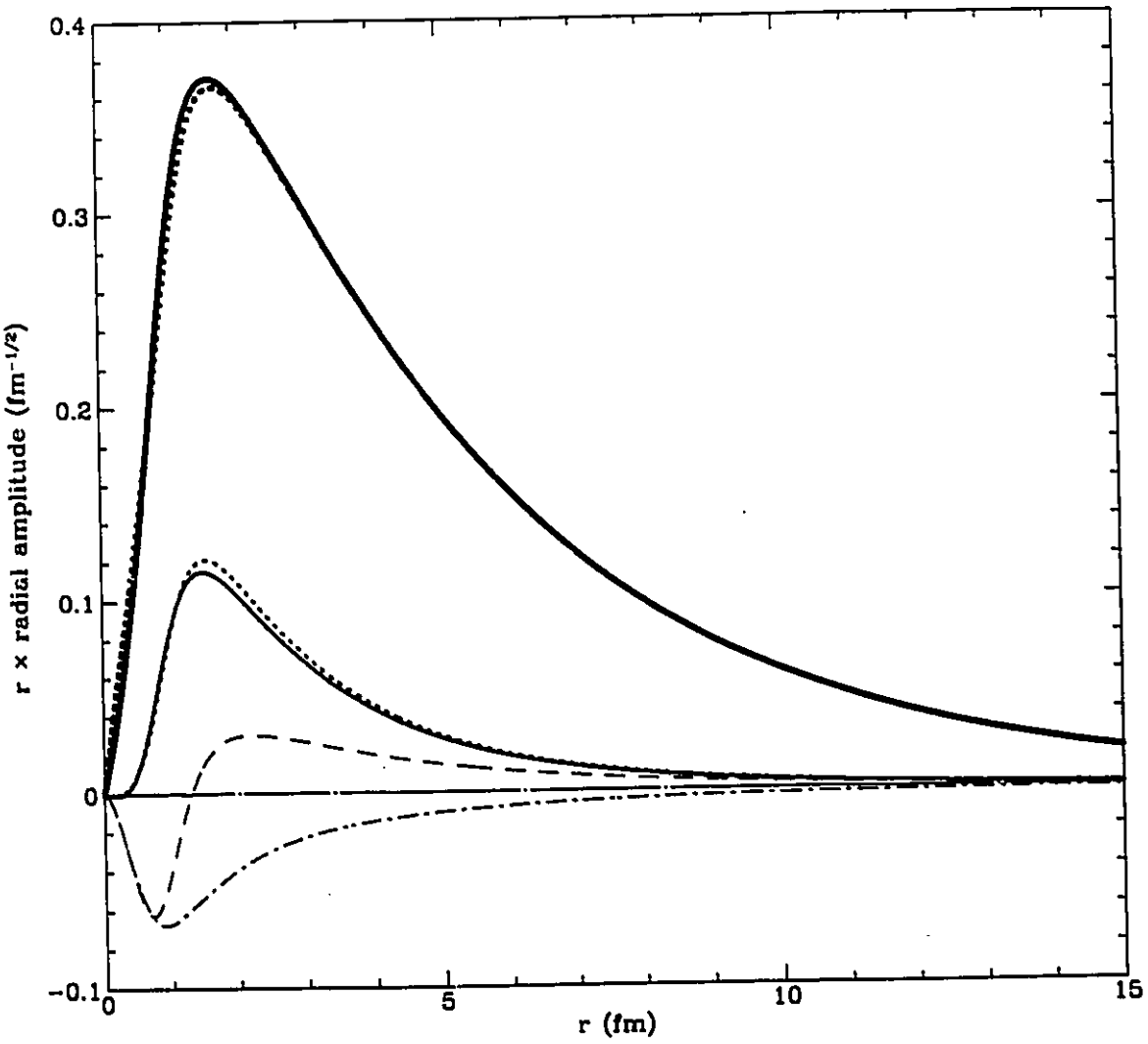

S–wave: ——— r $u_-(r)$, ····· r $g_-(r)$.
D–wave: ——— r $u_+(r)$, ····· r $g_+(r)$.
P–wave: – – – – –i r a(r), —— —— - –i r J(r).
.—.—.—.— –i r f(r), —·—·—·— –i r $u_o(r)$.

f and u_o hug the axis. (They would vanish identically for $m_n=m_p$).

Finally, although the elastic scattering data were not a fitting criterion beyond threshold, for completeness, the calculated phaseshifts of both models A and B are shown in Figure (5.4.5). The sign flip in $\bar{\epsilon}_1$ associated with model B illustrates clearly a trend that resulted in the abandonment of the $U_\Lambda(r=0)$ requirement in the first place. The sharp falling off of the D-wave phase shift (over-repulsion) is also a persistent feature of models within this parameter space.

Although the χ^2_{low} is dominated by r_m, the possibility that the proper r_m to relate to the Breit model *rms* radius (and the Blankenbecler-Sugar model for that matter) is shifted an amount close to 1 σ_{r_m} is intriguing. The best fit Breit model only just squeezes into the corner of the 1 σ box. Perhaps a not-so-contrived tuning of S-V interference may indeed move it into agreement with the experimental datum afterall. This is still an open question. The P-wave apparently does play a role in moving r_m in the right direction. Surprisingly, so does the D-wave part. The S-wave amplitudes alone would place r_m at 2.017 fm. for model-A. The P-wave *rms* radius alone is 1.194 fm., only slightly smaller than the D-wave value of 1.252 fm. Similarly, for model-B, we have values: 2.012, 1.216 and 1.314 for S,P, and D contributions respectively.

Figure 5.4.5 Breit models A and B: $^3S_1 - {}^3D_1$ phaseshifts

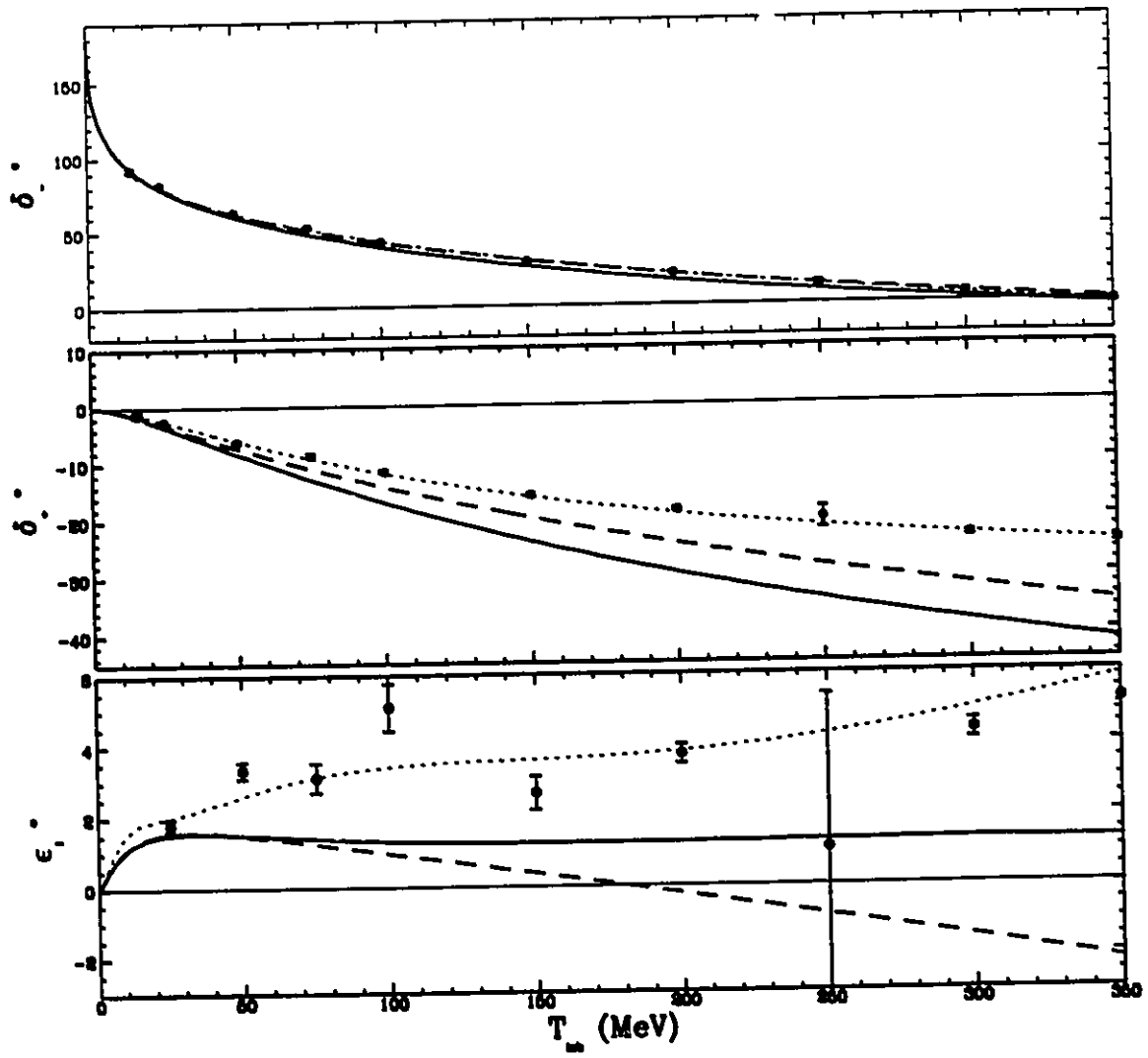

The solution set VL40 of SAID (Arndt *et.al.*[72]) is the fit of elastic scattering data below T_{lab} = 350 MeV. The light dotted line is their solution. (Points and error bars are their fixed energy solutions.) The best deuteron and effective range data fit, model–A, is shown as solid lines. The tapered OPEP solution model–B is represented by the dashed lines.

5.5 BREIT MODELS OF THE ${}^3S_1$ - ${}^3D_1$ NN SYSTEM

Since the scalar and vector ansatzes are simple Gaussians, a good fit of phaseshift data over the entire elastic scattering energy range is a bit too ambitious. A seemingly attainable goal would be to fit the phaseshifts at two widely separated energies: threshold and W_x: the energy at which the ${}^3S_1$ phaseshift crosses 0. Provided that the interactions are smooth and not pathological, smooth fitting phases like the S-wave of Figure (5.4.5) which do fit intermediate energies may arise anyway. If not, then intermediate points could probably be brought into line by additional shape enhancements on the basic ansatz.

The attempted total fit within the basic Gaussian model (+ OPEP) was therefore driven by a minimization algorithm acting on a quantity χ^2_{tot} which is χ^2_{low} of the previous section with an additional contribution:

$$\chi_{hiW} \equiv \sum_{\pm} \left(\frac{\bar{\delta}_{\pm}(W_x) - \bar{\delta}_{\pm \mathrm{targ}}(W_x)}{\Delta\bar{\delta}_{\pm}} \right) + \left(\frac{\bar{\epsilon}_1(W_x) - \bar{\epsilon}_{1\mathrm{targ}}(W_x)}{\Delta\bar{\epsilon}_1} \right)$$

Here the following target values were adopted.

$$\bar{\delta}_{-\mathrm{targ}}(W_x) = 0 \pm 0.0122$$

$$\bar{\delta}_{+\mathrm{targ}}(W_x) = -0.4211 \pm 0.0084\mathrm{rad} \qquad (= -24.12^\circ)$$

$$\bar{\epsilon}_{1\mathrm{targ}}(W_x) = +0.0971 \pm 0.0066\mathrm{rad} \qquad (= +5.56^\circ)$$

$$W_x = 2.17010 M_N \qquad (= 2037.550\mathrm{MeV})$$

The errors were estimated at W_x using a weighted average of Arndt *et al.* 's[71] fixed energy errors at $T_{lab} = 325$ MeV and $T_{lab} = 350$ MeV.

When one is attempting to simultaneously model the elastic scattering data[72] as well as the deuteron properties, a dichotomy arises. The

best deuteron fits, models A and B, yield an over-repulsed D-wave scattering phaseshift as can be seen in Figure (5.4.5). To offset this, the parameter search must provide more attraction for the D-wave while not seriously affecting the S-wave properties which are already reasonably described over the entire range. Hence, there is a preferential drive towards parameter configurations with $U_\Lambda(r)$ playing a larger role at small r (or higher energy, $T_{lab} \approx 350\text{MeV}$). Recall that to lowest order, U_Λ is the sole source of different dynamics in the S and D channels.

The parameter search is always restricted to select a range of g_S such that singular effective interactions at finite r are avoided. Parametrically the most severe danger is posed by g_V which can be large and positive (and is so in the Bonn model[58]). Of the four key quantities which appear in the denominators of radial equations (2.6.6)a and b, $\mathcal{W}_s(r)$ which includes the combination $W - 4V(r)$ proves to be the most restrictive on g_V.

This restriction apparently (as encountered in this study) is too dominating and as the search algorithm samples repulsive $U_{\sigma\sigma}(r)$ values at low r, it finds favourable configurations (lower χ^2_{tot}) in which the role of $U_{\sigma\sigma}(r)$ at small r is directed to offsetting $V(r)$ in the quantity $\mathcal{W}_s = W - 4V(r) + 3U_{\sigma\sigma}(r) + \ldots$. Eventually, the completely phenomenological $U_{\sigma\sigma}(r)$ (for small r) provides essentially *all* the short range repulsion while g_V is actually driven to *negative* values. This now harkens back to the observations of earlier investigators, including Breit[10] from the onset, that the equation generated spectra which departs in second order (in couplings) from field theory (or empirical data at the time). A departure in second order in a strong coupling $g_V \sim \mathcal{O}(1)$ could easily leave a negative coupling as a signature of this disorder. The

apparent consistent movement of the parameter search into this regime is a black mark against the Breit choice of framework.

The exercise of obtaining best fit scattering solutions is still worthwhile however in that the influence of universal relativistic elements, such as non-traditional energy dependences in the effective interactions of the radial equations, can be gauged and held up in comparison to the conventional view of the nuclear force as a hard repulsive core with soft intermediate attraction. The relative softness of interactions in the relativistic formalism is likely to survive this simple quantum-mechanical picture. Extra repulsion is generated by ramping up the energy in the effective equations here in the triplet as was the case in the charge-symmetry breaking investigation of the $^1S_0$ system of chapter 3.

The fact that soft interactions are forced upon the Breit equation by the avoidance of the Klein paradox scenario is quite separate from this. The suggested energy scale of the dynamics in this work is apparently not soft enough. Ultimately though, the theme of energy dependent interactions suggests an attractive viable resolution of the saturation/binding difficulties with nuclear matter.[73] The effect is achieved here with the correct qualitative behaviour. (Higher energy ramps up the internucleon repulsion.)

There are two results to be presented here. As before, the two alternative OPEP short range splines are employed. The best overall fit hit randomly in the broad survey had $\chi_{tot} \sim 420$ in the untapered OPEP tensor case and ~ 475 for the tapered OPEP tensor spline. These starting points had positive $g_V \sim +0.15 - 0.30$ to begin with but soon the simplexes were drawn to highly positive $U_{\sigma\sigma}$ and negative V.

The best obtained model fit with the untapered OPEP tensor will be referred to as model-C while the tapered OPEP tensor case will be designated model-D.

Altogether, six seed points were tested with the minimization algorithm. Five attempts were with the untapered OPEP and three of these were "chosen" points far apart in the space particularly *w.r. to* the starting at the best two points of the random survey. After achieving five end or aborted solutions with negative g_V, the sixth attempt with the tapered OPEP ansatz was made. The search trajectory joined the other five by driving g_V down and $U_{\sigma\sigma}(r=0)$ up.

The dynamical parameters and "deuteron" properties are presented in Table 5.5.1 for model-C. The interactions and effective interactions as they occur in model-C are illustrated in Figures (5.5.1)*a* and *b*. As the table shows, the low energy and deuteron fit is sacrificed for very marginal gain on the high end of the elastic scattering. The wave-functions are presented in Figure (5.5.2). It should be noted that although *none* of the interactions as indicated in the top left frame of Figure (5.5.1)*a* have a particularly *short* range repulsion, the S-wave radial equation has an effective interaction with a deep well and steep $\frac{1}{r^2}$ repulsion below 1 fm. This is a signature of highly non-additive interactions entering the relativistic equation for amplitudes $v_-(r), v_+(r)$.

The tapered OPEP tensor approach offers the better overall fit this time. Model-D fits the deuteron and effective range data along with the 3 scattering parameters at $W = W_s$ to within a χ^2_{tot} of 200. This very modest result is of course brought about by seemingly unphysical combinations of $V(r)$ and $U_\Lambda(r)$. Table 5.5.2 and figures 5.5.3*a* and *b* illustrate this choice.

The one out of four physically believable models of these last two sections, model-B, with the conventional $S\&V$ interference mechanism, does not do well with the scattering. The deflection back to the axis (and frequent sign change) of the mixing parameter ϵ_1 unfortunately seems a persistent feature of the tapered OPEP tensor ansatz. There are exceptions however -notably Model-D.

Table 5.5.1 MODEL-*C*: PARAMETERS AND LOW ENERGY DATA

Dynamical model parameters			
Scalar coupling g_s:	$-0.65994\ M_N$	range b_s:	$3.59875\ M_N^{-1}$
Vector coupling g_v:	$-0.50662\ M_N$	range b_v:	$1.11341\ M_N^{-1}$
OPEP splines $U_{\sigma\sigma}\|_{r=0}$:	$+0.90487\ M_N$	$U_\Lambda\|_{r=0}$:	$+0.33509 M_N$

Quantity	Numeric value		$\Delta\chi^2_{low}$ contribution
W_{deut}:	1,875.6134	MeV	0.000
Q_{deut}:	0.28909	fm^2	4.244
μ_{deut}:	0.83120	μ_N	*n.a.*
A_s:	0.88824	fm$^{-\frac{1}{2}}$	5.176
$\eta_{D/S}$:	0.02683		0.114
$\eta_{P/S}$:	0.03444		*n.a.*
r_m:	1.97912	fm	15.21
% D-state:	5.52442	%	0.069
% P-part:	0.99510	%	*n.a.*
a_t:	5.43365	fm	5.820
r_o:	1.77154	fm	6.290
P: (shape parameter)	-0.01169		*n.a.*
		total χ^2_{low}:	37.38

Figure 5.5.1a Breit model solution C dynamic components (C = untapered OPEP tensor)

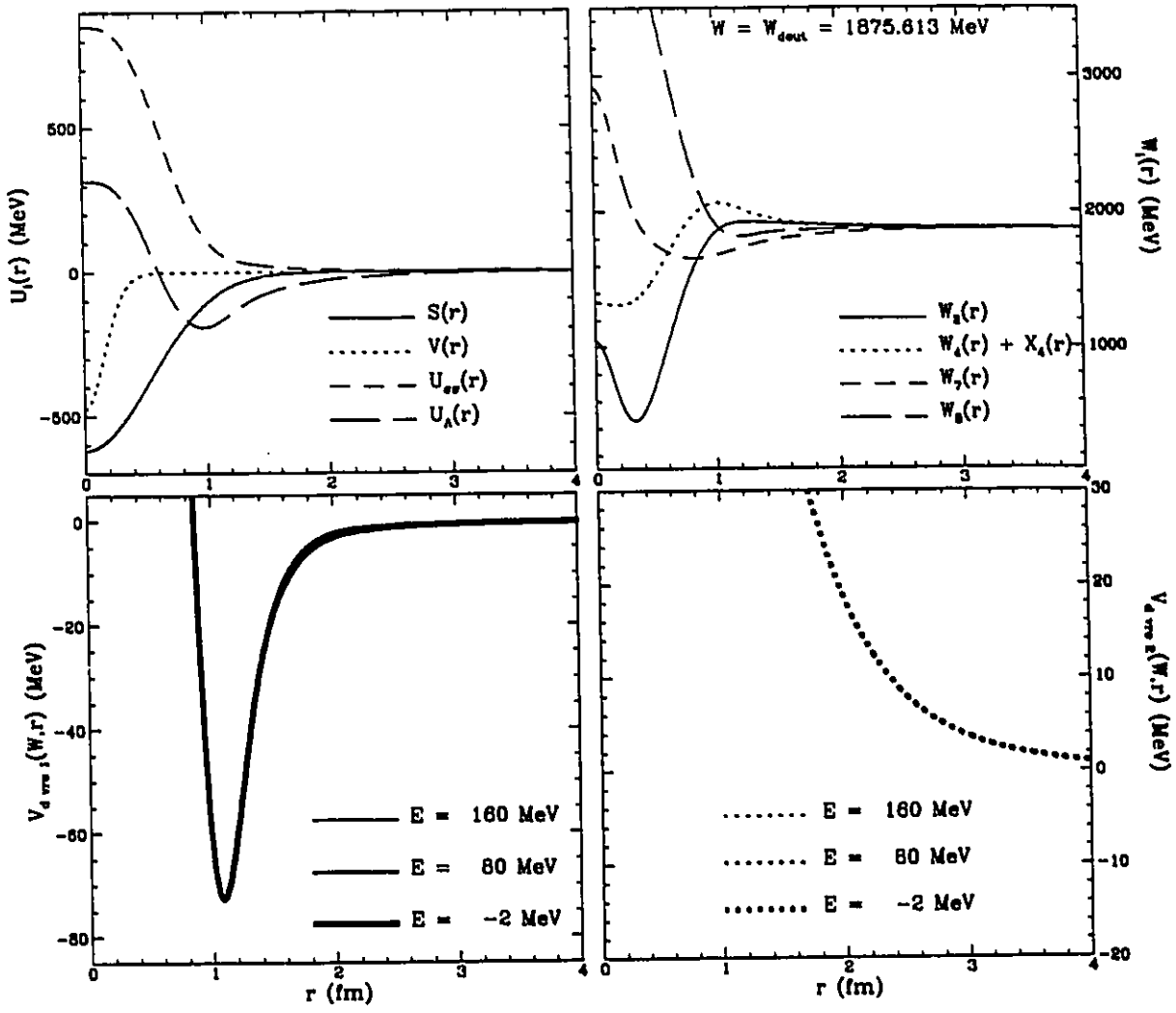

Top-left: The four simple dynamic model components
Top-right: The four crucial linear combinations which occur in denominators of equations (2.6.6)a & b (Zeroes of these quantities lead to the Klein paradox.)
Bottom-left/right: Energy dependent effective direct interactions of radial equations (2.6.6)a (solid lines) & (2.6.6)b (dotted lines). (E =W - $2M_n$)

Figure 5.5.1b Breit low energy model solution C dynamic components (continued)

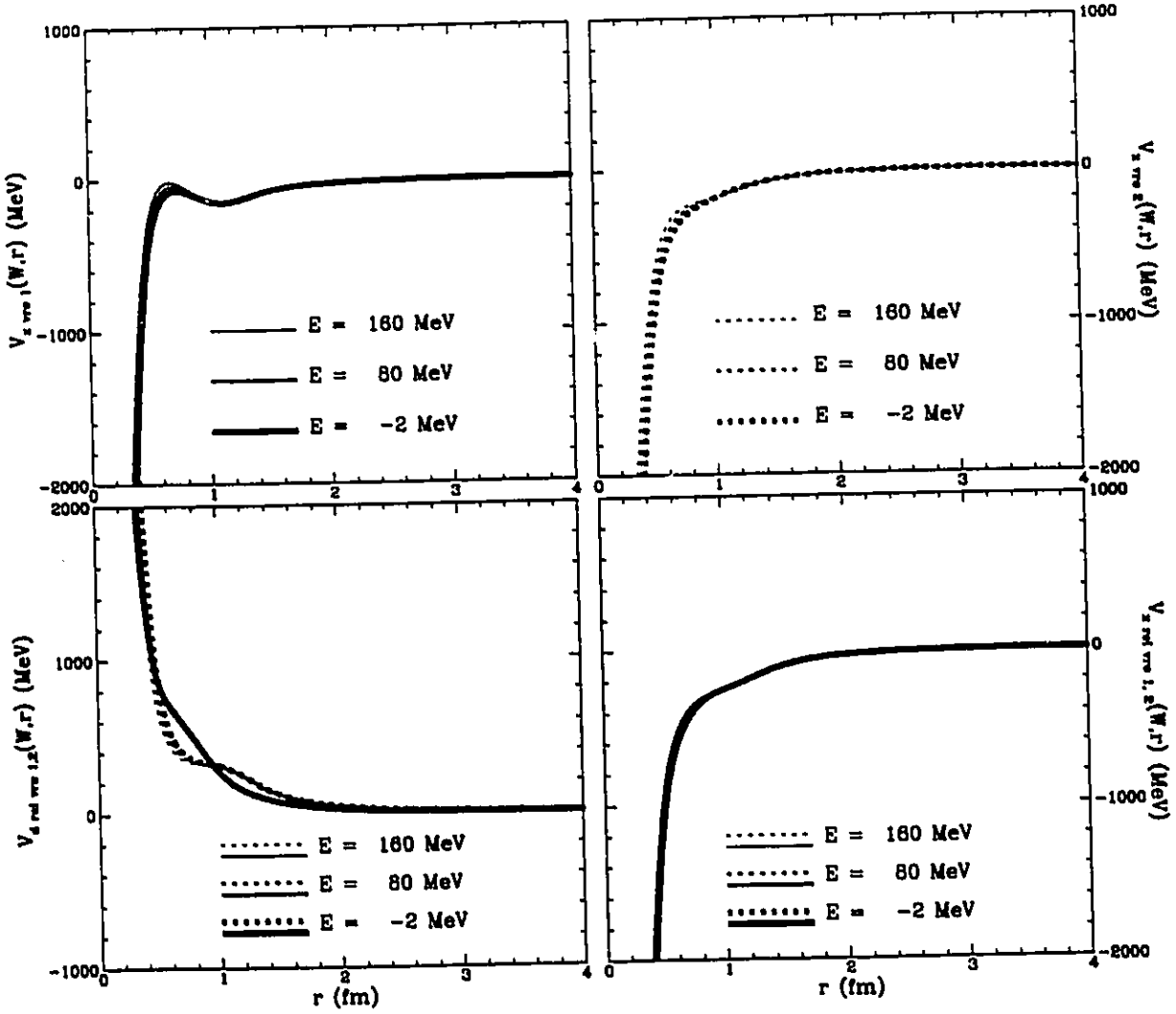

Top-left/right: Energy dependent effective S-D crossterm interactions of radial equations (2.6.6)a (solid lines) & (2.6.6)b (dotted lines).
Bottom-right/left: Purely relativistic interaction after subtraction of non-relativistic reduction in the direct and cross channels.

Figure 5.5.2 Breit radial amplitudes for Model C

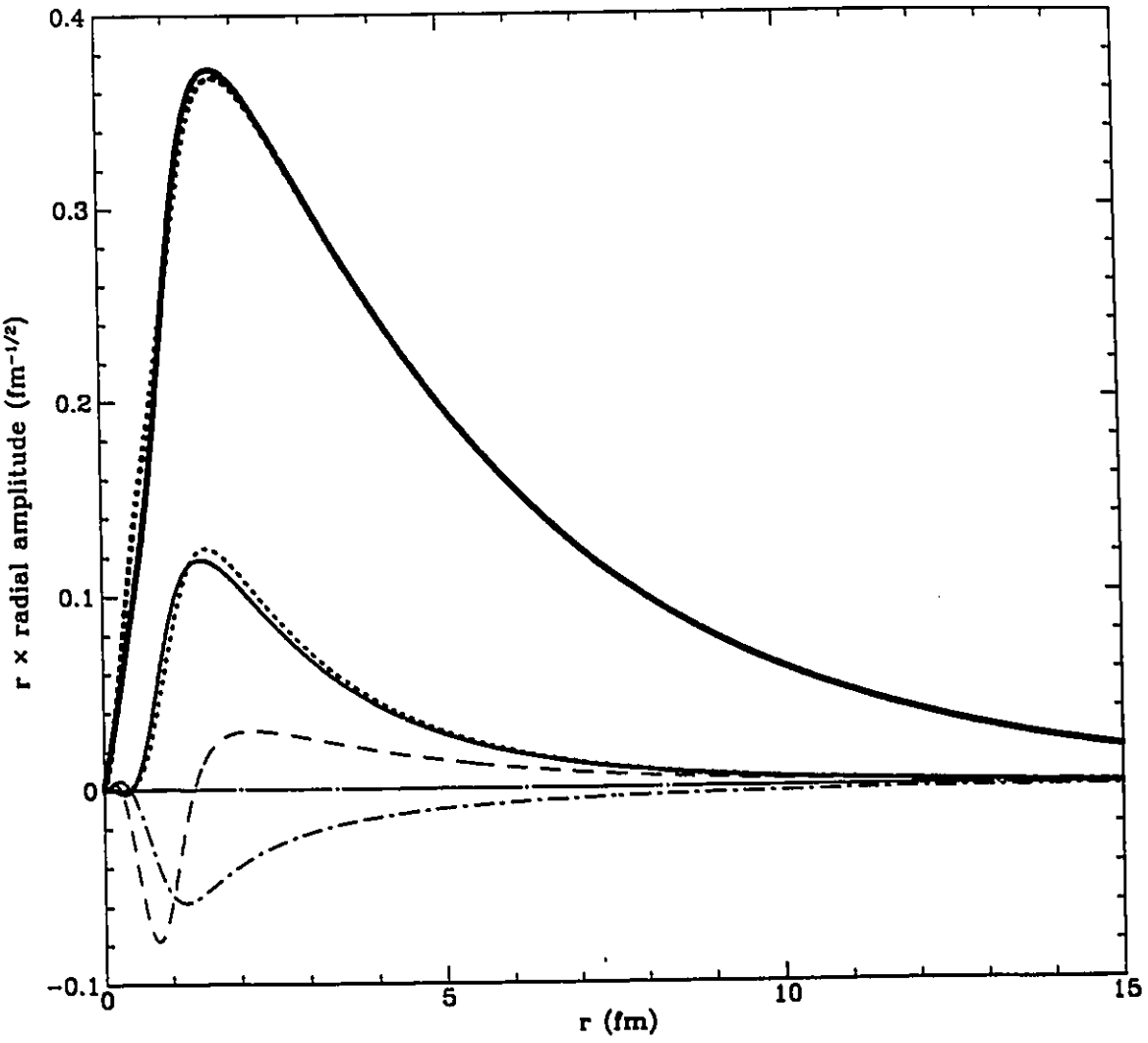

S–wave: ——— r $u_-(r)$, ... r $g_-(r)$.
D–wave: ——— r $u_+(r)$, ... r $g_+(r)$.
P–wave: – – – – –i r a(r), —— —— - –i r J(r).
.–.–.–.– –i r f(r), ——·——·—— –i r $u_o(r)$.

f and u_o hug the axis. (They would vanish identically for m_n=m_p).

Table 5.5.2 MODEL-*D*: PARAMETERS AND LOW ENERGY DATA

Dynamical model parameters			
Scalar coupling g_s:	$-0.07494\ M_N$	range b_s:	$3.87240\ M_N^{-1}$
Vector coupling g_v:	$-1.17388\ M_N$	range b_v:	$3.15588\ M_N^{-1}$
OPEP splines $U_{\sigma\sigma}\|_{r=0}$:	$+1.30468\ M_N$	$U'_{\Lambda}\|_{r=0}$:	$+0.12231 M_N$

Quantity	Numeric value	$\Delta\chi^2_{low}$ contribution
W_{deut}:	1,875.6134 MeV	0.000
Q_{deut}:	0.29752 fm^2	58.98
μ_{deut}:	0.82037 μ_N	*n.a.*
A_s:	0.88542 fm$^{-\frac{1}{2}}$	0.263
$\eta_{D/S}$:	0.02754	0.302
$\eta_{P/S}$:	0.03444	*n.a.*
r_m:	1.97488 fm	7.752
% D-state:	6.75591 %	0.771
% P-part:	1.00407 %	*n.a.*
a_t:	5.41918 fm	1.452
r_o:	1.75130 fm	2.372
P: (shape parameter)	-0.00900	*n.a.*
	total χ^2_{low}:	71.19

Figure 5.5.3a Breit model solution D dynamic components (D = tapered OPEP tensor)

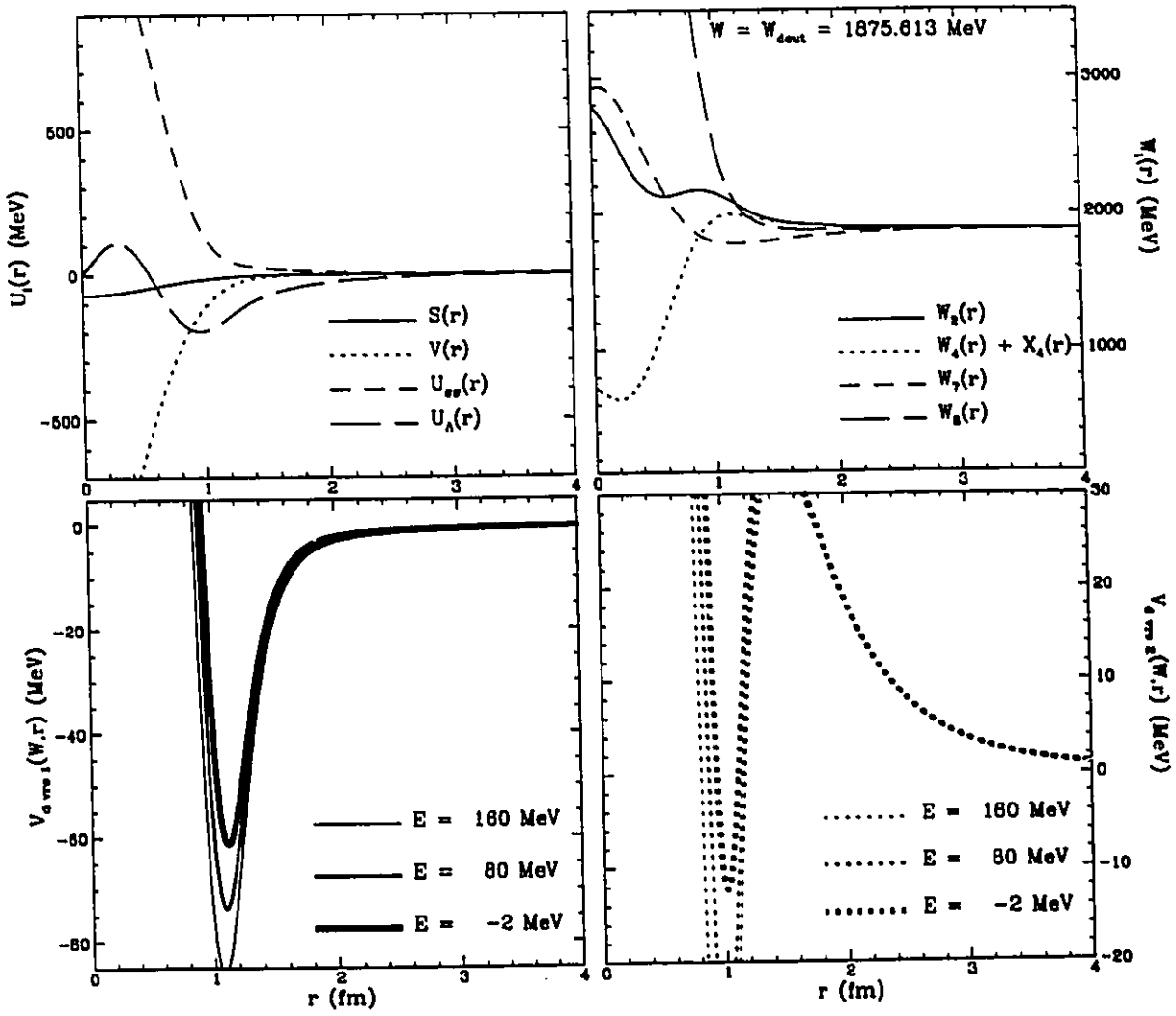

Top-left: The four simple dynamic model components
Top-right: The four crucial linear combinations which occur in denominators of equations (2.6.6)a & b (Zeroes of these quantities lead to the Klein paradox.)
Bottom-left/right: Energy dependent effective direct interactions of radial equations (2.6.6)a (solid lines) & (2.6.6)b (dotted lines). (E =W − $2M_e$)

Figure 5.5.3b Breit low energy model solution D dynamic components (continued)

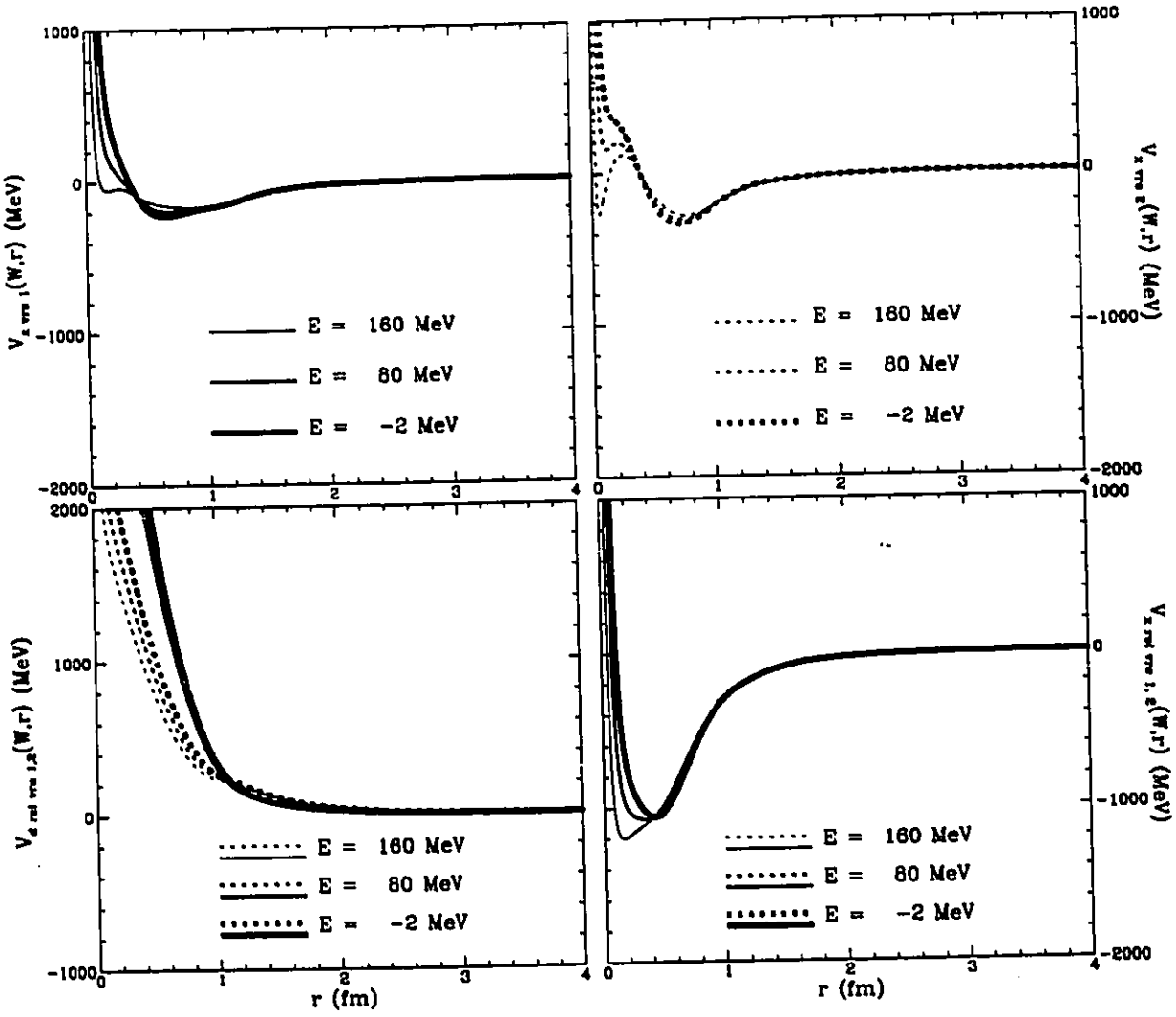

Top-left/right: Energy dependent effective S-D crossterm interactions of radial equations (2.6.6)a (solid lines) & (2.6.6)b (dotted lines).
Bottom-right/left: Purely relativistic interaction after subtraction of non-relativistic reduction in the direct and cross channels.

Figure 5.5.4 Breit radial amplitudes for Model D

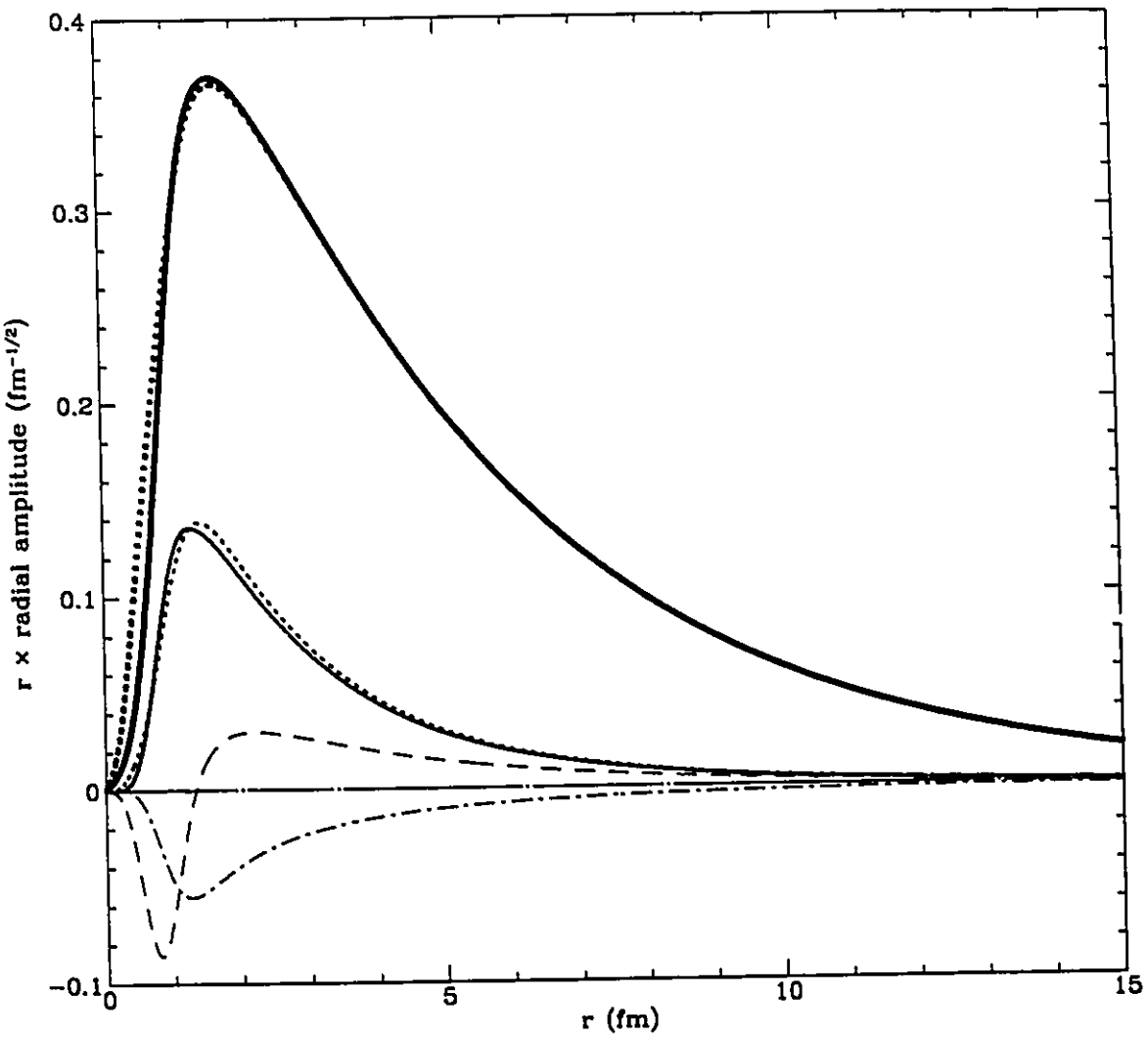

S–wave: ——— r $u_-(r)$, ... r $g_-(r)$.
D–wave: ——— r $u_+(r)$, ... r $g_+(r)$.
P–wave: – – – – –i r a(r), —— —— - –i r J(r).
.–.–.–.– –i r f(r), ——·——·—— –i r $u_o(r)$.

f and u_o hug the axis. (They would vanish identically for $m_n=m_p$).

Figure 5.5.5 Breit models C and D: $^3S_1$ – $^3D_1$ phaseshifts

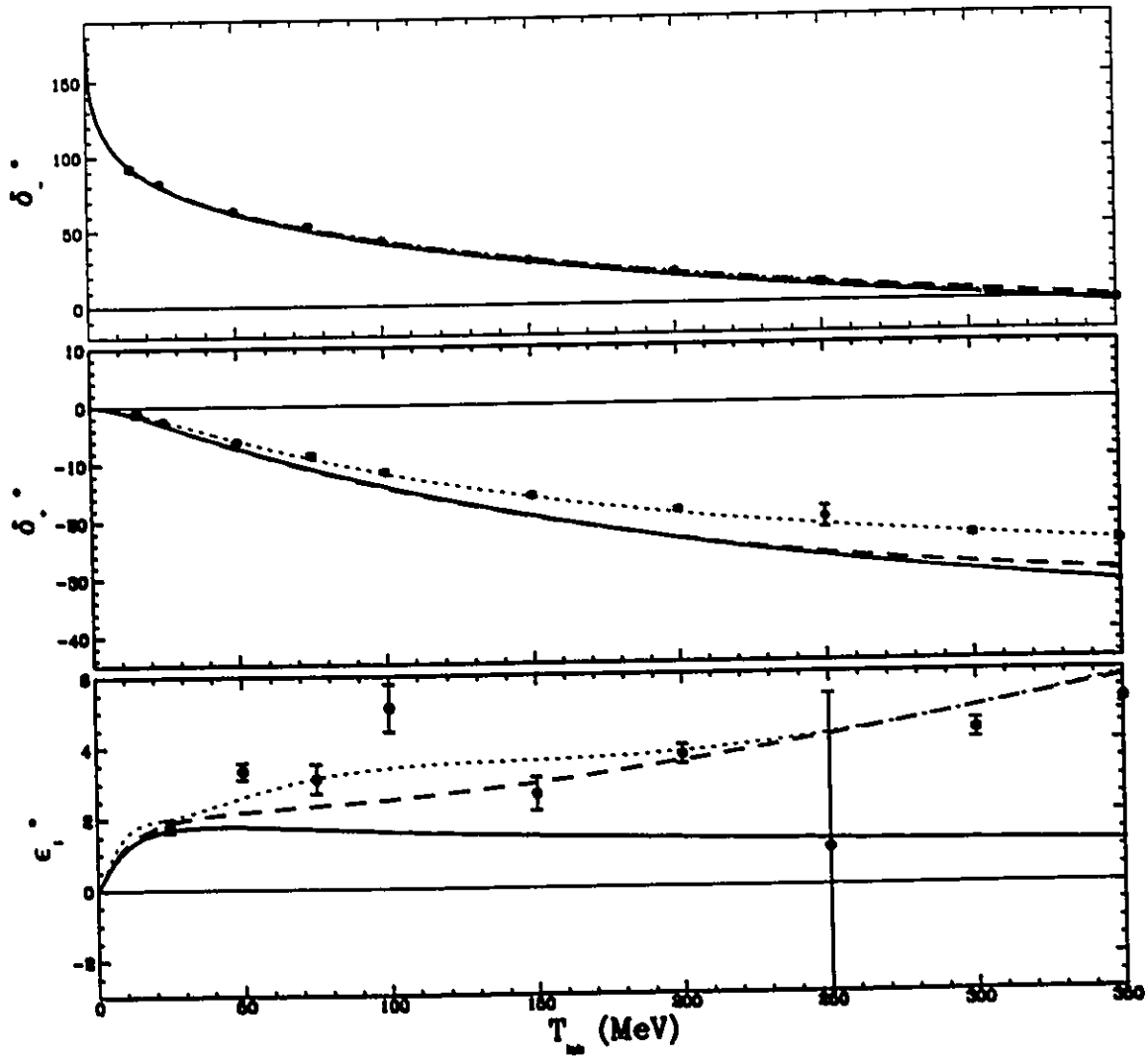

The solution set VL40 of SAID (Arndt *et.al.*[72]) is the fit of elastic scattering data below T_{lab} = 350 MeV. The light dotted line is their solution. (Points and error bars are their fixed energy solutions.) The best overall fit of scattering *and* low energy data, model–D, is shown as dashed lines. (It is the tapered OPEP tensor. As before, the untapered OPEP tensor fit, model–C is represented by the solid lines.

5.6 DISCUSSION OF THE TRIPLET RESULTS

In section 5.4, it was found that the Breit equation does not resolve the outstanding a_t-r_m discrepancy *if* the conventional non-relativistic reduction of r_m holds up. There is some dispute over the $\frac{3}{4m^2}$ contribution to the Zitterbewegung correction *as it applies to relativistic equations.*[66] The proposed correct deduction of r_m from electromagnetic scattering involves one-half of the usual correction.

The shift of the relativistic r_m to larger value combined with sufficient tuning of an interference mechanism which enhances the 4 P-wave amplitudes can indeed lead to a smaller r_m but the interference can happen between a number of interaction types. The S-V mechanism which has a lot of empirical and theoretical support generates a best fit (model-B) that falls a little more than 1 σ away from the experimental value. An anomalous solution (model-A) that relies on the purely adhoc short-range OPEP interaction can fit the experiment to an even better degree but this must in all likelihood be attributed to a kinder set of Klein paradox restrictions. A more sophisticated framework could allow g_S and g_V to become sufficiently large to solve the discrepancy more definitively.

From a purely kinematical point of view, the Breit equation seems to corroborate this. The P-amplitudes exist and take up a piece of the normalization, have concentrated strength at small r, and can be enhanced by dynamics acting differentially on the large and small components. The Breit equation may not lend itself to the right dynamics if couplings become large but certainly it does provide a window on "how" relativistic interference mechanisms impact on the problem if not "why".

The solution model-B is also reasonably close to the a_t-r_m point so that even with its moderate couplings, additional shape effects beyond the basic Gaussian ansatz may resolve this particular problem *within* the Breit framework afterall.

When an attempt is made to explain the elastic scattering for the $j = 1$ triplet in addition, the parameter searches are driven into the regions of large couplings. The Breit equation cannot be reliable because surely the vacuum must be playing an important role. Although it cannot be ruled out that the Gaussian choice of ansatz with no shape embellishments could be responsible for the bad fit, the fit attempted was at the energy end points of the elastic scattering range. Initial efforts in this work did involve extra parametric freedom among S and V. The ansatz: $g_i(1 + c_i r)e^{-(r/b_i)^2}$ was used for S and V although the parameter search was more crude and less systematic. For that matter, cut-off Yukawa potentials with two-boson exchange and single exchange tails were also utilized but in both cases, the OPEP used was frozen through all the work. The χ^2's of model's A,B,C, and D of this chapter are the best results of the accumulative attempts.

An attempt to resolve the problem through variable free parameters of both the OPEP (short range) generating part and the additional ones of the scalar and vector interactions was not undertaken because of the large number of parameters especially in light of the small number of data to be fitted. This will be undertaken in a subsequent study subject building from the results given here.

There are perhaps additional reasons that the Breit equation may still be a viable equation in this setting. Firstly, the parameter search took place in a diabolical space of funnels, long winding tunnels (in 5 dimensions

usually) and abrupt precipices. (Suddenly, at an incremented potential range, the deuteron state acquires an excited partner for instance.) It may yet be the case that most of the fit trajectories taken miss converging to a stable configuration of mildly strong scalar/vector couplings with OPEP clearly in the background.

If the strong couplings are unavoidable as this chapter leads us to believe, then perhaps a brand of quasi-potential formalism can be worked out, relating the Breit couplings to the "true" couplings as suggested by a more fundamental theory to a higher perturbative order than second.

Finally, although the total χ^2 for all data were dominated by the D-wave phaseshift $\bar{\delta}_+$ at $W = W_z$, and the $j = 1$ mixing parameter $\bar{\epsilon}_1$, the purely low energy fits for the deuteron and effective range were driven almost entirely by the dominating influence of r_m on the χ^2. The experimental value of r_m that entered this function was that obtained involving the $\frac{3}{4m^2}$ Zitterbewegung subtraction from the deuteron charge radius. It is an open question whether the suggested target for the Breit equation would have led to a gentler configuration of couplings.

Chapter 6

Discussion

In the previous pages, we tried to apply an equation to the two nucleon system that would allow a "simple" relativistic extension (the apparent complexity of chapter 2 notwithstanding) of the very familiar Schrödinger equation with local interactions.

The work of chapters 3 and 4 dealt exclusively with the $^1S_0$ system and chronologically, in the development of this study, preceded the triplet work of chapter 5. Several shortcomings of the Breit equation were exposed, even in the spin-singlet work. The handling of the electromagnetic interaction in the charge-symmetry-breaking (CSB) study, for example, is one such sensitive point. Still, an effort to correct for the departure from field theory is made by adopting Breit's own form of the electromagnetic interaction[10], $\{1 - \frac{1}{2}\vec{\alpha}_1 \cdot \vec{\alpha}_2 - \frac{(\vec{\alpha}_1 \cdot \vec{r})(\vec{\alpha}_2 \cdot \vec{r})}{r^2}\}V_{em}(\vec{r})$, for Dirac particles. Thus, the electromagnetic field, a Lorentz 4-vector, enters the dynamics in a modified form, quite

different from the strong nuclear vector field which has massive quanta and enters the interaction as $\{1 - \vec{\alpha}_1 \cdot \vec{\alpha}_2\}V(\vec{r})$.

The use of the Breit magnetic part is a tacit admission that the massless photon field cannot be handled properly in our purely quantum mechanical equation without *some* modification. The massive vector mesons, on the other hand, are more inhibited from popping in and out of the vacuum and so we enter the strong vector into the Breit equation as an unmodified covariant 4-vector. Keeping in mind that electromagnetic effects to *first* order in $\frac{v}{c}$ (as opposed to α_ϵ) are electric and *not* magnetic, and that the energy W, strong scalar S, and strong vector V all enter the Breit equation to lowest order correctly, the bilinear combinations of these quantities in the next order must therefore also be correct. These are the terms which are most important in the interference effect, a novel *apparent* charge-symmetry-breaking mechanism which appears in the *non*-relativistic singlet scattering length a_s discussed in chapter 3.

Due to the simplicity of the Breit equation, the effective range expansion of the ${}^1S_0$ singlet of chapter 4 provides an opportunity to examine general relativistic extensions of the usual expansion. The key to remember here is that this expansion relies primarily on elementary properties of wave functions such as continuity and asymptotic behaviour which are cemented concepts in *any* framework. The dynamics of the equation certainly influence the parameters of the various discussed expansions, but the kinematic correction $\frac{3\alpha^2}{m^2}$ of equation (4.15) (of the contained reprint) in the expansion of ratio $\{\frac{r_p}{a}\}^2$, will certainly remain as long as the modulus squared of all spinor components enters the calculation. (As mentioned briefly in chapter 5, when comparing with similar non-relativistic expansions, a part of this amount is

already accounted for in subtractions of the Zitterbewegung but apparently not the total.)

In chapter 5, difficulties with the OPEP came to light that did not appear in the singlet studies because of the neutrality of the tensor portion of the interaction. The essential problem is that the potential tail is characterized by a strength $g^2 \approx 0.08$ which is very approximately nonrelativistic. The nonrelativistic analyses corroborate this tail quite consistently and it *must* be generated to both extend any model consistently to higher partial waves in scattering and to place the asymptotic deuteron properties "in the right ball park".

The pseudoscalar inclusion of the OPEP in the Breit equation runs head on into the Klein paradox. Methods of regularizing the $P(r)\gamma_1^5\gamma_{25}$ form of the interaction must brutally damp the interaction at all values of r that $G^2\frac{e^{-m_\pi r}}{r}$ is greater than or even of the same order as M_n. The avoidance of a singularity at finite r (which would come at roughly 1.3 fm) requires severe damping in that very tail region. (The interaction is of course very benign at $r >> 1$ fm, where there is no need of damping and where, of course, nuclear scattering data is sparse to none!)

The alternative method of entering OPEP in an axial form cannot properly generate the tensor force. The deuteron d-state related properties and the $\bar{\epsilon}_1$ scattering mixing parameter are utterly unreproducible.

The OPEP *must* be part of the model. Both of the natural avenues for its inclusion in the Breit framework, $P(\vec{r})$ and $A(\vec{r})$, are closed. A sure-fire way to generate the proper tail without the singularity problem is to put in, by hand, the spin-dependent pieces of the interaction. The interaction, as it appears in the radial equations of the pure large components is the

traditional OPEP tail merely dressed with tiny transient pieces associated with the algebraic elimination of the small components. If we allow the short range phenomenological part of this interaction to be governed by two 0-range strength parameters and a smooth attachment to the tail, a fit of the scattering and deuteron data should fix these parameters in a benign way and presumably let the scalar and vector potentials cover most of the physics in the intermediate and short range regions.

This did not happen. With a blind eye to the scattering data, a good fit with physically meaningful interpretation, model-B of chapter 5, was attained. At this, the deuteron matter radius, r_m was still highly resistant to the fit and contributed the lion's share of χ^2_{low}. The added requirement of a simultaneous fitting of scattering data proved too restrictive altogether.

We can ask a few pointed questions. Can the interference scheme, which incrementally improves the fits until the point where singular effective interactions defeat the Breit equation framework be tuned with additional shape parameters *within* this context? Or alternatively, must the couplings keep ramping upward in strength, forcing our hand and making us discount the Breit equation in the nuclear context altogether? In chapter 5, it was stated that the attempt to fit the scattering was already directed at the meagre goal of producing a reproduction of scattering data at threshold and at one other fixed energy only, W_x, where the $\bar{\delta}_-$ crosses 0. It was argued that this already accounts for the crudity of the shape ansatz. Intuitively, if nothing was wrong with the framework, a crude model would likely fit the end point phase data and perhaps butcher the fit in between. Basic ingredients of range and strength parameters attached to each of attractive S and repulsive V were not able to fit this minimal scattering data.

A very pathological χ^2 behaviour in the 5-dimensional parameter space leads us not to discount entirely the possibility of a overlooked solution that does lend itself to physical interpretation *within* the Breit framework's sphere of description. The narrow tunnels that appear in the space are likely symptomatic of the interferences between the interactions. The parameter space was widely sampled however with points all playing to the more and more established scalar-vector interference mechanism (in section 5.3). In the wide survey, V was pegged to be repulsive which tended to drive S negative to bind the deuteron. *All* of the best seed points from this survey in addition to a few widely separated hand-picked points were drawn into areas of the parameter space where *other* interference mechanisms, of dubious physical interpretation, dominated the physics. (Constrained searches with $g_v \geq 0$ leads to $g_v \equiv 0$. Try to interpret *that*!)

What we are essentially left with is a high degree of certainty that the Breit framework is not a viable one for nuclear dynamics. This is unfortunate because of the ease of interpretation and the amount of overlap between traditional non-relativistic calculations and those of our minimally relativistic apparatus.

There is definite insight to be gained from this work however if attention is turned away from an incorrect dynamics (a result of a choice of framework) and turned instead to asking how does a relativistic wave-function, whatever the dynamics, twist and turn to offer a possible resolution of some outstanding problems? We think we have the answer. The p-wave amplitudes of the mid-sized spinor components can be pulled inward and enhanced in magnitude quite apart from the behaviour of the pure large spinor component.

A relativistic framework that properly describes the vacuum will not allow the Klein paradox. We would very likely be able to find positive g_v and negative g_s outside the Breit framework sphere of description that resolves the celebrated a_t-r_m discrepancy *within* some *higher* relativistic framework. Of course, if the dynamics requires much tuning to arrive at a highly contrived interference to resolve the discrepancy *completely*, then other dynamical data which come into play, to fix the meson-nuclear couplings for example, will then help elucidate whatever true divide exists between a resolution attributable to relativity and that attributable to intrinsic non-locality. Afterall, we are reasonably assured of both notions: that nature marches to Einstein's beat as opposed to Newton's, and that nucleons are indeed, like us and our pets, extended objects in more than one place at once.

Appendix I

Vacuum polarization in one dimension -elementary examples

1.1 INTRODUCTION

The content of this appendix is certainly removed, in subject matter, from the thrust of this thesis. It does point out some notable consequences of the "physics of the small component" which permeate all of relativistic formulations of fermion physics, either of fermions in isolation, pairs, or many body systems.[74],[14] In particular, what it holds in common with the Breit equation work is the novel physics associated with *enhanced* small spinor components due to constructive addition of repulsive vector and attractive scalar interactions. The lower component of the spinor sees stronger dynamics than the upper component and consequently the $E < 0$ single particle states of the Dirac Sea, in which the lower components *are* the large components acquire much structure in the vicinity of an external potential. We introduce two 1-dimensional toy models here in which we calculate both the redistributed

fermion number density of the vacuum and the peculiar acquired fractional fermion number, or charge, of the dynamically altered vacuum. The section immediately following was published as a short note to Europhysics Letters. It describes the treatment of a 1-dimensional external potential of a spatial δ-function form with mixed scalar and vector couplings. It is remarkable in its simplicity as an illustration of vacuum polarization. The section following that involves a simple embellishment. We exchange the spatial dependence for that of a square well. The problem is less amenable to analytic techniques however and offers essentially the same physics at a glance.

1.2

EUROPHYSICS LETTERS 1 November 1986

Europhys. Lett., 2 (9), pp. 661-665 (1986)

Vacuum Polarization and Fractional Fermion Number: an Elementary Example.

Y. NOGAMI(*)

Theoretische Physik II, Ruhr-Universität Bochum
D-4630 *Bochum* 1, *Federal Republic of Germany*

D. J. BEACHEY

Department of Physics, McMaster University - Hamilton, Ontario, Canada L8S 4M1

(received 28 April 1986; accepted 16 July 1986)

PACS. 03.65. – Quantum theory; quantum mechanics.
PACS. 11.90. – Other topics in general field and particle theory.
PACS. 21.60. – Nuclear structure models and methods.

Abstract. – For the Dirac field in one space dimension subjected to an external static potential in the form of a delta-function, we obtain the density $\rho(x)$ and the fermion number $\int_{-\infty}^{\infty}\rho(x)\,dx$ of the vacuum. The fermion number varies continuously depending on the strength of the potential.

In recent years there has been a growing interest in the role played by the vacuum in quantum field theory (see, *e.g.* ref. [1]). The vacuum probably has a rich structure yet to be disclosed, and it would be useful to study models such that one can work out the vacuum structure explicitly. The purpose of this note is to examine the vacuum of the Dirac field in one space-dimension under the influence of an external static potential of the form of a delta-function. For this system we can explicitly obtain the vacuum density $\rho(x)$ and the fermion number $N=\int_{-\infty}^{\infty}\rho(x)\,dx$. It is interesting that N turns out to be nonvanishing in general; it varies continuously depending on the strength of the external potential. There are several systems known to have fractional fermion numbers [2], but our example is perhaps the most elementary.

The Dirac equation in one dimension reads as

$$(\alpha p+\beta m+V)\psi=E\psi\,, \tag{1}$$

where ψ has two components. For α and β we use the Pauli matrices σ_x and σ_z, respectively.

(*) On leave (January-July 1986) from McMaster University, Hamilton, Ontario, Canada L8S 4M1.

Other notations are standard. We use units such as $c = \hbar = 1$. The potential that we assume is

$$V = -\begin{bmatrix} 2\lambda_1 & 0 \\ 0 & 2\lambda_2 \end{bmatrix} \delta(x) . \tag{2}$$

The potential can be written as a combination of a scalar and a vector type, *i.e.* $V = 3V_s + V_v$. If $V = V_s$, then $\lambda_1 = -\lambda_2$. If $V = V_v$, then $\lambda_1 = \lambda_2$.

The solutions of the Dirac equation can be classified in terms of parity. Let us begin with the even-parity solutions. The lower component of an even-parity ψ is an odd function of x, and hence the λ_2-part of V has no effect on it. If (and only if) $\lambda_1 > 0$, there is an even-parity bound state. Its energy is given by [1]

$$E_1 \equiv m_1 = m(1 - \lambda_1^2)/(1 + \lambda_1^2) . \tag{3}$$

The wave function is

$$\psi_b(x) = \sqrt{\frac{\varkappa_1(E_1 + m)}{2m}} \begin{bmatrix} 1 \\ \dfrac{i\varkappa_1}{E_1 + m} \dfrac{x}{r} \end{bmatrix} \exp[-\varkappa_1 r] , \tag{4}$$

where $r = |x|$, and

$$\varkappa_1 = \lambda_1(E_1 + m) = 2m\lambda_1/(1 + \lambda_1^2) . \tag{5}$$

The density is $|\psi_b|^2 = \psi_b^\dagger \psi_b = \varkappa_1 \exp[-2\varkappa_1 r]$, which is normalized as $\int_{-\infty}^{\infty} |\psi_b|^2 \, dx = 1$.

The scattering states are given by

$$\psi_k(x) = \sqrt{\frac{E + m}{2\pi E}} \begin{bmatrix} \cos(kr + \delta_1) \\ \dfrac{ik}{E + m} \dfrac{x}{r} \sin(kr + \delta_1) \end{bmatrix} , \tag{6}$$

where $E = \pm\sqrt{m^2 + k^2}$. The phase shift δ_1 is given by

$$\operatorname{tg} \delta_1 = \lambda_1(E + m)/k = \lambda_1 k/(E - m) . \tag{7}$$

The normalization of $\psi_k(x)$ is nontrivial. It is determined such that the completeness relation

$$\psi_b^\dagger(x)\psi_b(x') + \sum_{E \gtrless 0} \int_0^\infty dk \, \psi_k^\dagger(x)\psi_k(x') = \delta(x - x') \tag{8}$$

is satisfied. Here it is understood that the term $\psi_b^\dagger \psi_b$ is dropped when there is no bound state, *i.e.* $\lambda_1 < 0$. Also the summation in (8) implies that the sum is taken over positive- and negative-energy states. What we have obtained is a relativistic generalization of [4].

In the odd-parity case, there is a bound state when $\lambda_2 < 0$. Its energy is

$$E_2 = -m_2 = -m(1 - \lambda_2^2)/(1 + \lambda_2^2) , \tag{9}$$

---

[1] If we take a square-well potential and let the width of the well approach zero after solving the Dirac equation, $\operatorname{tg} \lambda_1$ appears in place of λ_1 in all the following results. This «discrepancy» has been discussed in detail recently [3]. We do not focus on this problem in this note because it is not essential.

and its wave function is

$$\psi_b(x) = \sqrt{\frac{\varkappa_2(E_2 - m)}{-2m}} \begin{bmatrix} \frac{i\varkappa_2}{E_2 - m} \frac{x}{r} \\ 1 \end{bmatrix} \exp[-\varkappa_2 r] , \tag{10}$$

where

$$\varkappa_2 = \lambda_2(E_2 - m) = -m(1 - \lambda_2^2)/(1 + \lambda_2^2) . \tag{11}$$

The odd-parity scattering states are given by

$$\psi_k(x) = \sqrt{\frac{E - m}{2\pi E}} \begin{bmatrix} \frac{ik}{E - m} \frac{x}{r} \sin(kr + \delta_2) \\ \cos(kr + \delta_2) \end{bmatrix} \tag{12}$$

with

$$\operatorname{tg} \delta_2 = \lambda_2(E - m)/k = \lambda_2 k/(E + m) . \tag{13}$$

One notices that $\psi^\dagger\psi$ for odd-parity states is obtained from the even-parity counterpart by $\lambda_1 \to \lambda_2$ and $m \to -m$.

Having determined the wave functions, we can now examine the vacuum structure. The density in the vacuum is

$$\rho(x) = \sum_{i, E<0} \{|\psi_i(x)|^2 - |\psi_i(x)|^2_{\lambda=0}\} . \tag{14}$$

Here the suffix i refers to b or k, and the summation is over all negative-energy states. The second term in the brackets differs from the first in that the interaction is switched off. Let us show how we calculate ρ for the even-parity states. With ψ_k of (6), we obtain, for $xx' > 0$,

$$\psi_k^\dagger(x)\psi_k(x') =$$

$$= \frac{1}{2\pi}\left\{\cos k(r - r') + \frac{m_1}{E}\cos(r + r') - \left(1 + \frac{m_1}{E}\right)\frac{\varkappa_1}{k^2 + \varkappa_1^2}[\varkappa_1 \cos k(r + r') + k \sin k(r + r')]\right\} . \tag{15}$$

This equation is valid irrespectively of the sign of λ_1. When $\lambda_1 < 0$, $\varkappa_1 < 0$ and there is no bound state. We still use m_1 defined by (3), although it no longer represents a bound-state energy. Using (15), we obtain

$$\rho_{\text{even}}(x) = -\frac{1}{2}\varkappa_1 \theta(\varkappa_1) \exp[-2\varkappa_1 r] +$$

$$+ \frac{1}{2\pi}\int_0^\infty \frac{dk}{\sqrt{k^2 + m^2}}\left\{\left(m - m_1 + \frac{m_1\varkappa_1^2}{k^2 + \varkappa_1^2}\right)\cos 2kr + m_1\varkappa_1 \frac{k \sin 2kr}{k^2 + \varkappa_1^2}\right\} , \tag{16}$$

where $\theta(x) = 1$ (0), if $x > 0$ ($x < 0$) [2]. The k-interpretation can be changed into an integration along the imaginary k-axis from im to $i\infty$. Then with $k \to i\eta$, we arrive at

$$\rho_{\text{even}}(x) = \frac{1}{2\pi}\left\{(m - m_1) K_0(2|m|r) - \frac{1}{2} m_1\varkappa_1 \int_{|m|}^\infty d\eta \frac{\exp[-2\eta r]}{(\eta - \varkappa_1)\sqrt{\eta^2 - m^2}}\right\} , \tag{17}$$

---

(2) We assumed that $\lambda_1 < 1$. If $\lambda_1 > 1$ a negative-energy bound state of positive parity appears which gives an additional contribution to ρ_{even}.

where $K_0(2|m|r)$ is a Hankel function. The reason why we write $|m|$ for some of the m's will become clear in the next paragraph. The fermion number of the vacuum is given by

$$N_{\text{even}} = \int_{-\infty}^{\infty} \varrho_{\text{even}}(x)\,dx = \frac{-1}{\pi} \operatorname{tg}^{-1} \lambda_1 . \tag{18}$$

If the particle is charged, then N is the «vacuum charge». Equation (18) resembles the fermion number obtained by GOLDSTONE and WILCZEK [5] for a soliton model (their eq. (9)). But our model is entirely different from theirs. Since m is the only parameter with dimension in the model, it is natural that N_{even} is independent of m. On the other hand, ϱ_{even} obviously depends on m. Its range is $\sim 1/2m$.

The ϱ_{odd} can easily be obtained from ϱ_{even} by the substitutions: $\lambda_1 \to \lambda_2$, $m \to -m$ (hence $\varkappa_1 \to \varkappa_2$). Perhaps it would be worthwhile noting that $\varrho(x)$ of (14) can be rewritten as [6]

$$\varrho(x) = \frac{1}{2}\Big\{ \sum_{\nu, E<0} |\psi_\nu(x)|^2 - \sum_{\nu, E>0} |\psi_\nu(x)|^2 \Big\} . \tag{19}$$

This expression holds for $\varrho = \varrho_{\text{even}} + \varrho_{\text{odd}}$, but not separately for ϱ_{even} and ϱ_{odd}. If the potential is a pure scalar, *i.e.* $\lambda_1 + \lambda_2 = 0$, then there is a complete symmetry between the positive- and negative-energy spectra, and hence $\varrho(x) = 0$. The fermion number is given by

$$N = -\frac{1}{\pi}(\operatorname{tg}^{-1}\lambda_1 + \operatorname{tg}^{-1}\lambda_2) .$$

If $\lambda_1 + \lambda_2 = 0$, $N = 0$ as expected.

As a numerical illustration, let us take $m = 4.76\ \text{fm}^{-1} = 939$ MeV, and $\varkappa_1 = \varkappa_2 = 0.6\ \text{fm}^{-1}$. Then $m_1 = m_2 = 932$ MeV. We have in mind a «nucleon» bound in a pure vector type potential with a binding energy of 7 MeV. Noticing that $\operatorname{tg}^{-1}\lambda_1 = \frac{1}{2}\sin^{-1}(\varkappa_1/m)$, we obtain $N = 0.040$. Table I shows ϱ_{even} and ϱ_{odd} *vs.* r. The ϱ's blow up as $r \to 0$. At $r = 0.1$ fm, $\varrho = -0.067\ \text{fm}^{-1}$, which is nonnegligible compared with the even-parity bound-state density $\varkappa_1 \exp[-2\varkappa_1 r] = 0.53\ \text{fm}^{-1}$ at the same distance.

TABLE I. – *The densities* ϱ_{even} *and* ϱ_{odd} *in* $10^{-4}\ \text{fm}^{-1}$ *vs.* r *in* 10^{-2} fm *for the parameters given in the text.*

r	$-\varrho_{\text{even}}$	$-\varrho_{\text{odd}}$
2	978	1012
3	845	855
4	735	733
5	643	633
10	342	327
20	108	101
30	36	33

There is an interesting possibility which may have relevance to real nuclear structure. Consider a «shell model potential» of the form of $V = \beta V_s + V_v$. Suppose $V_s < 0$ and $V_v > 0$; they are both very large in magnitude, but $V_s + V_v$ is only weakly attractive (negative). Then $-V_s + V_v$ will be positive and very large. In terms of our model, this means that $-\lambda_2 \gg \lambda_1 > 0$ and hence $-\varkappa_2 \gg \varkappa_1 > 0$. In this case, for the same «nuclear binding» which is determined by λ_1, the vacuum polarization can be very large. Recent Dirac phenomenology

in nuclear physics suggests that the nuclear shell model potential is a combination of such V_s and V_v [7]. Therefore, «nuclear» vacuum polarization may have significant effects. It is possible, however, that the fractional fermion number is a peculiar feature of the problem in one dimension. If this arises also in three dimensions, it would lead to various bizarre possibilities.

* * *

We would like to thank Drs. A. DE RÚJULA and W. GLÖCKLE for interesting discussions and D. KIANG for bringing ref. [2] to our attention. One of us (YN) also thanks Dr. W. GLÖCKLE for the warm hospitality extended to him at RUB. The work was supported by Deutsche Forschungsgemeinschaft and by Natural Sciences and Engineering Research Council of Canada.

REFERENCES

[1] RAFELSKI J. and MÜLLER B., *Die Strucktur des Vakuums* (Verlag Harri Deutsch, Frankfurt) 1985.
[2] JACKIW R., *Effects of Dirac's Negative Energy Sea on Quantum Numbers*, MIT preprint, CTP No. 1306 (1985).
[3] CALKIN M. G., KIANG D. and NOGAMI Y., *Proper treatment of the δ-function potential in the one-dimensional Dirac equation*, to appear in *Am. J. Phys.*
[4] BROWNSTEIN K. R., *Am. J. Phys.*, 43 (1975) 173.
[5] GOLDSTONE J. and WILCZEK F., *Phys. Rev. Lett.*, 47 (1981) 986.
[6] WICHMANN E. H. and KROLL N. M., *Phys. Rev.*, 101 (1956) 843.
[7] MCNEIL J. A., SHEPARD J. R. and WALLACE S. J., *Phys. Rev. Lett.*, 50 (1983) 1439.

1.3 VACUUM POLARIZATION AND FRACTIONAL FERMION NUMBER FOR A SQUARE-WELL POTENTIAL

The development in this section mirrors that of the previous section in the choice of spinor matrices and notation. We can explicitly write the dynamical equations for each isolated component as:

$$-\psi_i'' = \left\{(E-V)^2 - (m+S)^2\right\}\psi_i \qquad (A1.3.1)a$$

The scalar and vector interactions are now of a form:

$$V(x) = V_\circ\Theta(x+a)\Theta(-x+a) \qquad (A1.3.1)b$$

$$S(x) = S_\circ\Theta(x+a)\Theta(-x+a) \qquad (A1.3.1)c$$

The fact that, piecewise, S and V have no x-dependence is responsible for the interchangability of spinor components ψ_1 and ψ_2 in $(A1.3.1)a$. The continuity of each component at the boundaries of the interaction region $(-a,a)$ assures current conservation. As before, we define the quantities

$$\lambda_{\frac{1}{2}} = (V_\circ \pm S_\circ) \qquad (A1.3.2)$$

such that $\lambda_1 = \lambda_2 \Rightarrow V_\circ = 0$ We also, for simplicity, retain the definition: $r \equiv |x|$.

Inside the well, $(r \leq |a|)$ the positive parity bound state wave-function takes on the simple form:

$$\psi_1(x) = Q\cos(kx) \qquad (A1.3.2)a$$

$$\psi_2(x) = \frac{+ikQ\sin(kx)}{(E+m-\lambda_2)} \qquad (A1.3.2)b$$

while outside it becomes:

$$\psi_1(x) = Ne^{-\kappa r} \qquad (A1.3.2)c$$

$$\psi_2(x) = +(\frac{x}{r})\frac{+iN\kappa e^{-\kappa r}}{(E+m)} \qquad (A1.3.2)d$$

Continuity of both components at the boundary and overall normalization enable us to eliminate N in favour of Q:

$$N = Qe^{\kappa a}\cos(ka) \qquad (A1.3.3)a,$$

then to obtain Q entirely in terms of dynamical quantities:

$$Q = \left\{\frac{\cos^2(ka)}{\kappa}\left[\frac{2m}{E+m}\right] + a\left[\frac{2E+\lambda_1-\lambda_2}{E+m-\lambda_2}\right] + \frac{\sin(2ka)}{2k}\left[\frac{2m-\lambda_1-\lambda_2}{E+m-\lambda_2}\right]\right\}^{-\frac{1}{2}} \qquad (A1.3.3)b,$$

and finally to establish an eigenvalue equation:

$$cot^2(ka) - \frac{(E-m+\lambda_1)(E+m)}{(E+m-\lambda_2)(m-E)} = 0 \qquad (A1.3.3)c.$$

In the above, κ and k are given by:

$$\kappa = \sqrt{m^2 - E^2} \qquad (A1.3.4)a$$

and

$$k = \sqrt{(E-m+\lambda_1)(E+m-\lambda_2)} \qquad (A1.3.4)b$$

For the odd parity bound state, the wave-function is given by

$$\psi_1(x) = \frac{+iR\sin(kx)}{(E-m+\lambda_1)}, \qquad (A1.3.5)a$$

$$\psi_2(x) = R\cos(kx) \qquad (A1.3.5)b$$

and

$$\psi_1(x) = +\left(\frac{x}{r}\right)\frac{+iS\kappa e^{-\kappa r}}{(E-m)} \qquad (A1.3.5)c$$

$$\psi_2(x) = Se^{-\kappa r} \qquad (A1.3.5)d$$

inside and outside the well respectively.

$$S = Re^{\kappa a}\cos(ka) \qquad (A1.3.6)a,$$

$$R = \left\{ \frac{\cos^2(ka)}{\kappa} \left[\frac{-2m}{E-m} \right] + a \left[\frac{2E + \lambda_1 - \lambda_2}{E - m + \lambda_1} \right] + \frac{\sin(2ka)}{2k} \left[\frac{-2m + \lambda_1 + \lambda_2}{E - m + \lambda_1} \right] \right\}^{-\frac{1}{2}} \quad (A1.3.6)b.$$

The energy eigenvalue E is determined by:

$$cot^2(ka) - \frac{(E + m - \lambda_2)(m - E)}{(E - m + \lambda_1)(m + E)} = 0 \quad (A1.3.6)c.$$

Turning now to the scattering states, for positive parity, we have:

$$\psi_1(x) = A\cos(\eta x) \quad (A1.3.7)a$$

$$\psi_2(x) = \frac{+i\eta A \sin(\eta x)}{(E + m - \lambda_2)} \quad (A1.3.7)b$$

for $r \leq a$ and

$$\psi_1(x) = B\cos(\xi x + (\frac{x}{r})\delta) \quad (A1.3.7)c$$

$$\psi_2(x) = \frac{+i\xi B}{(E + m)} \sin(\xi x + (\frac{x}{r})\delta) \quad (A1.3.7)d$$

for $r > a$. Analogous to κ and k, we have introduced:

$$\xi = \sqrt{E^2 - m^2} \quad (A1.3.8)a$$

and

$$\eta = \sqrt{(E - m + \lambda_1)(E + m - \lambda_2)} \quad (A1.3.8)b$$

Matching conditions yield

$$A = B\frac{\cos(\xi a + \delta)}{\cos(\eta a)} \quad (A1.3.9)$$

where the remaining normalization B will be discussed further later on. In the negative parity case, the scattering continuum states have the form:

$$\psi_1(x) = \frac{+i\eta C \sin(\eta x)}{(E - m + \lambda_1)} \quad (A1.3.10)a$$

$$\psi_2(x) = C\cos(\eta x) \quad (A1.3.10)b$$

for $r \leq a$ and

$$\psi_1(x) = \frac{+i\xi D}{(E-m)} \sin(\xi x + (\frac{x}{r})\delta) \qquad (A1.3.10)c$$

$$\psi_2(x) = D\cos(\xi x + (\frac{x}{r})\delta) \qquad (A1.3.10)d$$

for $r > a$. Continuity eliminates C quite simply:

$$C = D\frac{\cos(\xi a + \delta)}{\cos(\eta a)} \qquad (A1.3.11)$$

and D will be discussed in the same context as B, in the light of the normalization convention and interplay with the density of states. The scattering phase-shifts for the positive (δ_+) and negative (δ_-) parity continuum states can be compactly expressed by the following:

$$\cot(\delta_{\pm}) = \frac{\xi(E \pm m \mp \lambda_{\frac{2}{1}})\cot(\eta a)\cot(\xi a) + \eta(E \pm m)}{\eta(E \pm m)\cot(\xi a) - \xi(E \pm m \mp \lambda_{\frac{2}{1}})\cot(\eta a)} \qquad (A1.3.12)$$

The normalization convention coupled with the density of states in the two continuums must be consistent with the completeness relation (equation (8) of the previous section). If we enclose the entire system in a box of length $2L$ and demand no leakage of current at the edges, the surviving lowest order term of the normalizations B and D scale with L as:

$$B \rightarrow \sqrt{\frac{E+m}{2LE}} \qquad (A1.3.13)a$$

$$D \rightarrow \sqrt{\frac{E-m}{2LE}} \qquad (A1.3.13)b$$

The density of states $g(\xi)$ is readily seen to be a constant *w.r.to* ξ and linear *w.r.t.* L in the limit of $L \rightarrow \infty$. In the positive and negative energy continuums, this translates into a density *w.r.to* energy E:

$$g(E) \rightarrow (\frac{L}{\pi})\frac{|E|}{\sqrt{E^2 - m^2}} \qquad (A1.3.13)c$$

The polarization of the vacuum due to the square well is simply the net change in aggregate density of the filled negative Dirac sea from the unperturbed free negative energy continuum.

$$\Delta\rho(x) = \int_{-\infty}^{-m} dE g(E)\Big\{\psi^\dagger(x)\psi(x) - \phi^\dagger(x)\phi(x)\Big\} + \sum_{E_i} \psi^\dagger_{E_i}(x)\psi_{E_i}(x) \quad (A1.3.14)$$

The last sum above refers to bound states pulled from the negative energy continuum, regardless of whether or not E_i is pulled above 0. The free continuum states $\phi(x)$ are generated from $(A1.3.7)c,d$ or $(A1.3.10)c,d$ by setting $\lambda_i = 0$ and $\delta_{\pm} = 0$.

We denote $\Delta\rho_-$, $\Delta\rho_+$, and $\Delta\rho_b$ as the respective contributions from the negative parity scattering states, positive parity scattering states, and bound states pulled from the vacuum. ($\Delta\rho_b$ is simply the final term of (A1.3.14).) The continuum contributions for $r \le a$ can be written:

$$\Delta\rho_{\pm}(r) = -\frac{1}{2\pi}\int_0^\infty \frac{d\xi}{\sqrt{\xi^2+m^2}}(E\pm m)\left\{\frac{\cos^2(\eta r) + h_2^{\pm 1}\sin^2(\eta r)}{\cos^2(\eta r) + h_1^{\pm 1}h_2^{\pm 1}\sin^2(\eta r)} - \cos^2(\xi r) - h_1^{\mp 1}\sin^2(\xi r)\right\} \quad (A1.3.15)a$$

where the compact dimensionless quantities:

$$h_1 \equiv \frac{E+m}{E-m} \quad (A1.3.15)b$$

$$h_2 \equiv \frac{E-m+\lambda_1}{E+m-\lambda_2} \quad (A1.3.15)c$$

have been introduced. Since E, in this integral, is drawn from the negative range $(-\infty, -m)$, we must select the negative root: $E = -\sqrt{\xi^2+m^2}$. For $r \ge a$ we have the very simple:

$$\Delta\rho_{\pm}(r) = \pm\frac{m}{\pi}\int_0^\infty \frac{d\xi}{\sqrt{\xi^2+m^2}}\Big\{\sin^2(\xi r + \delta_{\pm}) - \sin^2(\xi r)\Big\} \quad (A1.3.15)d$$

where (A1.3.12) can be utilized to yield $\delta_{\pm}$.

We obtain, from analytic integration of the density of states over negative energy, and confirm numerically via coordinate integration of $\rho(x)$ above, that the vacuum acquires a net fractional fermion number of:

$$\begin{aligned} N_f &= \frac{1}{\pi}\int_{-\infty}^{-m} dE(g(E) - g_o(E)) \\ &= \frac{1}{\pi}\int_{0}^{+\infty} d\xi(g(\xi) - g_o(\xi)) \\ &= \frac{1}{\pi}\int_{0}^{+\infty} d\xi(\frac{\partial\delta_-}{\partial\xi} + \frac{\partial\delta_+}{\partial\xi}) \\ &= \frac{1}{\pi}\left\{\delta_-(\infty) - \delta_-(0)\right\} + \frac{1}{\pi}\left\{\delta_+(\infty) - \delta_+(0)\right\} \\ &= \frac{1}{\pi}\left\{\frac{(\lambda_2 - \lambda_1)a}{2}\right\} + \frac{1}{\pi}\left\{\frac{(\lambda_2 - \lambda_1)a}{2}\right\} \\ &= \frac{1}{\pi}(\lambda_2 - \lambda_1)a \end{aligned} \qquad (A1.3.16)$$

We must add a unit of charge for every bound state originating from the $-E$ continuum. This structure could be made arbitrarily richer than in the δ-function case by strengthening the λ_i's and/or increasing the well radius a. With a selective combination of the three dynamical parameters, we can generate a less crude 1-dimensional simulation of nuclei than in the previous section. We include two examples for this purpose. In the first case, we set:

$$\lambda_1 = 0.066fm.^{-1}; \qquad \lambda_2 = 0.440fm.^{-1}; \qquad a = 3.0fm.$$

and in the second, we have:

$$\lambda_1 = 0.066fm.^{-1}; \qquad \lambda_2 = 3.000fm.^{-1}; \qquad a = 3.0fm.$$

In both instances we roughly simulate the average nuclear binding of about 6-7 MeV. We augment the strengths of the scalar and vector couplings unreasonably in the second example while maintaining their sum $S+V$ to bind an assortment of vacuum states. The vacuum polarization density for both these examples is shown in Figures A1.1 and A1.2 following.

Figure A1.1 Square well vacuum polarization density for small λ_1

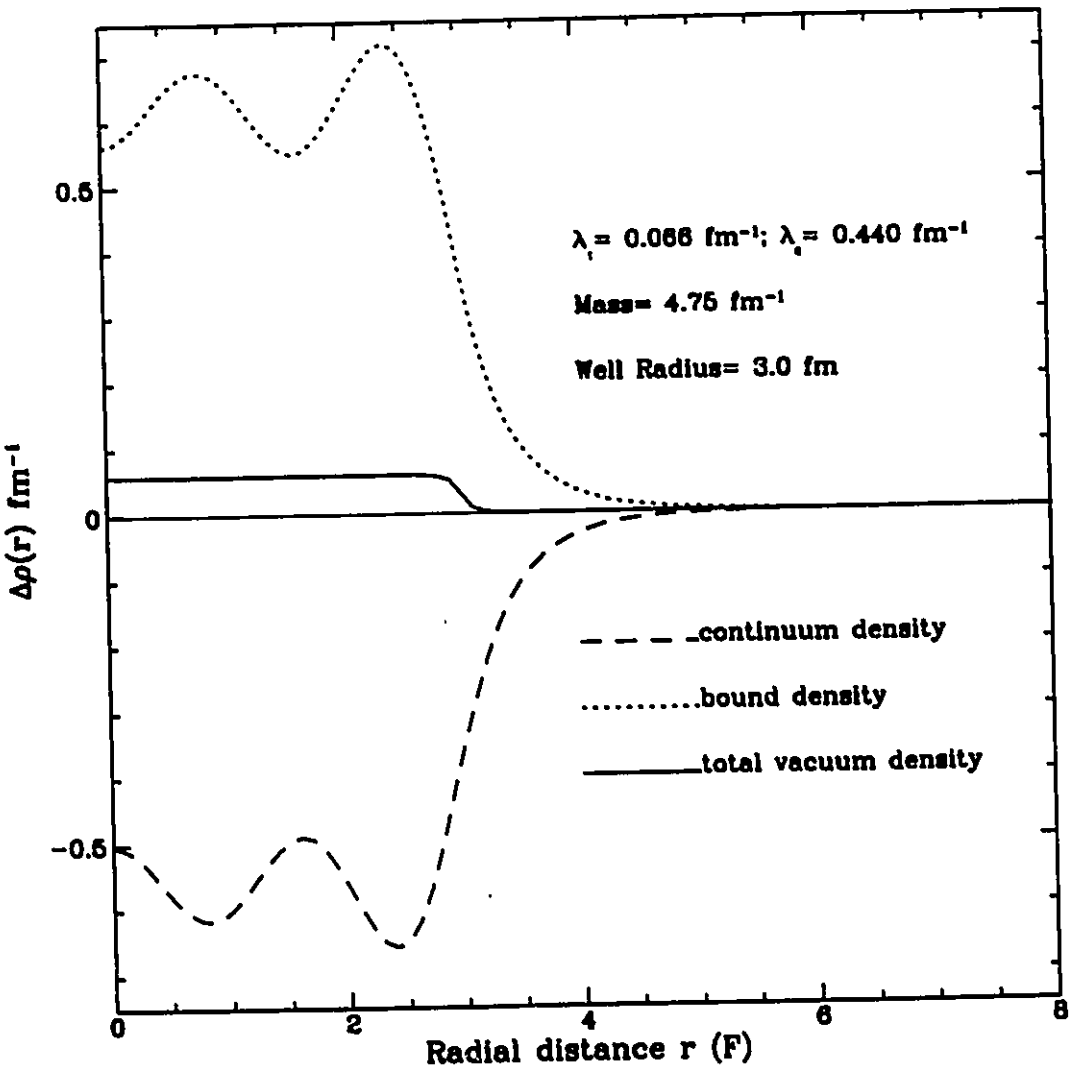

Figure A1.2 Square well vacuum polarization density for large λ_1

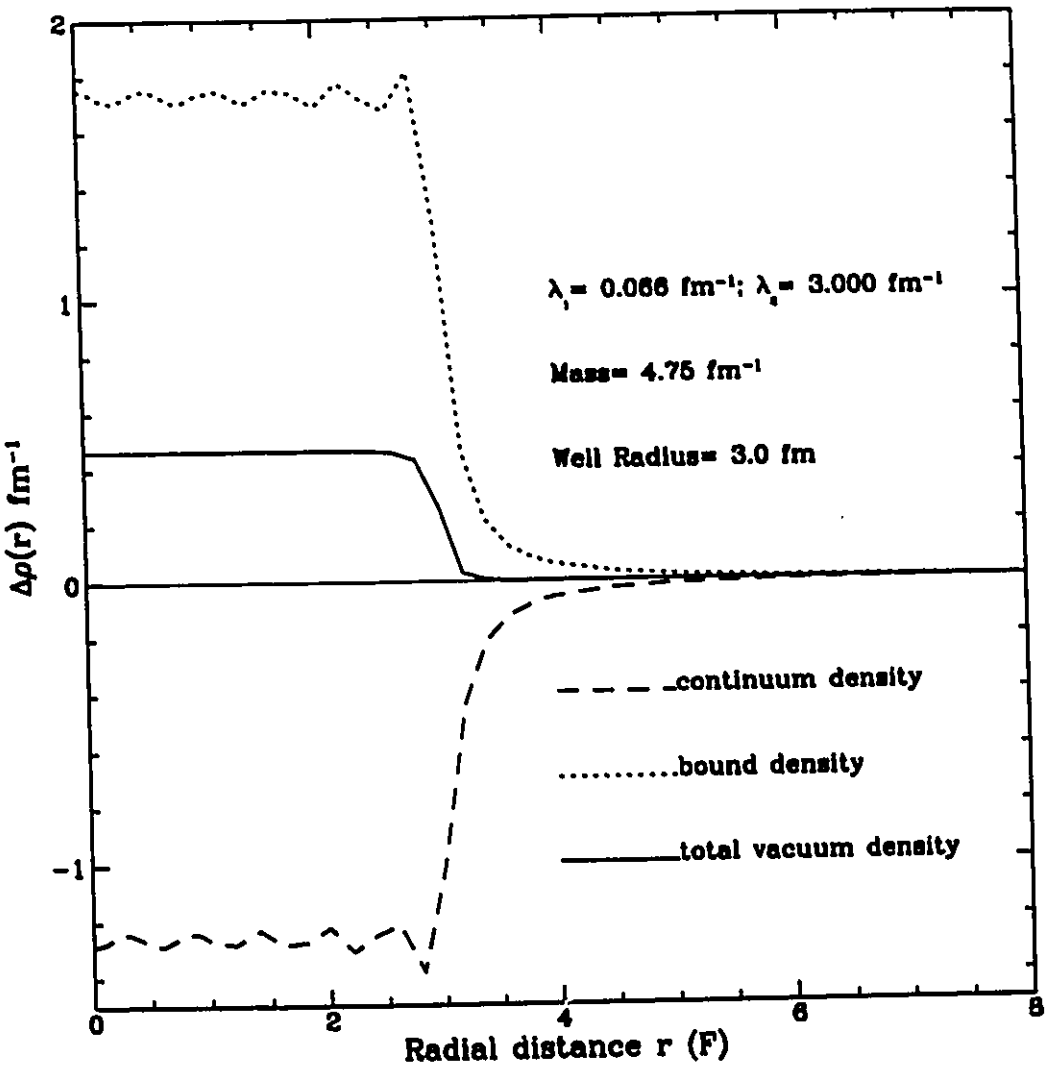

With the added parametric freedom supplied by the range a, we have in the square well, the additional observation that the vacuum polarization density profile is more or less featureless other than being tightly confined to the potential range. As we see in Figures A1.1 and A1.2, however, the vacuum bound state and continuum densities can exhibit many features on their own. One might have supposed that spatial oscillations in $\Delta\rho(x)$ would appear much like Friedel oscillations in crystals around an impurity. The key difference here is that we have a Fermi sea of infinite depth with energies $\in (-\infty, 0)$. We could see structure on a length scale $\frac{1}{\xi_{cutoff}}$ arise if the integrals of (1.3.15)a, d were truncated at a finite cutoff. The two illustrated vacuum polarization profiles of Figures A1.1 and A.1.2 are for a lightly and a heavily polarized vacuum respectively. There are respectively 4 and 11 bound vacuum states. One positive and one negative parity particle valence state is supported in each example. The bindings for the weak polarization case are 10.2 and 2.85 MeV. For the strong polarization example, they are shifted slightly to 9.83 and 1.43 MeV. The continuum particle number is (from direct spatial integration of $\Delta\rho_{continuum}(x)$, -3.6429 for the light polarization case. The total vacuum fermion number N_f is: +0.3571, consistent with equation (A1.3.16). The heavily polarized case, has a continuum contribution to N_f of -8.2 which offsets the integer 11 from the rich bound state vacuum structure. The total N_f is, as expected, +2.8.

Appendix II

Two body relativistic equations with a separable interaction in one dimension

2.1 INTRODUCTION

In a recent paper Munakata, Ino, and Nagamura[75],(MIN) solved for the wave function and energy eigenvalue of a fully relativistic bound two-body system in one dimension. Their system consisted of two equal mass Dirac particles bound together by a contact interaction – *i.e.*, the particles interact only at zero separation. They examined this system with scalar, vector and pseudoscalar couplings and solved both the Breit and Salpeter equations. (The Breit equation is sometimes referred to as the Kemmer equation or Fermi-Yang equation.)

They concluded that a field-theoretic formulation –namely the Salpeter equation yields no bound state solutions for such a system. A lone solution with vector coupling was found using the single particle formalism –the Breit equation. They suggested that pair effects, accounted for in the Salpeter

treatment, but omitted in the more naive Breit treatment, are responsible for weakening the interaction to an extent that binding becomes impossible.

The conclusion that bound states which exist in the Breit treatment fail to survive in a Salpeter treatment was also reached by Glöckle, Nogami, and Toyama [76],(GNT), who assumed a spatially extended Gaussian interaction. To obtain the fully covariant contact interaction limit, the Gaussian range was made to approach zero. They found that Salpeter solutions became more tightly bound, contrary to MINs' suggestion. GNT further suggested that the solutions would vanish at a critical range $a = a_c = \beta_c \approx \frac{2}{m} exp\{\frac{-2\pi}{g_{V,S}}\}$ where m is the particle mass and $g_{V,S}$ is the coupling strength of the vector or scalar interaction. At this point the binding reaches $-2m$. GNT's spectrum as the range $a \to 0$ was extracted numerically and they experienced difficulty in their calculation for a range $a < 10^{-4}(1/m)$.

The impetus for the investigations in this appendix is as follows. Partly, we wish to clarify the difference between the two investigations MIN and GNT. This is, admittedly, slightly removed from the central theme of this thesis, but it is an interesting exercise and mathematical curiosity. In addition though, we seek insight in this section on the divergence of the field-theoretic Salpeter formulation and purely quantum-mechanical Breit formulation from one another. We can draw some comfort here from the similar spectra of the two pictures when interaction ranges are of the order $\geq (1/m)$ (like the physical models in our 3-dimensional Breit treatments of chapters 3-6).

In regard to the first motivation, MIN's zero-range interaction is subtly different from GNT's and leads to subtly different spectra in the Breit

treatment. In addition, GNT obtained a bound solution to the Breit equation with a scalar coupling -a state which has no counterpart in the analysis of MIN. If the Breit solutions are sensitive in this way to the prescription to obtain the contact interaction, might not this hold also for the Salpeter solutions? In the following pages, an interaction of the separable type is used to analyse this problem. A limiting procedure, not unlike that of GNT, is employed to obtain the contact limit. A distinct advantage of the separable ansatz is that the spectrum is obtainable by analytic means over all range length scales. We find that the Breit and Salpeter spectra with this form closely mimic the spectra of GNT at finite ranges. We confine the discussion to the states with positive parity only.

The Salpeter solutions do indeed disappear at a critical range: $a_c = \frac{2}{m} exp\{\frac{-2\pi}{g_{V,S}} - \frac{1}{2}\}$ near the value GNT suggest. However, we find a *second* critical range $a_{c_2} = \frac{2}{m} exp\{\frac{-4\pi}{g_{V,S}} - \frac{1}{2}\}$ two orders of magnitude lower than the first, at which a scalar coupling solution to the Salpeter equation reappears. This is a lightly bound state which survives all the way to the contact limit. The numerical work of GNT stopped at a much longer range so possibly their system also has a zero range scalar solution to the Salpeter equation. Sections 2.4 and 2.5 are devoted to the analysis of the separable interaction with vector and scalar couplings respectively.

Breit and Salpeter equations with finite range interactions are, in general, not strictly covariant. Despite this, much use is made of them in modelling physical systems such as the deuteron ($N - N$ bound pair) [20],[27] or meson ($q - \bar{q}$) bound pair.[36],[38]

In practise, the Breit equation is simpler to solve and interpret. However, physically it breaks down at length scales of about the Compton length

$1/m$ because of the improper accounting of antiparticle effects. Thus the two alternative frameworks are expected to diverge at small ranges. In section 2.6 we take a quantitative look at this divergence and suggest a lower cutoff interaction range for which the Breit formulation is acceptable. First, however, the model and the calculations will be sketched and then detailed in the next two sections.

2.2 OVERVIEW OF THE MODEL AND PROCEDURE FOR EXTRACTING THE BOUND STATE SPECTRUM

The Breit equation for two like-mass particles can be written as:

$$\left\{(\alpha_1 - \alpha_2)p + (\beta_1 + \beta_2)m - E\right\}\Psi(p) - \frac{1}{2\pi}\int dq\ I(p-q)\Psi(q) = 0 \qquad (A2.2.1)$$

Here, $p = \frac{1}{2}(p_1 - p_2)$ represents the conjugate momentum to the relative co-ordinate $x = (x_1 - x_2)$ and E is the total energy of the system in the center of mass (c.o.m.) frame. In one dimension, the particle spinors have two components each and the two-particle wave function Ψ therefore has four components. We take the interaction to be of either the scalar or vector types.

$$I_S(p-q) = g_S\beta_1 \otimes \beta_2 U(p-q) \qquad (A2.2.2)a$$

$$I_V(p-q) = g_V(1 - \alpha_1 \otimes \alpha_2)U(p-q) \qquad (A2.2.2)b$$

Here, $U(p-q)$ is a simple function which we will take to be the same in both scalar and vector interaction cases. Also, for simplicity, we will adopt the spinor representation of GNT who wrote:

$$\Psi(p) = \begin{pmatrix} \chi_1(p) \\ \chi_2(p) \\ \chi_3(p) \\ \chi_4(p) \end{pmatrix}$$

This basis is chosen such that $I(p-q)$ is always a diagonal matrix. (This representation was introduced in an earlier publication involving the same authors.[77]) The $\chi_i(p)$ satisfy a system of coupled integral equations dictated by (A2.2.1).

$$-E\chi_1(p) \qquad + 2m\chi_2(p) = \frac{g_1}{2\pi}A_1(p) \qquad (A2.2.3)a$$

$$2m\chi_1(p) - E\chi_2(p) - 2p\chi_4(p) = \frac{g_2}{2\pi}A_2(p) \qquad (A2.2.3)b$$

$$-2p\chi_2(p) - E\chi_4(p) = \frac{g_4}{2\pi}A_4(p) \qquad (A2.2.3)c$$

Here, $A_i \equiv \int dq \;\; U(p-q)\chi_i$. A fourth equation $\chi_3 = 0$ follows from the selection of the c.o.m. frame of reference where $(p_1 + p_2) = 0$. The coupling constants (g_1, g_2, g_4) of equations $(A2.2.3)a-c$ become $(g_S, g_S, -g_S)$ in the case of a scalar coupling and $(0, g_V, g_V)$ for a vector coupling. As pointed out by GNT, a positive parity state has even $\chi_1(p)$ and $\chi_2(p)$ and odd $\chi_4(p)$.

The Salpeter equation is identical in form to the Breit equation with the following modification as pointed out by Salpeter.[3] We alter equation (A2.2.1) by:

$$I(p-q) \rightarrow \Big(\Lambda_{1+}(p_1)\Lambda_{2+}(p_2) - \Lambda_{1-}(p_1)\Lambda_{2-}(p_2)\Big)I(p-q)$$

where

$$\Lambda_{i\pm} \equiv \frac{1}{2}\left\{1 \pm \left[\frac{\alpha_i p_i + \beta_i m}{\sqrt{p_i^2 + m^2}}\right]\right\}$$

is the projection operator onto free particle states of $\pm$ energy.

In the c.o.m. frame and in the χ_i basis, we obtain the following system of equations in the Salpeter treatment:

$$-E\chi_1(p) \qquad + 2m\chi_2(p) = \frac{g_2}{2\pi}\frac{m}{\omega}A_2(p) \qquad (A2.2.4)a$$

$$2m\chi_1(p) - E\chi_2(p) - 2p\chi_4(p) = \frac{g_1}{2\pi}\frac{m}{\omega}A_1(p) - \frac{g_4}{2\pi}\frac{p}{\omega}A_4(p) \qquad (A2.2.4)b$$

$$-2p\chi_2(p) - E\chi_4(p) = -\frac{g_2}{2\pi}\frac{p}{\omega}A_2(p) \qquad (A2.2.4)c$$

Here, $\omega = \omega(p) = \sqrt{p^2 + m^2}$.

Equation sets $(A2.2.3)a - c$ and $(A2.2.4)a - c$ represent the Breit and Salpeter treatments respectively and are applicable in general for any static interaction in one space dimension. The dependence of the equations on the interaction is entirely contained in the $A_i(p)$.

At this point we can introduce the separable ansatz chosen for our interaction. $U(p,q)$ introduced in equations $(A2.2.2)a$ and b takes on a form:

$$U(p,q) = v(p)v(q) \qquad (A2.2.5)a$$

with

$$v(p) = \frac{\beta^2}{\beta^2 + p^2} \qquad (A2.2.5)b.$$

Details of the solutions of systems $(A2.2.3)a - c$ and $(A2.2.4)a - c$ with this selection are included in a *sub*-appendix but we will outline the procedure here.

The $A_i(p)$ now take on a simple form:

$$A_i(p) = \left(\int_{-\infty}^{+\infty} dq v(q) \chi_i(q) \right) v(p) = B_i v(p) \qquad (A2.2.6)$$

where the B_i are constants to be determined. The left hand side (*l.h.s.*)of both systems of equations $(A2.2.3)a - c$ and $(A2.2.4)a - c$ can be manipulated to isolate the $\chi_i(p)$. One can then simply carry out the operation $\int dp v(p) \cdot \{\text{both sides}\}$ to obtain two systems of algebraic equations in the constants B_i pertaining to the Breit and Salpeter treatments. Both systems are homogenous however and we must seek trivial determinants among the coefficients of the B_i. This sifts out the energy eigenvalue(s) as a function of coupling strength g_i, mass m, and interaction parameter β (introduced in $(A2.2.5)b$). $1/\beta$ is essentially an interaction range. At this point we note that

in the limit $\beta \to \infty$, $v(p), U(p,q) \to 1$ which corresponds to MIN's contact interaction. The Fourier transform of $v(p)$ is $\pi\beta e^{-\beta|x|}$ which combined with the $\frac{1}{2\pi}$ of (A2.2.1) behaves as a spatial δ-function in the $\beta \to \infty$ limit. Normalization of the momentum-space wave function uniquely determines the B_i-constants and consequently the $A_i(p)$ functions on the (*r.h.s.*)of equations (A2.2.3)$a-c$ and (A2.2.4)$a-c$. The $\chi_i(p)$ on the (*l.h.s.*)of these equations can be isolated algebraically to determine the wave function itself.

2.3 DETAILS OF THE CALCULATIONS

The separable nature of the interaction in this work greatly simplifies the solution of the Breit and Salpeter equations. Take, for example, the Breit system. Using (A2.2.3)$a-c$, one can isolate $\chi_1(p)$:

$$\chi_1(p) = \frac{1}{2\pi E\left(E^2 - 4(p^2+m^2)\right)}\left\{g_1(4p^2 - E^2)A_1(p) - g_2(2mE)A_2(p)\right\} \quad (A2.3.1)$$

Letting $\alpha \equiv \sqrt{m^2 - E^2/4}$ and using equation (A2.2.6) to replace the $A_i(p)$ by $B_i v(p)$ we obtain:

$$\chi_1(p) = \frac{v(p)}{8\pi E(p^2+\alpha^2)}\left\{g_1(E^2 - 4p^2)B_1 + 2mEB_2\right\}.$$

Likewise, $\chi_2(p)$ and $\chi_4(p)$ can be isolated. Now taking

$$\int_{-\infty}^{+\infty} dp v(p)\chi_1(p) = B_1$$

we obtain:

$$\left\{-1 + \frac{1}{8\pi E}\int_{-\infty}^{+\infty} dp \frac{g_1(E^2 - 4p^2)v(p)^2}{(p^2+\alpha^2)}\right\}B_1 + \left\{\frac{m}{4\pi}\int_{-\infty}^{+\infty} dp \frac{v(p)^2}{(p^2+\alpha^2)}\right\}B_2 = 0 \quad (A2.3.2)$$

This is one of three homogenous equations in the constants $B_{1,2,4}$. With the ansatz of (A2.2.5)b, the integration can be carried out simply. Equation

(A2.3.2) and its two counterparts must comprise a singular system to avoid $B_4 = 0$ trivially. Specifically, the (Breit) system is:

$$\left[g_1(K - L) - 1\right]B_1 + \left[2g_2\frac{m}{E}K\right]B_2 = 0 \qquad (A2.3.3)a$$

$$\left[2g_1\frac{m}{E}K\right]B_1 + \left[g_2K - 1\right]B_2 = 0 \qquad (A2.3.3)b$$

$$B_4 = 0 \qquad (A2.3.3)c$$

where $K = \frac{\beta E}{16\alpha}\frac{(\alpha+2\beta)}{(\alpha+\beta)^2}$ and $L = \frac{\beta^3}{4E(\alpha+\beta)^2}$. We see immediately that $B_4 = 0$. This is a consequence of $\chi_4(p)$ being odd in p. With a vector coupling, the energy eigenvalue is determined by:

$$1 - g_V K = 0 \qquad (A2.3.4)$$

With a scalar coupling, E is fixed by:

$$1 - \left(\frac{2g_S K\alpha}{E}\right)^2 - g_S(2K - L) - g_S^2 KL = 0 \qquad (A2.3.5).$$

These expressions yield the closed form expressions for E listed in Table A2.1 when $\beta \to \infty$. The momentum-space wave function in this limit reduces to the form:

$$\Psi(p) = \frac{g_2}{8\pi}\begin{pmatrix} 2m \\ E \\ 0 \\ -2p \end{pmatrix}\frac{N}{p^2 + \alpha^2}v(p) \qquad (A2.3.6)$$

Recall that as $\beta \to \infty$, $v(p) = \frac{\beta^2}{\beta^2+p^2} \to 1$. g_2 is either g_S or g_V. This is in agreement with MIN's equation (27) although our normalization constant N is considerably more complicated. For a scalar coupling, we obtain a term in the wave function component $\chi_1(p)$ which disappears for large β as $\mathcal{O}(1/\beta)$ but upon integration over p gives a finite contribution which is accounted for in N. The exact expression for N is not highly illuminating but it is important to point out that the $\mathcal{O}(1/\beta)$ contribution to $\Psi(p)$ behaves strangely upon

Fourier transforming to co-ordinate space. $\Psi(x)$, transform of $\Psi(p)$ in (A2.3.6) includes an additional term $\eta(x)$ in the component $\chi_1(x)$.

$$\eta(x) = -\frac{4Nm}{g_S E} e^{-\beta|x|}$$

As $\beta \to \infty$, the height of $\eta(x)$ does not vary and the area beneath it shrinks to zero. The Salpeter energy eigenvalue and amplitude are determined in the same way. Equations (A2.2.4)$a-c$ can be manipulated via the procedure (A2.3.1) $\to$ (A2.3.2) to obtain the following system of equations in the coefficients $B_{1,2,4}$:

$$\left[\frac{g_1 m^2}{\pi} I - 1\right] B_1 + \left[\frac{g_2 mE}{2\pi} I\right] B_2 = 0 \qquad \text{(A2.3.7)}a$$

$$\left[\frac{g_1 mE}{2\pi} I\right] B_1 + \left[\frac{g_2 m^2}{\pi} I - 1\right] B_2 = 0 \qquad \text{(A2.3.7)}b$$

$$\left[\frac{g_4}{\pi} J - 1\right] B_4 = 0 \qquad \text{(A2.3.7)}c$$

Here we have introduced the two integrals encountered in the Salpeter treatment, I and J.

$$I = \frac{\beta^4}{2(\alpha^2-\beta^2)}\left[\frac{\mathcal{I}_s(E) - J_1}{\alpha^2-\beta^2} + J_2\right] \qquad \text{(A2.3.8)}a$$

$$J = \frac{\alpha^4\beta^2}{(\alpha^2-\beta^2)^2} I + \frac{\beta^8(\beta^2-2\alpha^2)}{2(\alpha^2-\beta^2)^2} J_3 + \frac{\beta^{10}}{2(\alpha^2-\beta^2)} J_4 \qquad \text{(A2.3.8)}b$$

Here, $\mathcal{I}_s(E) \equiv \frac{1}{\alpha|E|}\cos^{-1}\{1 - \frac{E^2}{2m^2}\}$. The quantities $J_{1,2,3,4}$ are complicated expressions in β and m with the following forms: Let

$$A = \cos^{-1}\{\frac{2\beta^2}{m^2} - 1\} \qquad \text{for} \qquad \beta < m$$

$$= 2\ln\{\frac{m}{\beta - \sqrt{\beta^2 - m^2}}\} \quad \text{for} \qquad \beta > m.$$

and let

$$P_1(m,\beta) = 2\beta^2 - m^2$$

$$P_2(m,\beta) = 8\beta^4 - 8m^2\beta^2 + 3m^4$$

$$P_3(m,\beta) = 48\beta^6 - 72m^2\beta^4 + 54m^4\beta^2 - 15m^6$$

$$P_4(m,\beta) = 44\beta^4 - 44m^2\beta^2 + 14m^4,$$

then:

$$J_1 = \frac{A}{2\beta\sqrt{|\beta^2 - m^2|}}$$

$$J_2 = \frac{1}{2\beta^2(\beta^2 - m^2)}\left[\frac{P_1 A}{2\beta\sqrt{|\beta^2 - m^2|}} - 1\right]$$

$$J_3 = \frac{1}{8\beta^4(\beta^2 - m^2)^2}\left[\frac{P_2 A}{2\beta\sqrt{|\beta^2 - m^2|}} - 3P_1\right]$$

$$J_4 = \frac{1}{48\beta^6(\beta^2 - m^2)^3}\left[\frac{P_3 A}{2\beta\sqrt{|\beta^2 - m^2|}} - P_4\right].$$

For $\beta = m$, $\{J_1, J_2, J_3, J_4\}$ become simply $\{\frac{1}{m^2}, \frac{2}{3m^4}, \frac{8}{15m^6}, \frac{16}{35m^8}\}$ respectively. The energy of the bound state is determined by:

$$\left(1 - \frac{g_V}{\pi}J\right)\left(1 - \frac{g_V m^2}{\pi}I\right) = 0 \qquad (A2.3.9).$$

for a vector coupling, and by:

$$\left(1 + \frac{g_S}{\pi}J\right)\left(1 - 2\frac{g_S m^2}{\pi}I + (\frac{g_S m\alpha}{\pi})^2 I^2\right) = 0 \qquad (A2.3.10)$$

for a scalar coupling. In the $\beta \to \infty$ limit, these expressions reduce to those given in sections A2.4 and A2.5 respectively.

The Salpeter amplitude $\Psi(p)$ obtained with a scalar coupling in the $\beta \to \infty$ limit takes the form:

$$\Psi(p) = \frac{g_S}{8\pi}\begin{pmatrix} 2m \\ E \\ 0 \\ -2p \end{pmatrix}\frac{N'}{p^2 + \alpha^2}\left(\frac{mv(p)}{\sqrt{p^2 + m^2}}\right) \qquad (A2.3.11)$$

The amplitude contains a term which disappears as $\mathcal{O}(1/\ln(\beta/m))$ so it does not contribute to the above expression directly. However, this term, upon integration over p, contributes a finite amount to the normalization N'. This is quite similar to the situation found earlier with the Breit solution in this limit. Unlike the Breit case however, the co-ordinate space Salpeter amplitude $\Psi(x)$ does not pick up a residual term analogous to $\eta(x)$ which survives in the contact limit. The residual term here vanishes also as $\mathcal{O}(1/\ln(\beta/m))$ instead.

2.4 THE COVARIANT LIMIT WITH VECTOR INTERACTION

As seen in the last section, the determinant of the coefficients of the B_i yields a secular-type equation which can be quite complicated. Much simplification occurs in the $\beta \to \infty$ limit however. The Breit equation with a vector coupling reduces to the simple eigenvalue equation: $\frac{g_V E}{8\alpha} - 1 = 0$. This yields $E = \frac{2m}{\sqrt{1+(g_V/4)^2}}$ in agreement with the solution obtained by MIN. This agreement is somewhat coincidental since in general our spectra are different from those of MIN. A subtle conspiracy of relationships brings this about. The integrated quantities $A_i(p) = v(p)\int_{-\infty}^{+\infty} dq v(q)\chi_i(q)$ which appear in equations $(A2.2.3)a-c$ correspond to the A_i which MIN define as $A_i \equiv \int_{-\infty}^{+\infty} dq \chi_i(q)$. MIN's contact interaction simply amounts to setting $v(q) = v(p) = 1$ and therefore A_i is independent of p. Upon integrating $(A2.2.3)a$ over p, MIN obtain:

$$-EA_1 + 2mA_2 = \frac{g_1}{2\pi} A_1 \int_{-\infty}^{+\infty} dp$$

For this to describe a normalizable bound state, either g_1 or A_1 on the $(r.h.s.)$must be zero enabling the $(l.h.s.)$terms to remain finite. For an even

parity solution. $A_4 = 0$ since $\chi_4(p)$ is odd and A_1 and A_2 must be non-zero to avoid $\chi_1(p) = \chi_2(p) = \chi_4(p) = 0$. The requirement $g_1 = 0$ *is* satisfied in the vector coupling case. This allows the integrated equation (A2.2.3)*a* to be solved. In the separable interaction, the A_i themselves are integrable over p and remain so for any value of β, the inverse range. As mentioned in the detail of the last section, the amplitude $\Psi(p)$ is in near agreement with MIN but differs in a seemingly bizarre manner in the normalization.

MIN and GNT found no solutions to their Salpeter equations with vector coupled interactions. This is concluded in this work also. Our energy eigenvalues for the Breit and Salpeter equations as a function of β are illustrated in Figure A2.1 Our Salpeter solution becomes more tightly bound as β increases and disappears altogether at $\beta \approx \frac{m}{2}e^{2\pi+\frac{1}{2}}$ At this point, the binding reaches $2m$. This is in good qualitative agreement with the findings of GNT. MIN had speculated that the Salpeter equation would only allow a weaker binding as spatial range decreased. This is not supported by our result. We point out that the Salpeter equation yields a symmetric energy spectrum about $E = 0$. The secular-type equation (A2.3.9) which determines E is an even function. In the $\beta \to \infty$ limit, this equation reduces to:

$$\frac{g_v}{2\pi}\ln(\frac{m}{2\beta}) + 1 + \frac{g_v}{4\pi} - \frac{g_v E^2}{8\pi}\mathcal{I}_s(E) = 0$$

Here, $\mathcal{I}_s(E) \equiv \frac{1}{\alpha|E|}\cos^{-1}(1 - \frac{E^2}{2m^2}) > 0$ for $|E| \leq 2m$. The $\ln(\frac{m}{2\beta})$ term dominates for large β. The (*l.h.s.*)approaches $-\infty$ logarithmically. This offers strong support that the covariant 1-d Salpeter equation cannot support a bound vector coupled bound state regardless of the prescription used to define the covariant interaction. (See Table A2.1)

Figure A2.1 Separable Vector Interaction Energy Solutions

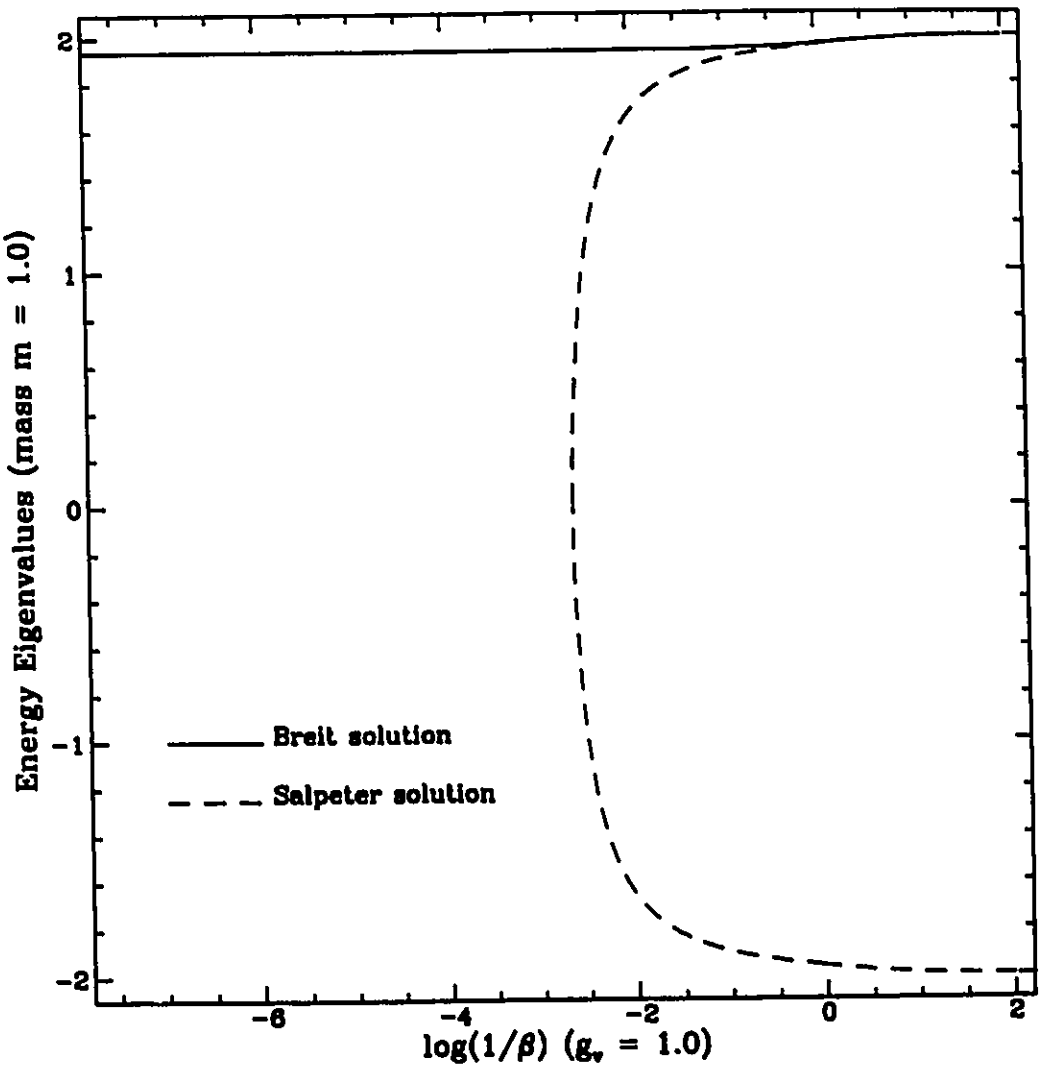

2.5 THE COVARIANT LIMIT WITH SCALAR INTERACTION

The Breit system of equations for the scalar separable ansatz yield the same asymptotic wave function and energy eigenvalue for $\beta \to \infty$ as in the vector coupled case (replacing g_V by g_S). Here also, the normalization is complicated by the nature of the ansatz. We once again obtain finite contributions to the normalization integral from terms in $\Psi^\dagger\Psi$ which disappear as $1/\beta$ in the limit.

Since none of the couplings g_1, g_2, g_4 vanish, MIN's coupled integral equations offer no solution for the scalar coupled Breit equation. GNT found a solution in the contact limit with energy $E = \frac{2m}{\sqrt{1+\tanh^{-1}(g_S/4)}}$. This falls into agreement with our solution in the weak interaction limit: $g_S \ll 1$. The difference is attributable to the separable nature of the ansatz used in this paper. [79]

Our scalar system within a Salpeter treatment provides a surprising result. As can be seen in Figure A2.2, the Salpeter spectrum has a lightly bound state for $\beta \approx m$ whose binding increases as β is increased until $E = 0$. This occurs very close to $\beta = \frac{m}{2}e^{2\pi+\frac{1}{2}}$. No bound solutions exist for the next three orders of magnitude in β! A weakly bound solution reappears for β very close to $\frac{m}{2}e^{4\pi+\frac{1}{2}}$. The approximate critical β-values are obtained by taking the asymptotic expansion for large β of the secular-type equation (in this case, (A2.3.10)). We retain orders $\mathcal{O}(\ln(\frac{\beta}{m}))$ and $\mathcal{O}(1)$ and ignore orders $\mathcal{O}(\frac{m^2}{\beta}\ln(\frac{\beta}{m}))$ and higher. We obtain:

$$\left[\left(-\frac{g_S}{2\pi}\ln(\frac{\beta}{m}) + 1 - \frac{g_S}{2\pi}(\ln(2) - \frac{1}{2})\right)\left(1 - \frac{g_S m^2}{8\pi}\mathcal{I}_s(E)\right)\right] - \frac{g_S E^2}{8\pi}\mathcal{I}_s(E) = 0$$

The $-\frac{g_S}{2\pi}\ln(\frac{\beta}{m})$ term changes the sign of the square bracket contents at $\beta = \frac{m}{2}e^{(4\pi+\frac{1}{2})} + \mathcal{O}(\frac{m^2}{\beta}\ln(\frac{\beta}{m}))$. For β larger than this critical value, the system retains

the solution shown in Figure A2.2. In the limit $\beta \to \infty$, E approaches the value ε which is the root of the equation: $\mathcal{I}_1(E) = \frac{2\pi}{g_S m^2}$. Again, $-\varepsilon$ is also a solution.

In their investigation with a Gaussian interaction, GNT concluded that no scalar solution seems to exist for a range smaller than a critical value $a_c \approx \frac{2}{m} e^{-\frac{2\pi}{g_S}}$. This corresponds quite closely to an inverse range $\beta \approx \frac{m}{2} e^{(\frac{2\pi}{g_S}+\frac{1}{2})}$. In fact, the solution of GNT at finite range agrees quite well qualitatively with our right-most Salpeter solution of Figure A2.2. GNT experienced difficulty in their numerical evaluation of the energy eigenvalue for short range (or large β). It is quite possible that their scalar interaction yields a bound state solution for very short ranges –say $a_{c_2} \approx e^{-(\frac{2\pi}{g_S})} a_c$. There is a strong possibility that these slightly different formulations corroborate one another qualitatively.

Figure A2.2 Separable Scalar Interaction Energy Solutions

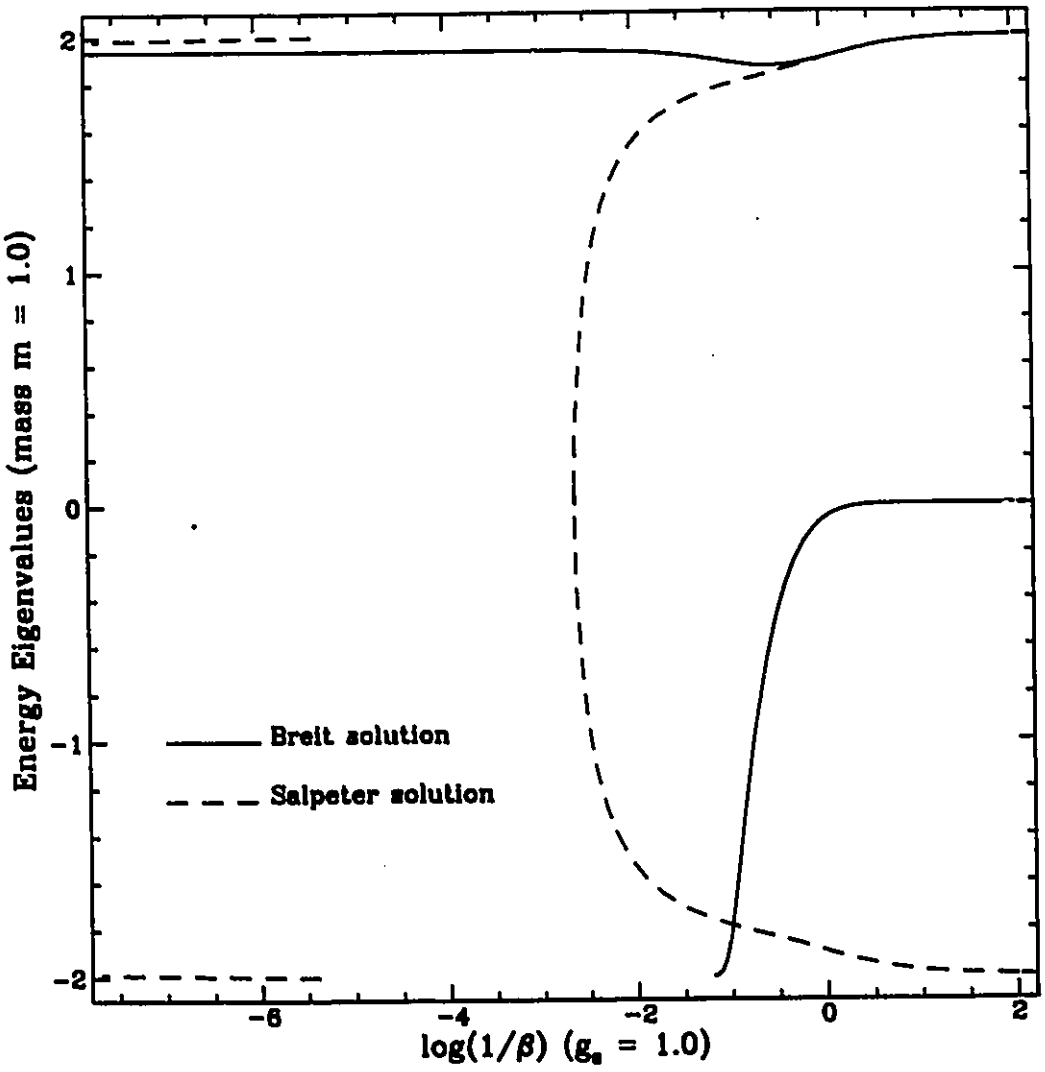

Table A2.1 SUMMARY OF CONTACT INTERACTION E-EIGENVALUES

Reference:	1.) MIN	2.) GNT	3.) This work
Ansatz $U(p,q)$:	1	$\lim_{a\to 0} e^{-[\frac{a}{2}(p-q)]^2}$	$\lim_{\beta\to\infty} \frac{\beta^4}{(\beta^2+p^2)(\beta^2+q^2)}$
Breit vector case:	$\frac{2m}{\sqrt{1+(g_V/4)^2}}$	$2m\cos(g_V/4)$	$\frac{2m}{\sqrt{1+(g_V/4)^2}}$
Breit scalar case:	*no solution*	$\frac{2m}{\sqrt{(1+\tanh(g_S/4)^2)}}$	$\frac{2m}{\sqrt{1+(g_S/4)^2}}$
Salp. vector case:	*no solution*	*no solution*	*no solution*
Salp. scalar case:	*no solution*	*no solution* *	ε **

* GNT found no solution in a numerical search for $a \gtrsim 10^{-4}m^{-1}$

** ε is the root of the equation $\cos^{-1}(1-\frac{\varepsilon^2}{2m^2}) - \frac{2\pi}{g_S m^2}\alpha(\varepsilon)|\varepsilon| = 0.$
For $g_s = 1, \varepsilon \approx \pm 1.95096m$

2.6 BREIT AND SALPETER EQUATIONS WITH EXTENDED RANGE INTERACTIONS

Figures *A*2.1 and *A*2.2 illustrate how differently behaved the Breit and Salpeter solutions can be for a short range interaction. This can be attributed to the inability of the Breit equation to properly account for anti-particle screening effects. The Breit equation involves fermions which propogate forward in time only.

The scalar and vector interactions with extended range yield the spectra illustrated in Figure *A*2.3. This is a magnification of the top right

corners of both Figures A2.1 and A2.2. At the range of the Compton wavelength ($\frac{1}{\beta} = \frac{1}{m}$), the Breit and Salpeter picture binding energies $2m - E$ differ by $\sim 10\%$ for the vector interaction and by $\sim 3\%$ for the scalar interaction. The discrepancy in the vector case is reduced to 1% at about $1/\beta = 7/m$. At this range, the scalar interaction discrepancy lies around 0.018%.

This has some significance for the nucleon-nucleon (N-N) interaction. If the N-N system indeed requires a relativistic treatment, the Breit equation may provide a sufficient description. It is more managable than the Salpeter equation technically and its interpretation is more straight forward. The interaction range for nucleons is an order of magnitude larger than the Compton wavelength -(1 to 2 fm *cf.* 0.21 fm).

It has long been considered that an admixture of attractive scalar and repulsive vector interaction components comprises a large portion of the N-N interaction.[2090] We reproduce the deuteron binding energy of $0.0024 m_N$ with couplings of $g_V = 0.30$ and $g_S = -0.25$. The Breit and Salpeter equations yield binding energies which differ by only 0.15%. The discrepancy increases rapidly as β approaches m and beyond. $\beta = m$ yields a discrepancy of 2.8% and at $\beta = 10m$, the bindings disagree completely ($B.E._{Sa} = B.E._{Br} \cdot 1.56$). Again, we see the binding strengthen, not weaken, as the interaction range becomes smaller.

On the whole, our model offers support for the utility of the Breit equation for the N-N system.

Figure A2.3 Extended S and V Interaction Bound State Energy

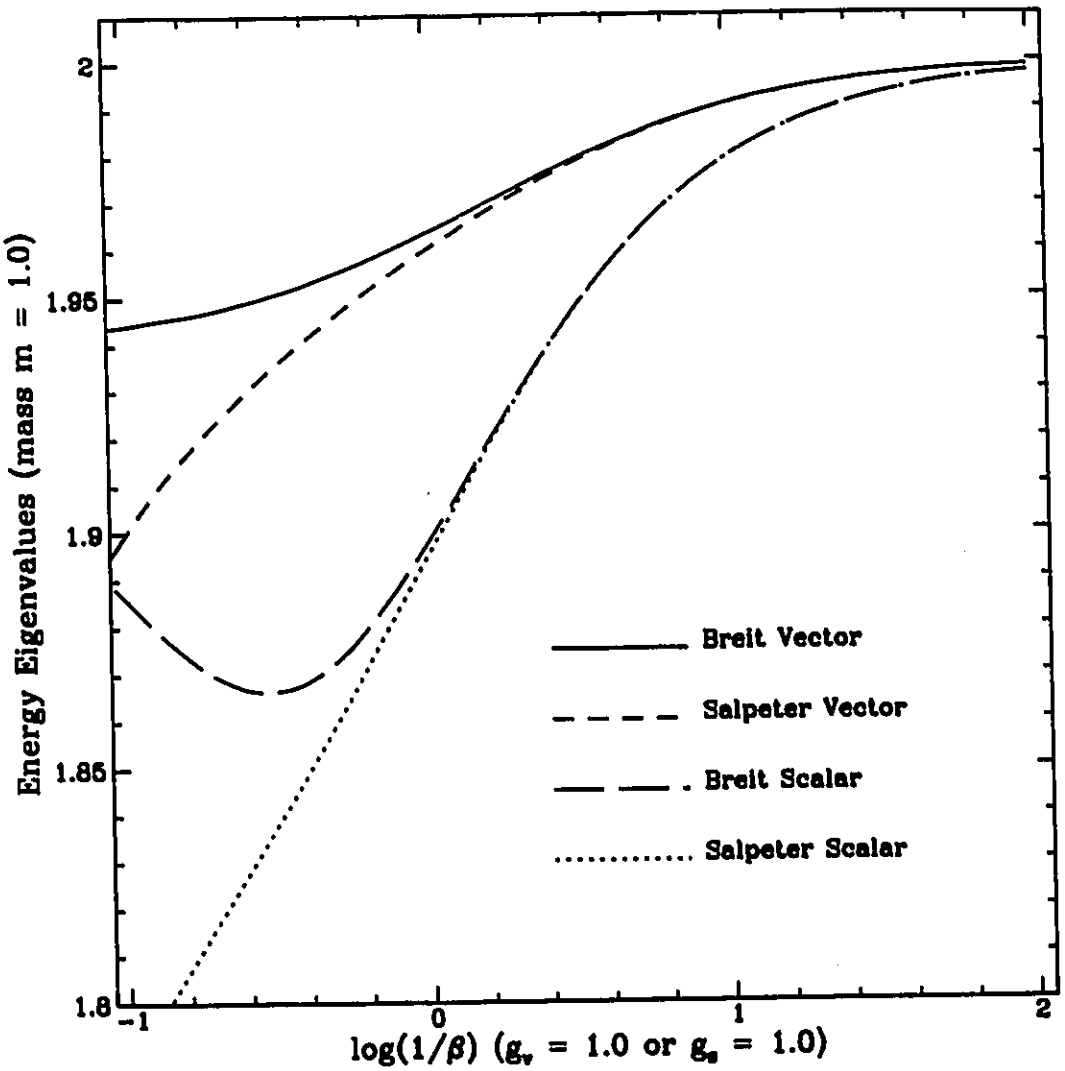

2.7 SUMMARY AND DISCUSSION

The separable systems treated in this appendix shed light on two areas of interest.

In the limit of the inverse range parameter approaching ∞ the Breit and Salpeter equations become fully covariant. We find three bound positive parity solutions to these covariant equations –one each for the Breit equation with scalar and vector coupling, and a third solution –a scalar mediated bound system in the Salpeter formulation. The Salpeter spectrum is fully symmetric about $E = 0$ so we obtain a mirror solution with $E < 0$ also which could be considered a fourth covariant system with properties identical to the $+E$ solution. It is interesting that the spectrum of the covariant interaction is sensitive to the prescription used to describe the interaction. The models of MIN, GNT, and this paper involve the Fourier representation of a δ-function in momentum space, a spatial Gaussian with width approaching zero, and a separable ansatz with range $(\frac{1}{\beta})$ approaching zero respectively. Our results would concur with MIN's if we interchanged the order of the operations of 1.) integrating the equation systems (A2.2.3) and (A2.2.4) over p and 2.) taking the contact interaction limit: $\beta \to \infty$. Our results agree qualitatively quite well with GNTs' Gaussian results for the values of range common to both investigations. They suggested that a scalar solution to the Salpeter equation did not exist but our surprising result hints that this conjecture may be incorrect.

We also looked briefly at the Breit and Salpeter equations for inverse range parameter $\beta \sim \mathcal{O}(m)$. The spectra of the two equations depart from

each other at around this order of β. Our model offers some support for the utility of the Breit equation for the N-N system.

Appendix III

OPEP and the Breit Equation

The best established feature of the N-N interaction is the "long" range tail and relatively strong tensor coupling associated with the exchange of a single pion. In the Schrödinger equation, the OPEP (One Pion Exchange Potential) is first derived field-theoretically from the pion propogator and nucleon form factors in the lowest order of perturbation theory. (See, in particular, p264-265 Eq.#s 4.370-4.375 of Sakurai [80].) The resulting spatial/spinor dependent quantity is then simply "placed" into the Schrödinger equation. It is characterized by the Yukawa tail radial dependence: $\mathcal{Z}_\pi(r) = \frac{e^{-m_\pi r}}{r}$.

The discussion which follows will touch on three possible ways of including the well established long range behaviour of the N-N interaction in the Breit equation: a pseudoscalar form, an axial vector form, and a contrived alternative.

The incorporation of the OPEP into the Breit equation is, at first glance, a straight forward operation. The pion is a pseudoscalar meson, so

the logical spinor/spatial dependence to include in $\hat{H}_{int}$ would seem to be:

$$(\mathcal{J}_1\mathcal{J}_2)(\Gamma_1\Gamma_2)P(r)$$

with $P(r) = -G^2\mathcal{Z}_\pi(r)$. The bare coupling $G^2 = 14.7$ is much too large. This presents an overriding difficulty which excludes this possibility. It sets the strength of the pseudoscalar interaction at one order of magnitude larger than the nucleon mass scale! In the reduction of the Breit equation to a Schrödinger-*like* equation, the form $W + P(r) + ...$ appears often and in the denominator of the effective interaction. The effective interaction obtains a singular point at some positive value of r. This situation in the Breit equation precipitates the infamous Klein paradox -a clear regime of inapplicability of a purely quantum mechanical equation.

When one carries through the reduction to a Schrödinger-*like* equation favouring the pure large spinor component, simply setting $P(r) = 0$ and retaining the derivatives $P'(r)$ and $P''(r)$ indeed yields the traditional OPEP interaction. This fact is anticipated by the agreement of the Breit formalism with full fledged Quantum Field Theory to first order in perturbation. [81]

In this sense, the Schrödinger equation of conventional nuclear physics is written with the OPEP put in by hand. $P'(r)$ and $P''(r)$ appear directly but $P(r)$ is strictly absent.

An axial vector coupling between the nucleon and pion, on the other hand, leads to no such difficulties with large coupling as the axial interaction is defined with a modified coupling constant. In the tail region,

$$\hat{H}_{int} = (\gamma_1^0\gamma_2^0)(\gamma_1^5\gamma_1^\mu\gamma_{25}\gamma_{2\mu})A(r)$$

with $A(r)$ taken to be: $-(\vec{\tau}_1 \cdot \vec{\tau}_2)/3g^2\mathcal{Z}_\pi(r)$ with the usual definition of the coupling: $g^2 \equiv (\frac{m_\pi}{2M})^2G^2$

In the case of the spin-singlet, this coupling leads exactly to the desired Yukawa tail favoured by the NN scattering data partial wave analysis [72] and so we made use of this form in the CSB problem of chapter 3 and the relativistic singlet state effective range case of chapter 4. However, the tensor dependence which mixes the $l = (j-1)$ and $l = (j+1)$-wave in the spin triplet configuration is an extra order in $(\frac{m_\pi}{2M})^2$ smaller than in the desired OPEP. This tensor coupling is far too small to remotely explain the triplet data, (including the $l = 2$ component of the deuteron) and hence for the triplet work, a more thorough treatment was necessary. The OPEP interaction plays a more significant role in our triplet analysis than in the singlet work in which our focus was charge symmetry.

To bring about a satisfactory resolution of these problems we are led to the remaining option. We drop any pretense that the Breit equation will retain more field theoretic rigour than the Schrödinger equation by virtue of it being relativistic. To obtain both the proper strength *and* tensor coupling in the OPEP part of the Breit equation, we must resign to putting it in by hand. It is therefore on the same footing as the OPEP in the Schrödinger equation. We appeal to a field-theoretic framework to obtain it but then use it in a less rigourous quantum mechanical framework. The lowest order contribution from pion exchange is:

$$H_{int_\pi} = (\frac{G}{2M})^2(\vec{\tau}_1 \cdot \vec{\tau}_2)\{-(\vec{\sigma}_1 \cdot \vec{p})(\vec{\sigma}_2 \cdot \vec{p})\}\mathcal{Z}_\pi(r)$$

To obtain direct and tensor strengths of the traditional OPEP (i.e. as in the pseudoscalar coupling) *and* avoid encountering the defeating bare coupling G^2 we must simply translate this into configuration space.

$$\hat{H}_{int_\pi} = \vec{\sigma}_1 \cdot \vec{\sigma}_2 U_{\sigma\sigma}(r) + \hat{\Lambda} U_\Lambda(r)$$

where:

$$U_{\sigma\sigma}(r) \equiv (\frac{G}{2M})^2(\vec{\tau}_1 \cdot \vec{\tau}_2)\frac{1}{r}\mathcal{Z}'_\pi(r) \qquad (A3.1)a$$

and:

$$U_\Lambda(r) \equiv (\frac{G}{2M})^2(\vec{\tau}_1 \cdot \vec{\tau}_2)[\mathcal{Z}''_\pi(r) - \frac{1}{r}\mathcal{Z}'_\pi(r)] \qquad (A3.1)b$$

The operator $\hat{\Lambda}$ is given by:

$$\hat{\Lambda} \equiv (\frac{1}{r^2})\{(\vec{\sigma}_1 \cdot \vec{r})(\vec{\sigma}_2 \cdot \vec{r})\}$$

In more traditional notations. the operator $\hat{S}_{12}$ is favoured over $\hat{\Lambda}$ and:

$$\hat{H}_{int_\pi} = (\frac{G}{2M})^2(\vec{\tau}_1 \cdot \vec{\tau}_2)\{\vec{\sigma}_1 \cdot \vec{\sigma}_2[\frac{1}{3}\mathcal{Z}''_\pi(r) + \frac{2}{3r}\mathcal{Z}'_\pi(r)] + \hat{S}_{12}[\frac{1}{3}\mathcal{Z}''_\pi(r) - \frac{1}{3r}\mathcal{Z}'_\pi(r)]\}$$

where:

$$\hat{S}_{12} \equiv 3\hat{\Lambda} - \vec{\sigma}_1 \cdot \vec{\sigma}_2$$

The elimination of the smaller spinor components in favour of the pure large component of Ψ leads to Schrödinger-*like* equation's with interaction tails in both the central and tensor parts which are in agreement with the nonrelativistic OPEP to lowest order in $(\frac{m_\pi}{2M})^2$ There are further spurious contributions which come about as signatures of the eliminated components but they are one *further* order removed in this ratio $\approx 1/200$.

We turn now to the regularizing of our OPEP within the region of nucleon overlap. The partial wave analysis which strongly favours the OPEP tail draws upon fits of the higher l partial waves in the $r > 2$fm. region where other nuclear forces are greatly diminished. Within the shorter range, the OPEP should depart from the pure Yukawa form due to the smeared out nucleons (i.e. form factors). Treatment of the pion exchange here is generally phenomenological since the other contributions to the nuclear force are thought

to dominate. The cutoff Yukawa used in the CSB. and singlet-effective range expansion work (chapters 3 and 4). namely. $\mathcal{Z}_\pi(r) = \frac{[e^{(-m_\pi r)} - e^{(-\frac{1}{2}\Lambda r)}]}{r}$, suffices to eliminate any singularity in the effective interaction at some finite r for the $^1S_0$ case. The same ansatz. however. leads to a large tensor part in the near region which overly restricts the parameter space for the strong couplings g_s and g_v which also must be small enough to avoid such singularities. We therefore desire to limit the OPEP influence in this region by a more moderate ansatz and introduce controlling parameters $c_{\sigma\sigma 0} \equiv U_{\sigma\sigma}(r=0)$ and $c_{\Lambda 0} \equiv U_\Lambda(r=0)$ to keep the OPEP contribution tame enough to not greatly intrude on the g_s, g_v parameter space but at the same time offer some control over the very important tensor portion of the interaction since it is vital to the S/D-mixing of the deuteron and scattering states. We acknowledge other possible contributions to the tensor portion at short range by relaxing the connection between $U_{\sigma\sigma}(r)$ and $U_\Lambda(r)$ in the region of small r. $c_{\sigma\sigma 0}$ and $c_{\Lambda 0}$ are therefore independent. Since the Yukawa tail is inviolable at larger r, we define $U_{\sigma\sigma}(r)$ and $U_\Lambda(r)$ as follows.

$$r \le \frac{2}{m_\pi} \Rightarrow U_{\sigma\sigma}(r) = g^2\{c_{\sigma\sigma 0} + c_{\sigma\sigma 4} r^4 + c_{\sigma\sigma 5} r^5 + c_{\sigma\sigma 6} r^6 + c_{\sigma\sigma 7} r^7 + c_{\sigma\sigma 8} r^8\}$$

$$r \le \frac{2}{m_\pi} \Rightarrow U_\Lambda(r) = g^2\{c_{\Lambda 0} + c_{\Lambda 4} r^4 + c_{\Lambda 5} r^5 + c_{\Lambda 6} r^6 + c_{\Lambda 7} r^7 + c_{\Lambda 8} r^8\}$$

Outside of the pion Compton length, the quantities $U_{\sigma\sigma}(r)$ and $U_\Lambda(r)$ revert to their dependences (A3.?)a, b above, on $\mathcal{Z}_\pi(r)$ of the Yukawa form:

$$r \ge \frac{2}{m_\pi} \Rightarrow \mathcal{Z}_\pi(r) = \frac{e^{(-m_\pi r)}}{r}$$

The coefficients $c_{\sigma\sigma i}$ and $c_{\Lambda i}$ are chosen to match radial derivatives up to 4th order at the matching radius. The 4th derivative of $\mathcal{Z}_\pi(r)$ appears explicitly in the Breit radial equations so continuity one derivative beyond that yields sufficiently smooth effective interactions.

References

[1] C.A. Dominguez, E. de Rafael, Ann. Phys. 174, p372, (1987)

[2] E.E. Salpeter and H.A. Bethe, Phys. Rev. 84, p1332, (1951)

[3] E.E. Salpeter, Phys. Rev. 87, p328, (1952)

[4] V.B. Mandelzweig and S.J. Wallace, Physics Lett. B 197, p 469, (1987)

[5] J. Sucher, Proc. NATO Institute for Advanced Study on Relativistic effects in atoms, molecules and solids (Vancouver), ed. G. Malli (Plenum, New York, 1982)

[6] J. Sucher, Phys. Rev. Lett. 55, p1033, (1985)

[7] G.E. Brown, D. Ravenhall, Proc. R. Soc. London, A 208, p552 (1951)

[8] N. Nakanishi, Supp. Prog. Theor. Phys. 43 p1, (1969)

[9] W. Krowlowski Act Polon. B 12 #9 p891, (1981)

[10] G. Breit, Phys. Rev. 34, p553, (1929)

[11] L.G. Arnold et. al. , Phys. Rev. C 25, p936, (1982)

[12] L.G. Arnold et. al. , Phys. Rev. C 23, p1949, (1981)

[13] L.G. Arnold, B.C. Clark , Phys. Lett. 843, p46, (1979)

[14] J.A. MacNeil, J.R. Shephard, S.J. Wallace, Phys. Rev. Lett. 50, p1439, (1983)

[15] S. Klarsfeld, J. Martorell, J.A. Oteo, M. Nishimura, D.W.L.Sprung, Nuc. Phys. A456, p373, (1986)

[16] W. van Dijk, Phys. Rev. C 40, p1437, (1989)

[17] D.W.L. Sprung, Hua Wu, J. Martorell, Phys. Rev. C 42, p863, (1990)

[18] R.K. Bhaduri, W. Leidemann, G. Orlandini, E.L. Tomusiak,
Phys. Rev. C 42, p1867, (1990)

[19] M.W. Kermode, S.A. Moszkowski, M.M. Mustafa, W. van Dijk
Phys. Rev. C 43, p416, (1990)

[20] N. Kemmer, Helv. Phys. Acta 10, p48, (1937)

[21] J. Schwinger, Phys. Rev. 61, p381, (1942)

[22] C. Møller and L. Rosenfeld, Proc. Cop. 17, #8, (1940)

[23] L. Rosenfeld, "Nuclear Forces" (North Holland Publ. Co., Amsterdam)
(1949)

[24] K. Erkelenz, Phys. Rep. 13 #5, p191 (1974)

[25] A.E. Green and T. Sawada, Rev. Mod. Phys. 39 #3 p594, (1967)

[26] S. Okubo and R.E. Marshak, Ann. Phys. 4, p166, (1958)

[27] S. Sato, Nuovo Cimento 82A #3 p339, (1984)

[28] S. Sato, Nuovo Cimento 103A #4 p471, (1990)

[29] R. Blankenbecler and R. Sugar, Phys. Rev. 142, p1051, (1966)

[30] J. Fleischer and J.A. Tjon, Nucl. Phys. B84, p375, (1975)

[31] J. Fleischer and J.A. Tjon, Phys. Rev. D 15, p2537, (1977)

[32] J. Fleischer and J.A. Tjon, Phys. Rev. D 21, p87, (1980)

[33] M.J. Zuilhof and J.A. Tjon, Phys. Rev. C 24, p736, (1981)

[34] K. Erkelenz, R. Machleidt, K. Hollinde, Nucl. Phys. A 194, p161, (1972)

[35] E. Fermi and C.N. Yang, Phys. Rev. 76, p1739, (1949)

[36] H.M. Moseley and N. Rosen, Phys. Rev. 80, p177, (1950)

[37] Y. Koide, Prog. Theor. Phys. 39, p817, (1968)

[38] R.W. Childers, Phys. Rev. D 26, p2902, (1982)

[39] P. Leal Ferreira and A.P. Galeão , Mod. Phys. Lett. A 5, p2523, (1990)

[40] H.M. Moseley, Ph.D. Thesis, University of North Carolina, (1950)

[41] C.Y. Cheung, S.P. Li, Phys. Lett. B. 234, p.444, (1989)

[42] A. Messiah, Quantum Mechanics Vol.2, New York:John Wiley & Sons, Amsterdam: North Holland Publ. Co. (1961). NH published en Francais, (J.Wiley handled Anglais translation)

[43] A.R. Edmonds, Angular Momentum in Quantum Mechanics, New Jersey: Princeton Univ. Press. (1957)

[44] D.J. Beachey, Y. Nogami, F.M. Toyama, J. Phys. G. 17 p1039 (1992)

[45] S. Klarsfeld, J. Matorell, J.A. Oleo, M. Nishimura, D.W.L. Sprung, Nucl. Phys. A.456, p.373, (1986)

[46] F.M. Toyama, Y. Nogami, Phys. Rev. C. 38, p.2881, (1988)

[47] W. van Dijk, Phys. Rev. C. 40, p.1437, (1989)

[48] D.W.L. Sprung, Hua Wu, J. Matorell, Phys. Rev. C. 42, p.863, (1990)

[49] R. Machleidt, Adv. Nucl. Phys. 19, p.189, (1989)

[50] M.W. Kermode, S.A. Moszkowski, M.M. Mustafa, W. van Dijk, Phys. Rev. C. 43, p.416, (1991)

[51] M.W. Kermode, W. van Dijk, D.W.L. Sprung, S.A. Moszkowski, J. Phys. G. 17, p.105, (1991)

[52] E.M. Henley, Isospin in Nuclear Physics. ed D.H. Wilkinson, Amsterdam: North Holland Publ. Co., p.15 (1969)

[53] J. Schwinger, Harvard lecture note (1947)

[54] H. Bethe, Phys. Rev. 76, p38 (1949)

[55] Particle Data Group, Physics Letters B. 204, p28,29,96, (1988)

[56] *ibid* p.24

[57] R. Vinh Mau, C. Semay, B. Loiseau, M. Lacombe Phys. Rev. Lett. 67, p. 1392, (1991)

[58] R. Machleidt, K. Holinde, Ch. Elster, Phys. Rep. 149, p1, (1987)

[59] R.W. Bérard, F.R. Buskirk, E.B. Dally, J.N. Dyer, X.K. Maruyama, R.L. Topping, T.J. Trowers, Phys. Lett. B47, p355, (1973)

[60] G.G. Simon, Ch. Schmitt and V.H. Walther, Nucl. Phys. A364, p285, (1981)

[61] D.W.L. Sprung and Hua Wu, Acta Phys. Pol. B 24, #3, p503, (1993)

[62] V.I. Kukulin and V.N. Pomerantsev, Prog. Theor. Phys. 88, #2, p159 (1992)

[63] N. Levinson, Kgl. Danske Videnskab. Selskab, Mat.-Fys. Medd. 25, p.9 (1949)

[64] M.J. Moravcsik, Rep. Prog. Phys. 35 #6, p587, (1972)

[65] W.H. Press, S.A. Teukolsky, W.T. Vetterling, B.P. Flannery, Numerical Recipes in Fortran: The Art of Scientific Computing 2nd ed., Cambridge: Cambridge University Press, (1992)

[66] D.J. Beachey, Y. Nogami, W. van Dijk, F.M. Toyama, to be submitted to Physical Review C

[67] M. Kohno, J. Phys. G, 9, p L85, (1983)

[68] B.M. Casper and F. Gross, Phys. Rev. 155 p1607 (1967)

[69] J. Schwinger, Phys. Rev. 78, p135, (1950)

[70] S. DeBenedetti, Nuclear Interactions, New York, John Wiley & Sons, (1964)

[71] R.A. Arndt, L.D. Roper, R.A. Bryan, R.B. Clark, B.J. VerWest, and P. Signell, Phys. Rev. D 28, p97 (1983)

[72] R. Arndt, L.D. Roper, R.L. Workman, and M.W. McNaughton, Phys. Rev. D 45, p3995, (1992) (Phases obtained from E-dependent solutions set VL40 from SAID dial-in facility.)

[73] L.S. Celenza and C.M. Shakin, "Relativistic Nuclear Physics -Theories of Structure and Scattering", Singapore, World Scientific, p6-7,(1986)

[74] R. Jackiw, MIT preprint, CTP No. 1306 (1985)

[75] Y. Munakata, T. Ino, F. Nagamura, Prog. Theor. Phys. 79 (1988), p1404

[76] W. Glöckle, Y. Nogami, F.M. Toyama, Prog. Theor. Phys. 81 (1989), p706

[77] W. Glöckle, Y. Nogami, I. Fukui, Phys. Rev. D. 35 (1987), p584

[78] A. E. S. Green, Phys. Rev. 76 (1949), p406

[79] M.G. Calkin, D. Kiang, Y. Nogami, Am. J. Phys. 55 (1987), p737

[80] J. J. Sakurai, Advanced Quantum Mechanics, Addison Wesley Publ. Co. Inc. Reading Mass. (1967)

[81] N. Parent M.Sc. Thesis McMaster Univ. (1991)